The Dissertation Committee for Brent Carl Norris Certifies that this is the approved version of the following dissertation:

Applications of N-Heterocycles in Electrically and Ionically Conductive Polymers

Committee:

Christopher W. Bielawski, Supervisor

Alan H. Cowley

Arumugam Manthiram

Eric V. Anslyn

Jonathan L. Sessler

Applications of N-Heterocycles in Electrically and Ionically Conductive Polymers

by

Brent Carl Norris, B. S.

Dissertation

Presented to the Faculty of the Graduate School of

The University of Texas at Austin

in Partial Fulfillment

of the Requirements

for the Degree of

Doctor of Philosophy

The University of Texas at Austin

August 2010

Dedication

To my family, for their love and support

Acknowledgements

I would like to thank Dr. Christopher Bielawski for all his guidance as well as all the members of the Bielawski group who I have called on for help too many times to count. I have been fortunate to work with people who were more like family than coworkers. In particular I would like to thank Dr. A.J. Boydston, Dr. Kyle Williams, Dr. Daniel Coady, Dr. Justin Kamplain, Mr. Matt Sanderson MA., Dr. Andrew Tennyson, Mr. Adam Stockett, Dr. Dimitri Kramov and Mr. Daniel Varnado MA. They have all been my mentors. I would also like to thank Dr. Jeff Strahan, Dr. Brian Long, Dr. Wen Li and Dr. Ryan Littich for all their help and friendship.

I would like to thank my sister for always being there for me and getting me through high school and college. The family dinners have always meant so much.

I would like to thank my father for instilling in me my love of science and my mother for her endless encouragement and support. They have gracefully pushed me to succeed in all aspects of life and are the loving parents that I hope to be. I owe them more than I can ever possibly repay.

Most importantly I would like to thank my wife Lauren for her patience, love and devotion. She is my best friend, my fishing buddy, and my life companion. Without her I would most certainly not have finished this.

Applications of N-Heterocycles in Electrically and Ionically Conductive Polymers
Publication No._____

Brent Carl Norris, Ph. D.
The University of Texas at Austin, 2010

Supervisor: Christopher W. Bielawski

The covalent bond formed between a N-heterocyclic carbene and an aryl-isothiocyanate was discovered to be thermally-reversible. This bond was incorporated into the backbone of an aromatic polymer which, when subjected to heat and excess monomer, would depolymerize to smaller oligomers. In addition these small molecules contain active chain ends and could be repolymerized to reform the original polymer. The high molecular weight material was made into freestanding sheets with desirable mechanical properties and could be made conductive by treatment with iodine.

A new poly(triazene) was formed from the reaction of a facially opposed, annulated, bis-N-heterocyclic carbene (NHC) and an organic bis-azide. The NHC as well as the azide were varied and combined to produce a series of polymers which were characterized by GPC, TGA, and NMR. These thermally robust polymers were also coated onto glass slides and rendered electrically conductive by exposure to iodine vapor.

A new reagent for Reversible Addition Fragmentation Chain Transfer Polymerization (RAFT) is described. This imidazolium based reagent shows unusually fast kinetics which allows it to control polymerizations at significantly reduced loadings compared to the more traditional neutral dithiocarbamates or dithioesters. The fast kinetics is explained by the rapid rotation of the dithioester about the plane of the cationic N-heterocycle.

Sulfonated poly(ether ether ketone) (sPEEK) membranes were blended with imidazoles with varying pKas. The proton conductivity of the membranes was evaluated as a function of pKa and temperature. Interestingly, the conductivity of the dry membranes showed a non-monotonous profile over a temperature range of 25 – 150 °C. We use a theoretical model to better understand the mechanistic origins of the observed temperature–conductivity profiles. This model is based on the reaction equilibria between sPEEK's sulfonic acid groups and the basic sites of the added heterocycles.

Using the copper-catalyzed 1,3-dipolar "click" cycloaddition reaction, poly(sulfone)s containing pendant azide moieties were functionalized with various amounts of sodium 3-(prop-2-ynyloxy)propane-1-sulfonate and crosslinked with 1,7-octadiyne. The degree of sulfonation as well as the degree of cross-linking was systematically varied by changing the ratios of the aforementioned reagents. The polymers were cast into membranes, acidified, and then tested for proton conductivity, methanol permeability, and membrane-electrode assembly (MEA) performance.

Table of Contents

List of Figures

List of Schemes

List of Tables

Chapter 1: Introduction

REVERSIBLE CONJUGATED POLYMERS

Conjugated polymers (CPs) are a unique subset of synthetic macromolecules that exhibit formal chemical unsaturation along their main chains,[1] wherein π-conjugation extends across multiple repeat units as a result.[2] Their highly-delocalized nature of CPs endows them with useful characteristics, such as intense π→π* transitions, accessible band-gap potentials, as well as photo- and electroluminescence. Consequently, CPs have enabled significant advances in applications ranging from sensing[3,4] to photovoltaics[5,6] to optoelectronic materials.[7,8,9,10] Given the burgeoning scope of CP-based applications, there is significant interest in variants that undergo functional changes in response to exogenous stimuli. Considering the physical and electronic properties displayed by CPs are intimately linked to their structures,[5,11,12,13,14,15,16] one avenue to effect such functional changes is through the development of structurally-dynamic CPs.

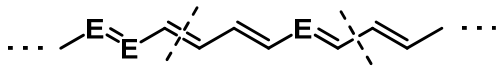

Figure 1.1 Conceptual dissection of a heteroatom-doped polyacetylene, wherein σ- and π-bond scission can occur reversibly in response to chemical, electrochemical, photochemical or thermal impetuses. E = sp2-hybridized atom such as C, N, P, etc.

Structural dynamism in CPs may be manifested by geometric isomerization, dissociation, or other chemical alteration of a covalent bond, and ultimately involves the reversible disruption and restoration of σ- and π-bonds. In general, these changes may

occur in response to (1) chemical, (2) electrochemical, or (3) thermal impetuses (Figure 1.1). Each stimulus features unique advantages and disadvantages, and is thus better suited for some applications more than others. For example, chemical impetuses can be administered in a well controlled fashion, given that a reaction that requires certain conditions will not occur in their absence. Electrochemically-impelled structural dynamism, however, displays significantly improved atom economy and benefits from the ease by which electrons can be supplied to or removed from solutions or films.

To imbue any of three aforementioned impetuses in a homogenous manner is an additional level of complexity. Moreover, each strategy necessitates impetus-specific functional groups (to react chemically with a specific molecule, to undergo redox change at a specific potential, etc). In contrast, solutions and solid materials can both be evenly heated with less difficulty, and thus thermally-impelled structural dynamism may be used in situations where the others may not.

Chemical Impetus

In many ways, the simplest strategy for impelling controllable structural dynamism in a CP is with the use of chemical reagents. If a polymer can only undergo structural change upon reaction with an exogenously supplied molecule, it will never exhibit this dynamism in its absence. Frequently, the same compounds and reagents can be used for these materials, thus precluding the need to incorporate additional chemically reactive or other stimulus-responsive functionalities. As a result, chemically-impelled structural dynamism can be initiated and controlled in a straightforward manner.

Amine–carbonyl condensation and the opposite process, imine hydrolysis, exist in equilibrium. Because the forward and backward reactions occur with such high fidelity, these chemical functionalities have been widely used for reversible covalent bonding strategies.[17,18] One of the earliest examples of using condensation chemistry to access a structurally dynamic CP was reported by Moore nearly a decade ago.[19] Condensation of imine-terminated m-phenylene ethynylene tetramers **1.1** and **1.2** with catalytic oxalic acid in $CHCl_3$ afforded primarily unreacted starting materials, along with dimers and trimers of **1.3** (M_w = 1.8 kDa) and byproduct **1.4** after 6 d (Figure 1.2). However, when the same reaction was performed in CH_3CN, nearly a 200-fold increase in the molecular weight of **1.3** was observed (M_w = 350 kDa). The authors attributed this variation to the dependence of m-phenylene ethynylene oligomer conformation on the chemical environment, where polar solvents induce the formation of helical structures,[20] thus stabilizing the polymeric structure and templating it for further reaction with monomer.

In a related approach, Lehn and coworkers described the condensation of diamines **1.8** and **1.10** with bisaldehyde **1.9** to afford polymer **1.11**, comprising a statistical distribution of alkyl and aryl diamines (i.e., $0 \leq x \leq 1$ and $y = 1–x$; Figure 1.3).[21] Analysis by ^{1}H NMR, UV/vis and fluorescence spectroscopies indicated a larger percent incorporation of **1.8** (~80%), reflecting its greater nucleophilicity vs. **1.10**. Adding 2 equiv of $Zn(BF_4)_2 \bullet 8H_2O$ caused a 3-fold increase in absorbance at 418 nm, a greater than 100 nm shift in λ_{em} (365 to 475 nm), and complete disappearance of the alkyl imine ^{1}H NMR signals. Subsequent addition of hexamethylhexacyclen (stoichiometric with respect to added Zn^{2+}) restored the spectroscopic features of the original statistical

polymeric mixture. Thus, **1.11** exists in equilibrium with its component monomers **1.8–1.10**. The polymer distribution can be driven to the fully-aromatic **1.11** (x = 0, y = 1) by

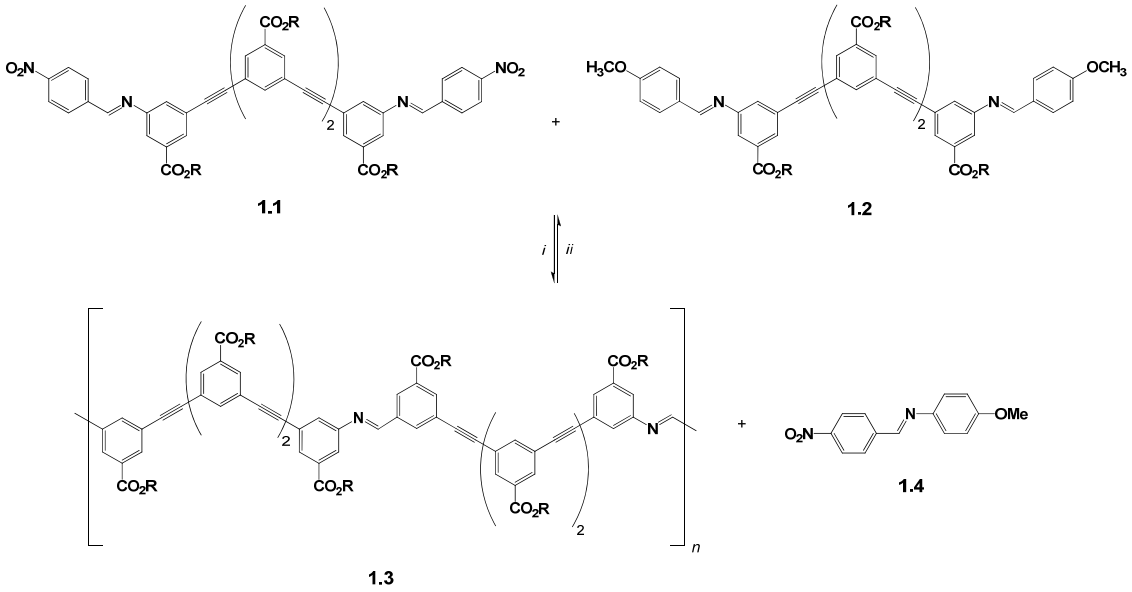

Figure 1.2. Reversible formation of poly(m-phenylene ethynylene)s via imine condensation. R = $(CH_2CH_2O)_3CH_3$. Conditions: 0.1 equiv $C_2H_2O_4$, RT, 6 d; i) CH_3CN; ii) $CHCl_3$.

trapping **1.8** with Zn(II) ions, and returned to the statistical mixture by sequestering the Zn(II) ions with hexamethylhexacyclen.(see Figure 1.3) Collectively, these results show that **1.11** (x = 0, y = 1) can be reversibly generated and consumed, enabling dynamic chemical control over the effective conjugation length – and hence the electronic properties – of the respective polymer. Subsequent studies by Lehn have shown that this strategy can be applied to a wide variety of diamines and that the structural dynamism is retained.[22] One limitation to using these reversible element–

nitrogen double bond linkages as a general strategy is that they, under certain conditions, can interrupt conjugation despite being formally unsaturated. [23,24]

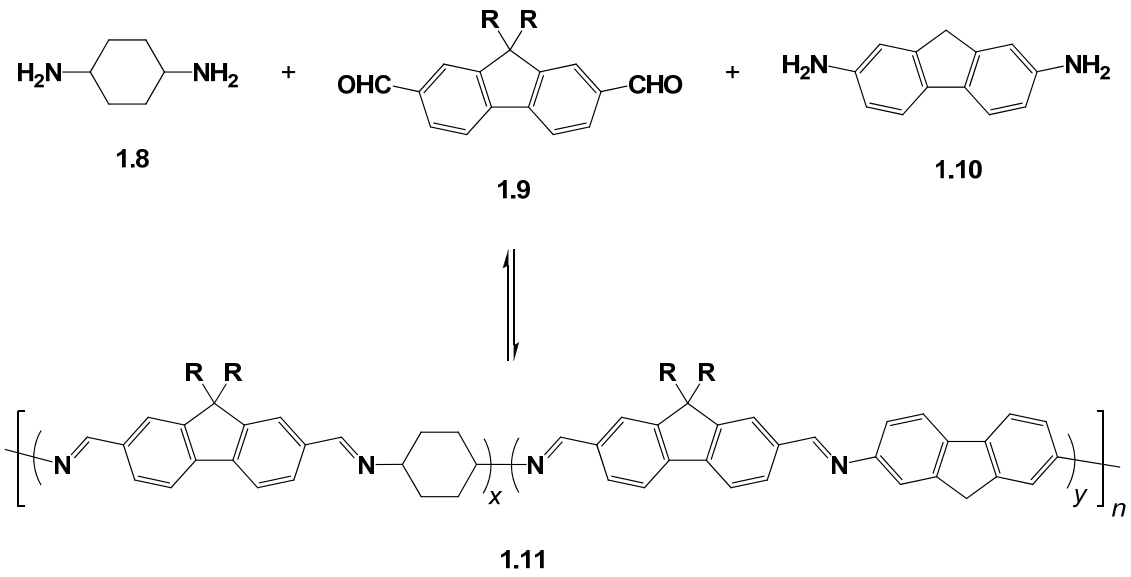

Figure 1.3. Reversible formation of poly(cyclohexyl-co-fluorene)s via imine condensation. R = n-hexyl. Conditions: RT, CH_3CN. Addition of $Zn(BF_4)_2 \bullet 8H_2O$ to **1.11** comprising a statistical mixture of monomers drives it to a fully-aromatic state (x = 0, y = 1). Subsequent chelation of Zn(II) restores the original distribution.

Carbon–carbon multiple bonds have both greater thermodynamic and kinetic stability than their heteroatomic analogues, and can often be efficiently formed and broken via metathesis catalysts. However, a complication inherent to the preparation of CPs via ring-opening metathesis polymerization reactions in particular is the competitive formation between linear polymers and cyclic oligomers,[25,26] reflecting the disparate entropic and thermodynamic properties of these two classes of molecules under solution equilibrium conditions.[27,28,29] For example, competitive formation of cyclic oligomers is frequently observed as a complication inherent to metathesis-based polymerization

strategies, especially at low concentrations. Moore demonstrated that this reversibility could be harnessed productively in alkyne–containing polymers, whereby treating poly(m-phenylene ethynylene) **1.12** with molybdenum alkyne complex [Mo(≡CEt){N(3,5-Me_2Ph)-(tBu)}$_3$] resulted in conversion of the open-chain polymer into macrocycle **1.14**, along with small amounts of short, open-chain oligomers (Figure 1.4).[30] Conversely, reaction of **1.14** with diphenylacetylene in the presence of the same Mo catalyst led to the reformation of polymeric material (**1.13**, R4 = Ph).

Overall, chemically-impelled structural dynamism benefits from the excellent controllability inherent to this strategy. However, in practice, this approach if often impeded by the phases of the components, where the polymer is typically a solid and the exogenous reagents are either in the liquid- or solid-state. Moreover, automation requires

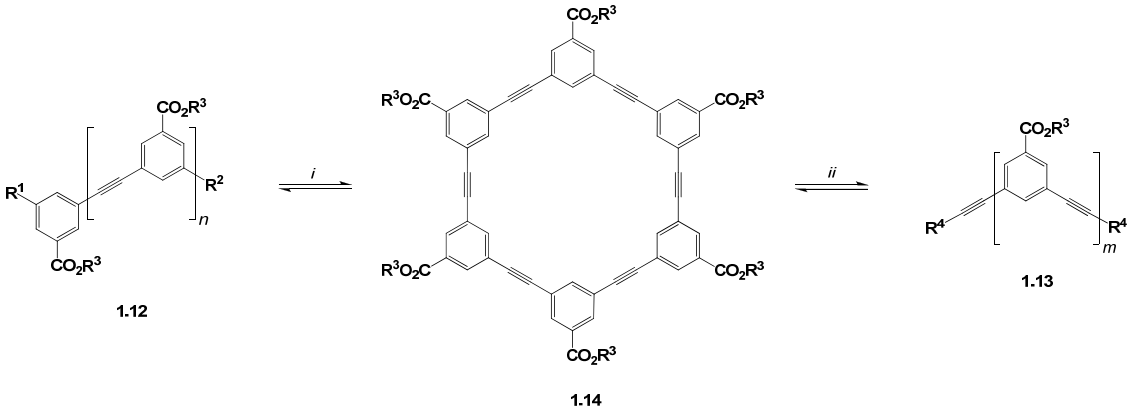

Figure 1.4. Reversible cyclodepolymerization and subsequent repolymerization of poly(m-phenylene ethynylene)s via alkyne metathesis. R_1, R_2 = I or C≡CH, R_3 = $(CH_2CH_2O)_3CH_3$, R_4 = Ph. Conditions: [Mo(≡CEt){N(3,5-Me_2Ph)(tBu)}$_3$], 4-nitrophenol, 30 °C; i) 1,2,4-trichlorobenzene; ii) CCl_4.

embedding reagents into a polymer matrix such that they are only released and reactive in response to a specific stimulus. This necessitates complicated and time-consuming

fabrication techniques. Given these characteristics, chemical impetuses are ideally suited for applications where significant changes in CP structure and properties, including such extremes as complete depolymerization or disruption of conjugation, must occur automatically. In stark contrast to the detailed molecular weight and macromolecular studies of CPs that exhibit chemically-impelled structural dynamism, however, very little attention has been directed toward attendant variations in the electronic properties of these materials. As a result, much of the structure–property relationships remain unexplored, and thus present opportunities for discovery.

Electrochemical Impetus

Despite the fundamental controllability of a chemical reaction (i.e., it will not proceed without all necessary reagents present), the reversible scission of covalent bonds via chemical reactions suffers from poor atom economy and bulk heterogeneity. Electrons, however, can be easily added and removed from both solutions and solids via bulk electrolysis. Moreover, the timescales for such electrochemical processes are often short, facilitating rapid activation and shutdown of the structural dynamism response. Biological macromolecules, such as enzymes and other proteins, for example, undergo redox mediated disulfide–dithiolate interconversions, which Nature uses to alter the structure and function of these biopolymers in a reversible and well-defined manner with perfect atom economy.[31,32,33]

Imitation and implementation of this strategy by chemists has endowed them with redox control over a wide variety of applications, ranging from molecular recognition[34] to template-directed synthesis[35] to targeted drug delivery.[36] Conjugated polymers were

added to this list by Su and coworkers, who prepared **1.15** via chemical and electrochemical polymerization of the corresponding disulfide–aniline precursor (Figure 1.5).[37] Cyclic voltammetric analysis of **1.15** revealed that the disulfide–dithiolate redox couple occurred at a lower energy and with better reversibility than the monomer. Conversion of **1.15** to **1.16** could afford a material with greater conductivity when combined with Brønsted- or Lewis-acid doping. Cleavage of these interchain cross-links resulted in the disappearance of the characteristic main-chain absorption for **1.15** and appearance of an intense band at lower energy in **1.16** (~400 nm vs. 820 nm), reflecting the lower band-gap potential in the latter. Because **1.15** is positively charged, it will exhibit much higher negative vs. positive charge mobility. Whereas **1.16** is formally neutral, it exhibits zwitterionic character, wherein the thiolate moieties can interact with cations (e.g. H+ and Li+), thus enabling it to transport both negative and positive charges. Collectively, these results represent electrochemically-impelled control over the electron/hole transport ability of a CP, as effected by the disruption and formation of interchain cross-links. Moreover, the band-gap potential can be adjusted by altering the overall CP charge. Thus, redox modulation of a CP by electrochemical methods can produce significant changes in polymer architecture and bulk electronic properties. Given these features, a material composed of a redox active CP, such as **1.15**, could be toggled between charge-transport and charge-storage functions, with potential for smart energy applications.

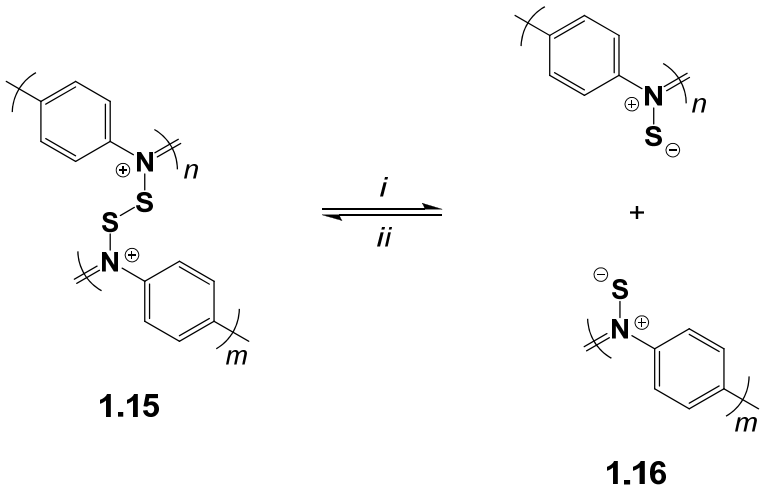

1.15 1.16

Figure 1.5. Reversible cleavage and reformation of interchain cross-links via electrochemical reduction of disulfide (i) and oxidation of dithiolate (ii) moieties, respectively. Conditions: 0.5 M $LiClO_4$, RT, CH_3CN; i) Eapp = –0.2 V; ii) Eapp = +1.0 V.

Electrochemically-impelled structural dynamism can actuate reversible covalent bonding with perfect atom economy and potentially allow near-instantaneous control over this process. However, the generality of this method is limited by the need for a conductive medium, and is only effective with solutions with high ionic strengths and materials that are intrinsically conducting or doped. Additionally, because the extended π-conjugation inherent to the CP scaffold renders its HOMO and LUMO energetically accessible, the addition of chemical redox agents could potentially cause oxidation or reduction of the entire polymer. As a result, this strategy is best suited to CPs designed for use in conductive materials whose function must be rapidly controlled, such as electronic self-protection, whereby a device is modulated between power-delivery and -storage behavior in response to abnormal operating conditions (e.g. short circuits, power surges, etc.). Despite its potential, electrochemically-impelled structural dynamism in

CPs has so far been limited to the formation and disruption of interchain cross-links. To achieve significantly greater control over properties and function, a similarly responsive CP should incorporate redox active functional groups within the main chain. Because such a CP has not yet been prepared, we believe there are great opportunities for electrochemically-impelled structurally-dynamic CPs.

Thermal Impetus

One disadvantage common to chemical, electrochemical and photochemical stimuli is the challenge associated with supplying them in a homogenous / isotropic manner. Moreover, many of the systems that exhibit dynamic structures in response to these stimuli are highly specialized, and cannot be readily adapted for general use. Compelled by these limitations, we reasoned that thermal energy would be a suitable alternative, given that applying heat to a solution or material is relatively straightforward and that all molecules interact with heat.

To understand the challenges associated with thermally-reversible CPs, we first conceptualized this behavior in polyacetylene, one of the simplest CPs. Retrosynthetic analysis of this polymer highlights how cleavage of the different C–C bonds therein can afford electronically-orthogonal precursors. Dissection of trans-polyacetylene along its carbon–carbon single or double bonds will afford either diradicals or biscarbenes (left or right, respectively, Figure 1.6). Although the carbon–carbon single bonds would have a lower thermodynamic activation barrier, the resulting vinyl radicals would be unstable. Conversely, cleavage of the carbon–carbon double bonds would require more energy, but produce carbenoid fragments with potential for achieving greater stability.

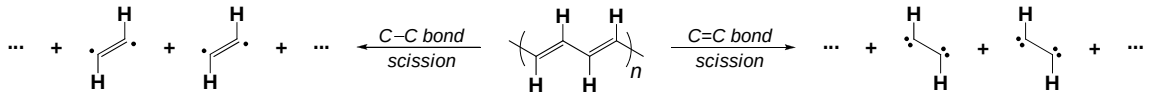

Figure 1.6. Deconstructions of trans-polyacetylene into diradicals (left) or biscarbenes (right).

Thermally-reversible carbon–carbon single bonds have been studied for over a century, with one of the most prominent historic examples detailed by Gomberg in 1900 (**1.17** ↔ 2 **1.18**; Figure 1.7).[38] Dehalogenation of trityl chloride produced an extremely air-sensitive compound that decomposed to trityl peroxide under aerobic conditions, indicating the equilibrium presence of trityl radical (**1.18**). Although these radicals originated from a dimeric precursor, reactivity studies indicated that this molecule contained an olefinic bond (**1.17**), and subsequent crystallographic analysis confirmed this structural assignment.[39] In contrast, reversible carbon–carbon double bonds were not reported until 1963 by Wanzlick, presumably due to the obvious difficulty associated with effecting a reversible 2→0 bond-order reduction (Figure 1.7).[40] Deprotonation of the imidazolinium precursor to **1.20** afforded the tetraazafulvene **1.19**, formally a dimer of two imidazolinylidene units. Subsequent reactivity studies indicated that **1.19** exists in equilibrium with the two N-heterocyclic carbenes (NHCs). Similarly reversible carbon–carbon single- and double-bonds have been successfully incorporated into non-conjugated polymers for nearly two decades,[41,42,43,44] yet these functionalities have remained relatively unexplored as components for thermoresponsive structurally dynamic CPs.

The simple ditopic hydrocarbon-based carbenes depicted in Figure 1.6 have the appropriate electronic configuration and connectivity to reform their parent CP, but their extreme reactivity could lead to decomposition or other irreversible chemical behavior. Inclusion of electron-donating heteroatoms, such as sulfur or nitrogen, adjacent to the carbene nuclei could enhance their stability sufficiently to allow recombination. N-Heterocyclic carbenes feature a carbene nucleus stabilized by two adjacent nitrogen atoms in a cyclic framework. Depending on the steric encumbrance of the N-substituents,

A) Reversible single bond

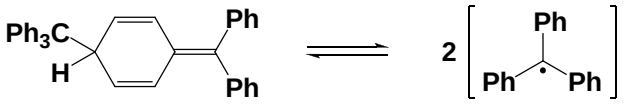

1.17 **1.18**

B) Reversible double bond

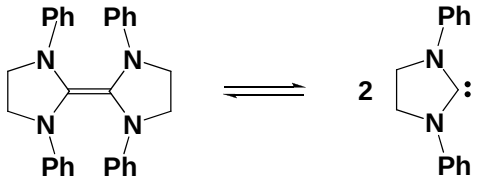

1.19 **1.20**

Figure 1.7. Examples of thermally-reversible carbon–carbon (A) single and (B) double bonds.

NHCs can exist either as dimeric tetraazafulvenes or free carbenes, where bulky groups are required to stabilize the latter.[45] Moreover, NHCs have been shown to couple with a range of electrophiles (such as organic azides and isothiocyanates; Figure 1.8,

left)[46,47,48,49] and to coordinate a variety of MLn fragments (Figure 1.8, right),[50, 51,52,53] whereby the resulting adducts and complexes, respectively, exhibit electronic properties and connectivity that are ideally-suited for structurally-dynamic CPs.

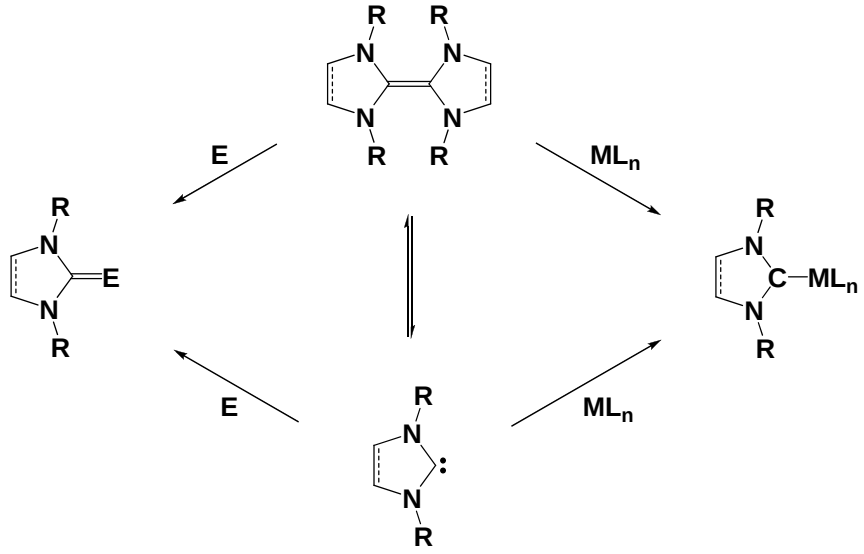

Figure 1.8. Wanzlick equilibrium between NHCs and tetraazafulvenes, along with the organocoupling and organometallic chemistries they undergo, where E = R–NCS, R–N3, etc.

Capitalizing on the rich chemistry of NHCs, we reasoned that appropriate bis(NHC)s could be used to access three major classes of polymers, potentially even those that are conjugated or extensively delocalized: (1) homopolymers featuring multiple tetraazafulvene linkages (Figure 1.9, top right), (2) alternating copolymers obtained via condensation polymerization of bis(NHC)s with ditopic electrophiles (middle right), and (3) metallopolymers comprising alternating NHC and MLn units (bottom right). Many of these reactions can be rendered thermally-reversible by tuning the stereoelectronic properties of the NHC (e.g. bulkier N-substituent) or coupling partner (e.g. more electron rich). In addition, NHCs and bis(NHC)s are stable and isolable

molecules, which significantly improves the stoichiometric control of step-growth polymerizations (e.g. those shown in Figure 1.9) and thus enables access to high molecular weight CPs. Guided by this precedence and potential, we have pursued bis(NHC)-derived polymers as suitable materials for thermally impelled structural dynamism.

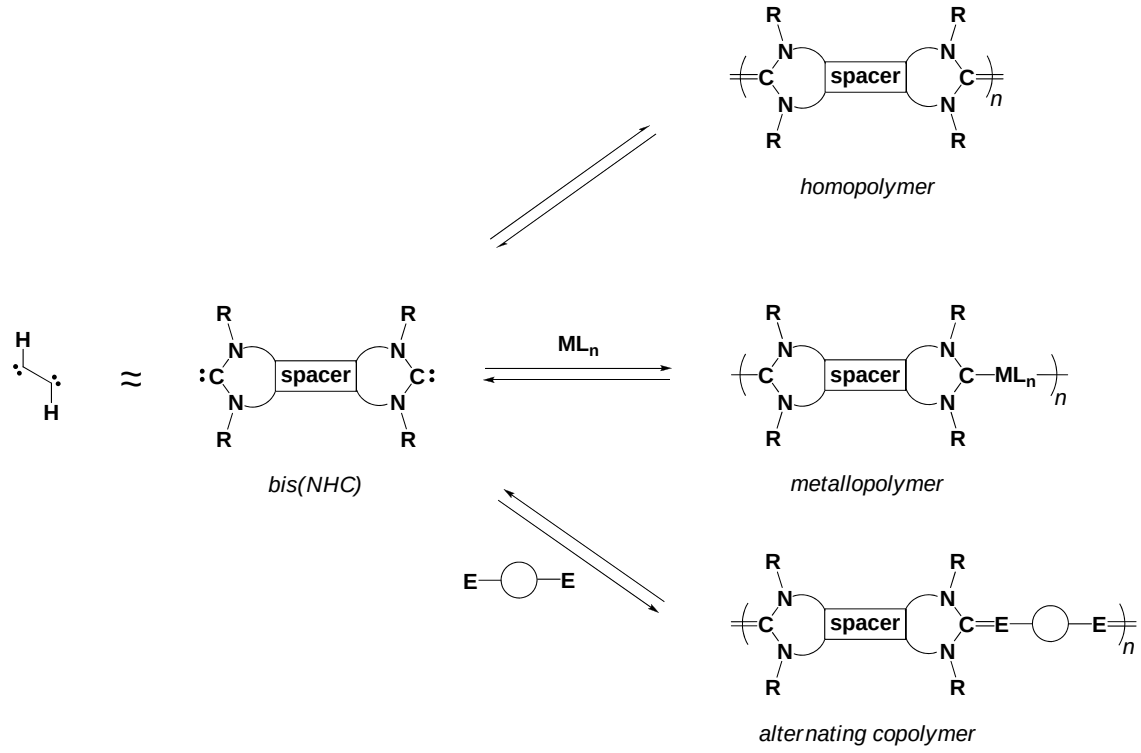

Figure 1.9. Conceptual homology depicting rationale for the bis(NHC) monomer scaffold (left) and the distinct classes of CPs they afford, ranging from homopolymers (top), to metallopolymers (middle), to alternating copolymers (bottom).

HOMOPOLYMERS. Building on the NHC–tetraazafulvene equilibrium discovered by Wanzlick (**1.19** ↔ 2 **1.20**, Figure 1.7), [40] we reasoned that a comparable bis(NHC) could afford homopolymer featuring tetraazafulvene linkages between monomers (Figure

1.9, top right). Deprotonation of readily-accessible bis(imidazolium) salts **1.20** and **1.23**, to generate bis(NHC)s **1.21** and **1.24** in situ, resulted in a gradual color change from near-colorless to dark red over the course of 12 h, suggesting the formation of a molecule with an extended π-system.[54] Interestingly, ^{1}H NMR spectroscopic analysis of these reactions revealed two unique sets of signals: one sharp and one broad, corresponding to free bis(NHC) (**1.21** and **1.24**) and polydisperse macromolecules (**1.22** and **1.25**), respectively (Figure 1.10). A dependence on the N-substituents was observed for the bis(NHC) / polymer ratio, whereby longer alkyl chains correlated with decreased macromolecular composition. Moreover, because the ^{1}H NMR signals for the N-methylene protons in the free bis(NHC)s and polymers could be resolved, the corresponding equilibrium constant could be measured (K_{eq} = 1.0–5.3 to >100, depending on the N-substituent).

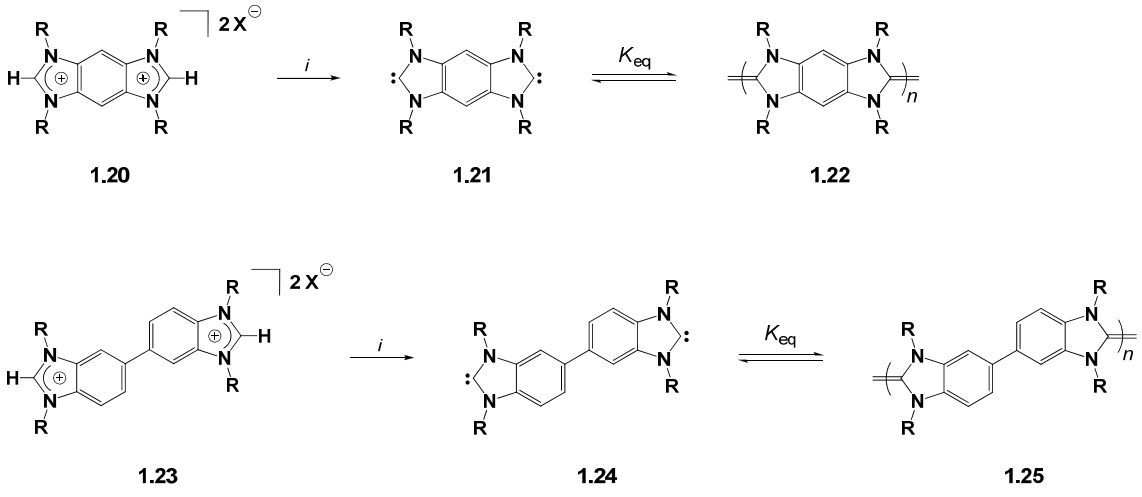

Figure 1.10. Synthesis and solution-phase structural dynamism of poly(tetraazafulvenes). Conditions: i) 2 equiv. NaH, RT, THF.

Replacing the primary alkyl groups in **1.20** and **1.23** with methyl afforded **1.22** and **1.25** as insoluble materials with high molecular weights, due to the decreased steric influence of the N-substituents. Conversely, the equilibrium could be shifted towards greater relative monomer composition by increasing the N-substituent alkyl chain length. Heating a solution of **1.25** (R = ethyl) to 90 °C decreased the relative amount of polymer and increased that of **1.24**, as judged by variable-temperature ^{1}H NMR spectroscopy, and then allowing the solution to cool restored the equilibrium to its original distribution. Paralleling these experiments, analysis of the bis(NHC)–poly(tetraazafulvene) mixture by UV/vis spectroscopy revealed characteristic absorbances at 300 nm and 450 nm, respectively, wherein the latter reflects the extended π-conjugation in **1.22** and **1.25**. As the relative amount of the bis(NHC) monomer increased, either by dilution or heating, the A300 / A450 ratio increased accordingly. Although these results represented an important fundamental achievement, i.e. thermally reversible C=C bond-formation and -breakage in a CP, **1.22** and **1.25** were unsuitable for practical applications as they decompose to their respective water adducts and bis(urea)s upon exposure to water and oxygen, respectively

METALLOPOLYMERS. Whereas tetraazafulvene linkages rapidly decompose under ambient conditions, NHC–metal bonds exhibit significantly greater stability.[55, 56] Guided by these observations, we concluded that inserting MLn spacers between the bis(NHC) monomers could afford an organometallic CP with better robustness than a poly(tetraazafulvene) and comparable formal conjugation (Figure 1.9, middle right). Metallopolymers **1.27** and **1.29** could be prepared via the Herrmann–Schwarz–Gardiner[57] method of simultaneous deprotonation and metallation of **1.26** and **1.28** with $M(OAc)_2$,

or alternatively by co-treatment with MX_2 and NaOAc (M = Pd or Pt, X = Cl or Br; Figure 1.11).[58] Although this approach was successful for Pd and Pt, attempts to prepare the Ni congeners were unsuccessful, presumably due to the greater lability of Ni–NHC bonds.[59] Incorporating metal chelating groups into the N-subtituents enabled access to organometallic CPs,[60] however these systems lacked structural dynamism. Analysis of **1.27** and **1.29** by GPC revealed a wide range of molecular weights (M_n = 8.0 kDa to 1.8 Mda; relatively to polystyrene standards) and polydispersities (PDI = 1.7 to 2.0) consistent with step growth polymerization.

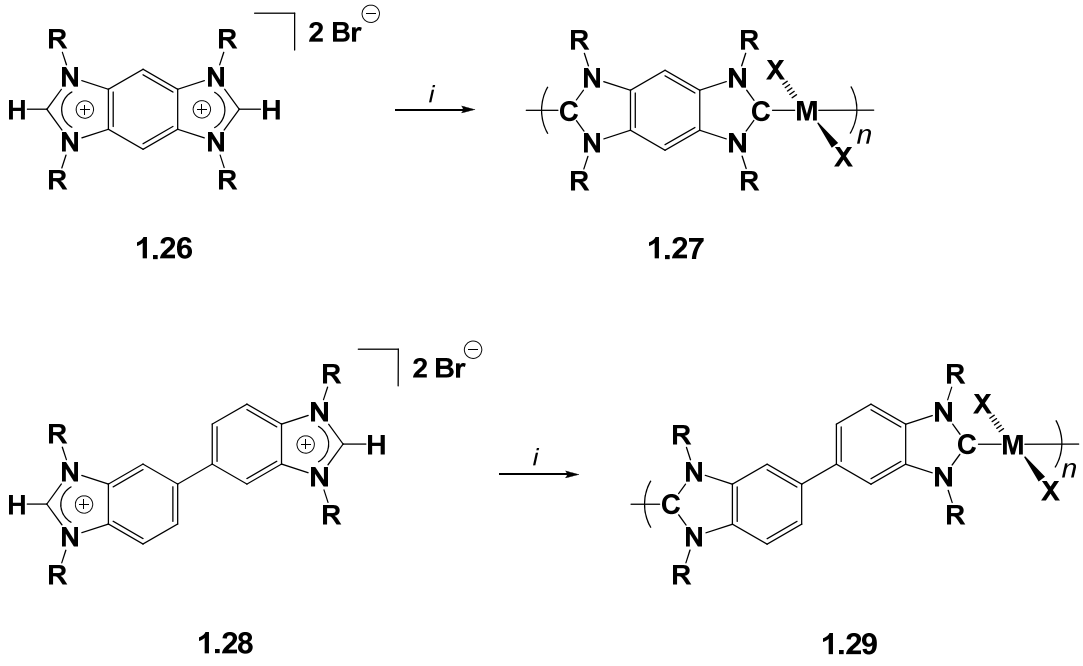

Figure 1.11. Synthesis of organometallic polymers comprising bis(NHC) linkers. R = n-butyl or benzyl, M = Pd or Pt, X = Cl or Br. Conditions: i) $M(OAc)_2$ or (M = Pd or Pt).

To determine whether reversible metal–NHC dissociation/binding was operative in these polymers, monomer exchange studies were performed and monitored by ^1H

NMR spectroscopy. Treatment of **1.30** with **1.31** in the presence of base resulted in the incorporation of the corresponding bis(NHC), affording metallopolymer comprising both monomers (**1.32**, Figure 1.12). Comparable post-polymerization exchange and incorporation of monomers was also found to occur between two homopolymers of different molecular weights, whereby combining two independently-prepared samples of **1.30** with different M_n values (13.0 and 10.4 kDa) afforded a homogenous polymer with an intermediate molecular weight (M_n = 11.1 kDa). Recently, metallopolymers capable of this thermally-impelled structural dynamism have been received interest as recyclable catalysts[61] and self-assembled materials.[62]

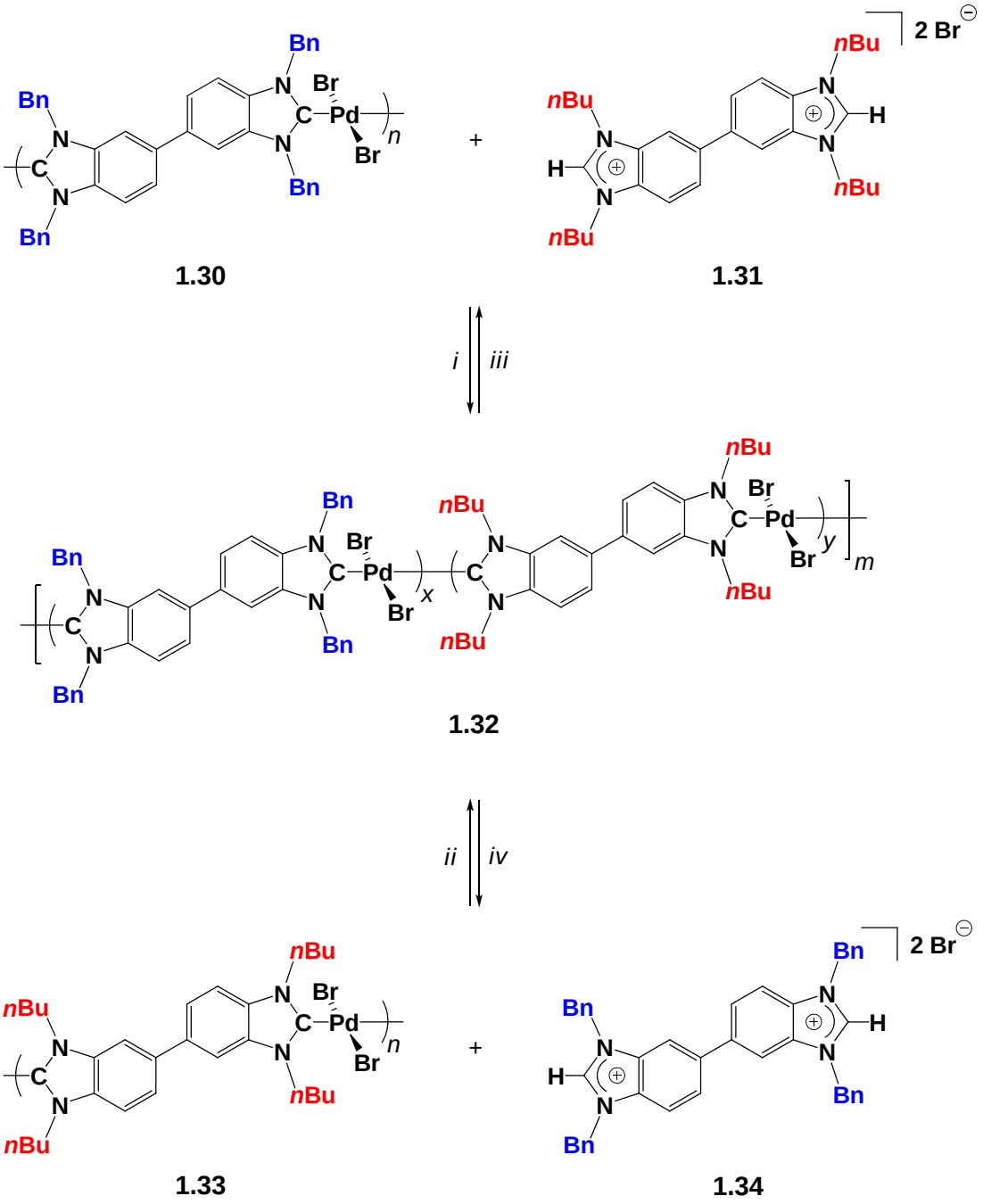

Figure 1.12. Reversible monomer exchange in **1.29**. Conditions: 110 °C, DMSO; i and iv) **1.31**; ii and iii) **1.34**.

To increase the mechanical properties of films comprised by **1.27** and **1.29**, a tritopic NHC capable of cross-linking various polymer chains was included in aforementioned polymeriziation reactions. For example, performing the polymerization of **1.30** in the presence of tris(imidazolium) **1.35** (10–30 mol%) yielded cross-linked materials (**1.37**) that were cast into films (Figure 1.13).[63] One important advantage to studying films of **1.37** is that they are intrinsically conducting (~10–3 S cm^{-1}), allowing undoped films to be imaged via scanning electron microscopy (SEM). Additionally, **1.37** exhibited thermoresponsive behavior, with a range of sol-gel transitions temperatures from 100 to 150 °C. To test the viability of **1.37** for self-healing applications, scored films of these materials were visualized by SEM; subsequent solvent vapor annealing at 150 °C for 15 min actuated the structural dynamism of **1.37**, resulting in a noticeable smoothing and partial repair of the damaged areas. Current efforts are focused towards **1.36** and related tris(NHC)s building blocks for organometallic polymers and metal-organic frameworks.[64]

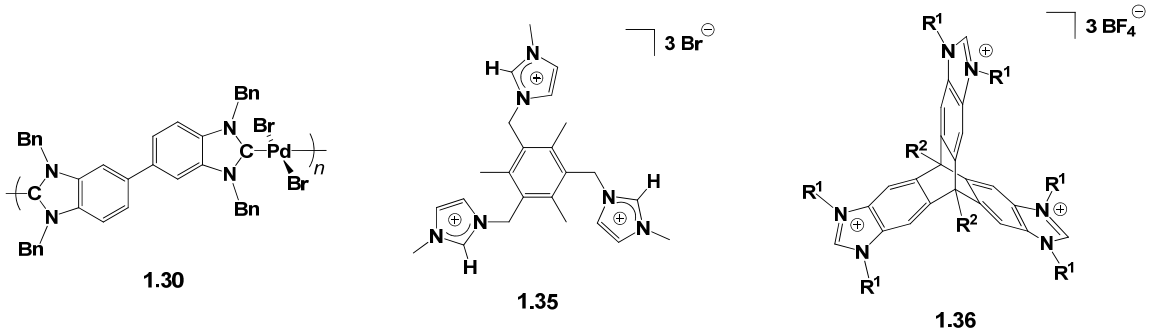

Figure 1.13. Components of cross-linked organometallic polymer networks (**1.37**). R1 = t-butyl; R2 = n-butyl or n-hexyl.

ALTERNATING COPOLYMERS. Despite the improved stability of the bis(NHC)-derived metallopolymers vs. homopolymers, the electronic and geometric requirements for the MLn linkages ultimately constrain CP synthetic diversity. In contrast, organic electrophiles span a much wider range of stereoelectronic properties, therefore combination of ditopic NHCs and electrophiles should enable access to a more diverse and tunable CP scaffold (Figure 1.9, bottom right).[47,48,65] Isothiocyanates are electrophiles that have been known to react reversibly with transition metal complexes for over two decades,[66,67] thus we reasoned that bis(isothiocyanate)s could couple with bis(NHC)s to yield CPs with thermally-reversible carbon–carbon bonds. Guided by this precedence, we reacted **1.38** with stoichiometric **1.39** (0.2 M each in DMF) at ambient temperature and, gratifyingly, obtained the corresponding CP in near-quantitative yield (**1.40**, Figure 1.14).[68] Analysis by GPC enabled determination of the absolute molecular weight (M_n = 14.8 kDa) and polydispersity index (PDI = 2.1) for **1.40**, values consistent with a step-growth polymerization. Higher molecular-weight materials (M_n values up to 29.0 kDa) could be accessed by increasing the initial monomer concentration from 0.2 to 0.8 M. Heating a solution of **1.40** (M_n = 14.8 kDa) containing 1.0 equiv **1.39** (relative to the repeat unit) to 120 °C caused this high molecular weight peak to disappear in the GPC trace, along with concomitant formation of multiple low molecular weight peaks (1.5 to 6.1 kDa). Analysis of this same transformation by UV/vis spectroscopy revealed a decrease in the absorbance at 410 nm, accompanied by a new peak at 392 nm, consistent

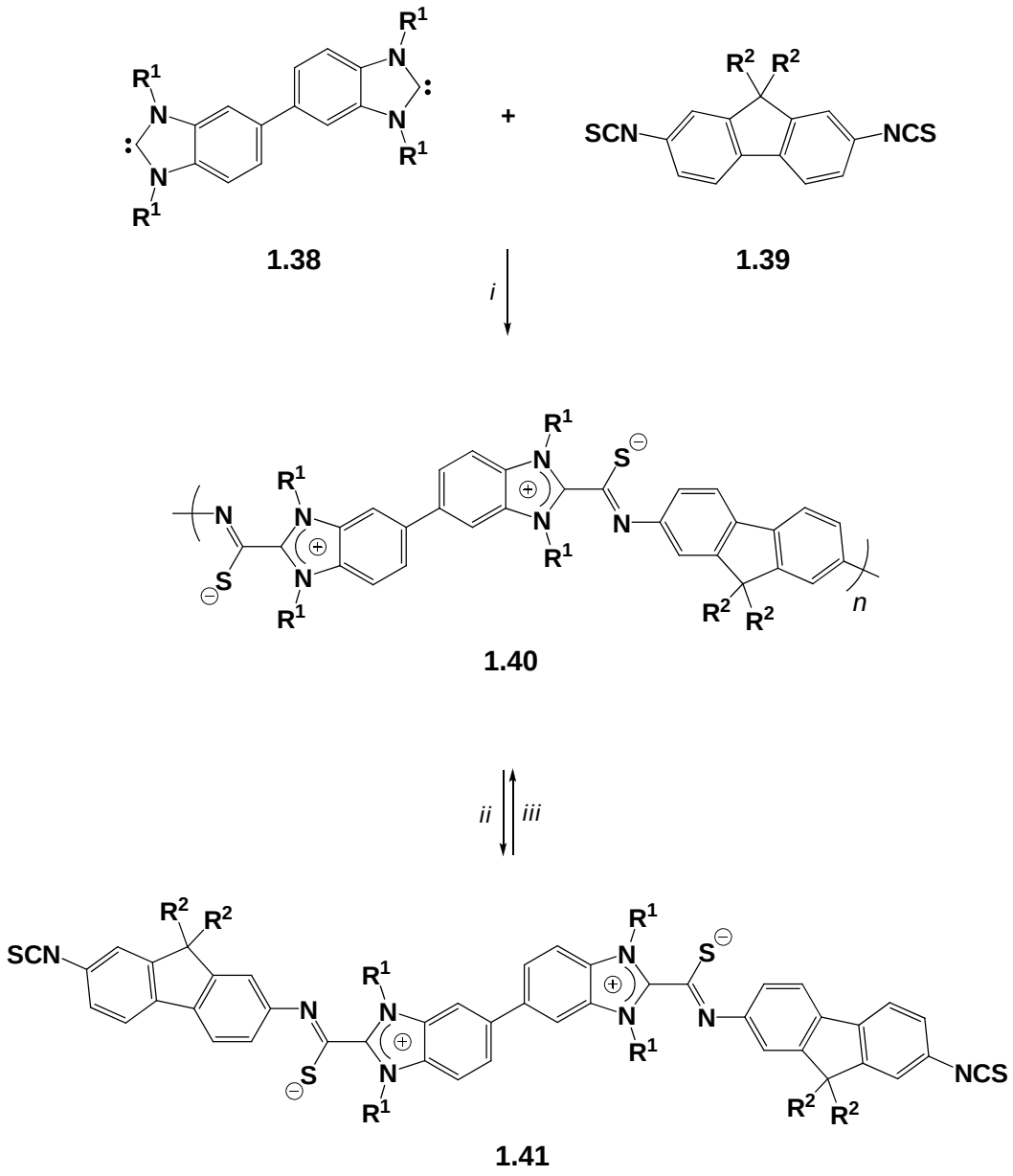

Figure 1.14. Synthesis of alternating bis(NHC)–bis(isothiocyanate) copolymers and their structural dynamism in solution. R1 = 2,2-dimethylbutyl, R2 = n-hexyl. Conditions: DMF; i) RT; ii) **1.39**, 120 °C; iii) **1.38**, RT.

with the shorter effective conjugation length in **1.41** vs. **1.40**. Following isolation and purification, the major component was unambiguously identified as **1.41** and confirmed

via comparison to independently-prepared material. Conversely, this mixture of low molecular weight oligomers could then reform **1.40** (M_n = 18.0 kDa) upon addition of **1.38**. Moreover, these depolymerization / repolymerization reactions could be cycled multiple times, indicating that the NHC–isothiocyanate bonds were fully reversible.

Heat can be generated and supplied to solutions and materials with greater ease and efficiency than chemical reagents, electricity or light, reducing overall complexity and cost. Moreover, this technique does not require chemically-reactive functional groups, conductive media or optical transparency, and thus is more general and compatible with a broader scope of materials. However, one disadvantage of using thermal energy to effect reversible structural changes in CPs is that the covalent bonds relevant to this process must be significantly weaker than the other bonds in the polymer. Given that molecules occupy a Boltzmann distribution, the energy required for thermoresponse must be sufficiently lower than the corresponding activation barriers for other chemical reactions, to avoid undesired structural or functional changes. Considering this limitation, thermally-impelled structural dynamism could be employed in situations where chemical, electrochemical or photochemical impetuses are infeasible or impractical. For example, device components or materials that cannot be accessed without causing damage, disrupting function or requiring shutdown would benefit from CPs whose functions could be modulated via thermally-impelled structural dynamism.

POLY(TRIAZENE)S

In 2005, the Bielawski group reported a new synthesis of triazenes from the reaction of organic azides with N-heterocyclic carbenes(Figure 1.15). [69] This reaction

proceeded to high conversions which made it a possible candidate for polymer formation. Furthermore it produced a highly conjugated chromophore[70] which illustrated it's potential for use in electronic materials. Given the previously discussed utility of poly(azomethine)s we proceeded with a synthesis of a series of polymers based on this bonding.

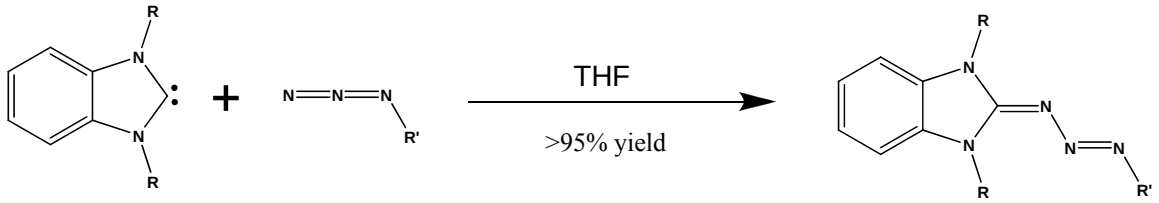

Figure 1.15. Triazene formation through NHC/azide coupling.

By incorporating bis-N-heterocyclic carbenes and bis-azides were able to form polymeric materials which had desirable mechanical properties. Varying nitrogen substituents on the carbene monomers had a large impact on the solubility and the thermal stability of resulting polymers which stretched over a range of more than 120 °C. In short, polymers containing bis-carbenes with long alkyl substituents produced more soluble polymers and those with tertiary groups on the nitrogen had lower decomposition temperatures. The polymers could be cast down onto glass substrates and were found to be electrically conductive when doped with iodine vapor.

IONIC CHAIN TRANSFER AGENTS

Free radical polymerization has become a staple in the polymer industry because of its relatively simple reaction conditions and wide range of vinyl monomers. However this poor selectivity produces side reactions which result in uncontrolled molecular weights and high distributions. Undesired side reactions such as bimolecular termination

can be minimized by lowering the concentration of propagating radicals. Methods such as Atom Transfer Radical Polymerization (ATRP),[71] or addition of nitroxide based radical trapping agents (ie. TEMPO) reversibly sequester the radical chain ends, thereby reducing the probability of bimolecular termination yet allowing chains to grow at a controllable rate

A third method of controlling free radical polymerizations is the addition of radical chain transfer reagents. These not only moderate the concentration of active radicals but also transfer the active radical from one growing polymer chain to another. By doing this a single radical is able to propagate multiple polymer chains, effectively minimizing the concentration of active radicals needed for polymerization. This method is known as Reversible Addition-Fragmentation Transfer (RAFT). (Figure 1.16)

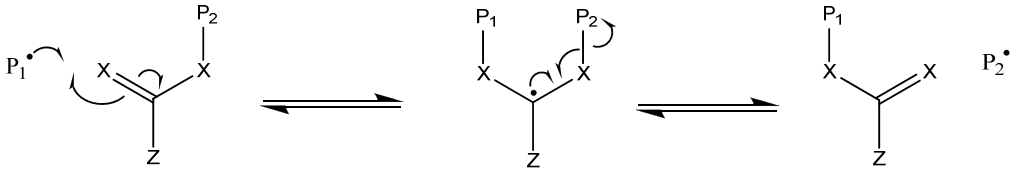

Figure 1.16 RAFT mechanism of radical transfer. Growing polymer chain P_1 transfers the radical to a stabilized intermediate which then fragments to form another active polymer chain P_2.

Typical RAFT reagents employ a xanthate, dithioester, or dithiocarbamate pendant to a group (Z) which either stabilizes or destabilizes the radical intermediate (Figure 1.16). The identity of the Z group is the determining factor for controlling the rates of addition and fragmentation, the key to maximizing the efficiency of the raft reagent for a specific monomer. Our research efforts have focused on imidazolium based Z groups coupled with sterically demanding nitrogen substituents to control the activity of the RAFT reagent.

DIRECT METHANOL FUEL CELLS

One major drawback to traditional hydrogen fuel cells is the need for pressurized gas cylinders to store the fuel. One method of circumventing this is to use liquid hydrocarbons in conjunction with a hydrogen reformer. Hydrogen reformers react hydrocarbons with water to produce hydrogen gas which is then consumed in the fuel cell. This process is not only very endothermic but requires high temperatures and complicates the design of the overall fuel cell. In small devices, where size, weight and cost are major concerns, the Direct Methanol Fuel Cell (DMFC) is a more attractive option. DMFCs oxidize methanol fuel on the surface of the cell electrode, with no need for a reformer.

Although some devices using DMFCs are showing up in the market place, their widespread use is limited by short lifetimes, poor efficiency and cost. A major factor responsible for the short lifetime and efficiency is methanol crossover through the electrolyte. Methanol quickly poisons the platinum catalyst on the cathode, dramatically reducing the performance and shortening the lifespan of the cell.

The most common electrolyte for these small devices is the proton exchange membrane (PEM), a polymeric membrane containing acidic groups (ie. sulfonic acids). The industry standard for this material is Nafion, a perfluoro-polyethylene containing pendant sulfonic acids. Nafion exhibits excellent stability and proton conductivity (when moist) but is highly permeable to methanol. The hydrated membranes exhibit much better conductivity because the primary charge carrier is the hydronium ion. Unfortunately, attempts at maximizing the conductivity by increasing the water content also showed an increase in methanol crossover. Likewise, approaches to lowering the methanol crossover typically result in also lowering the proton conductivity. However, it was recently

reported that N-heterocycles have a unique ability to act as proton carriers while simultaneously lowering the methanol crossover.

An alternative method to lowering the methanol uptake has been to crosslink polymer chains in the membrane. This has the effect of constraining the physical expansion of the membrane and limiting the liquid uptake. The application of crosslinks to PEMs in the literature has met with limited success, primarily due to the lower content of hydronium charge carriers. Our approach has been to combine these two strategies. We envisioned limiting the liquid uptake of the membranes with covalent crosslinks but relying N-heterocycles to carry the charge in instead of water.

Chapter 2: Structurally Dynamic Materials Based on Bis(N-Heterocyclic Carbene)s and Bis(isothiocyanate)s: Toward Reversible, Conjugated Polymers

INTRODUCTION

Demand for reconfigurable and self-healing materials suitable for use in electronic applications continues to grow.[72] Although shape memory alloys offer promise for use in some of the aforementioned applications,[73] they function at prohibitively high temperatures and are challenging to process. As an alternative strategy, we envisioned polymers with conjugated π-systems capable of altering their molecular structures, specifically through depolymerization to fluidic monomers, in response to changes in externally-applied stimuli. Access to such reversible, conjugated polymers (RCPs) presents a fundamental challenge in finding sets of building blocks that are capable of assembling and disassembling while maintaining unsaturation. For practical reasons, this dynamic process should also exhibit high atom economy (i.e., no by-product evolution) and function without the need for catalyst(s) or other exogenous species (i.e., solvents, additives, etc.) While an impressive range of dynamic covalent reactions and associated polymerizations are known,[74] the underlying chemistry[75] of these systems do not fulfill the aforementioned requirements.

Herein we show that an answer to these challenges may lie in the chemistry of N-heterocyclic carbenes[76] (NHCs), which are known to form reversible adducts with a variety of reagents, including other NHCs, organic electrophiles, and transition metals. [54, 58, 77], NHC coupling reactions with isothiocyanates[65, 78] were particularly appealing since they conserve unsaturation and create a formally conjugated linkage between the two moieties (see Figure 2.1), meeting important design criteria for constructing RCPs. Analogous to NHC dimerization, we reasoned that the NHC–isothiocyanate coupling

reaction may be rendered reversible[79] through steric tuning of the N-substituents. Ultimately, by combining aromatic bis(isothiocyanate)s with appropriate bis(NHC)s,[80] we envisioned the formation of a new class of RCPs.

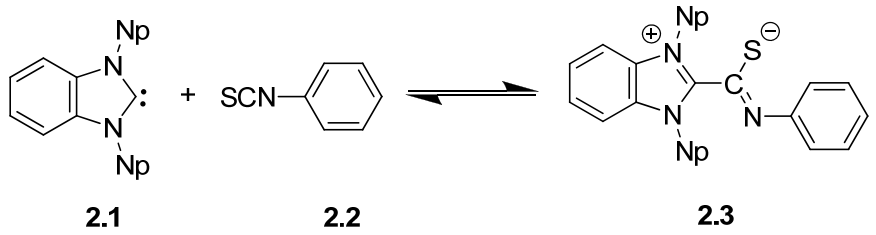

2.1 **2.2** **2.3**

Figure 2.1 reversible coupling of NHC's and isothiocyanates

RESULTS AND DISCUSSION

Initial efforts were directed toward investigating the reversible nature of the covalent bond formed between NHCs and isothiocyanates. As shown in Figure 2.2, heating a toluene-d_8 solution of adduct **2.3**, which was prepared from 1,3-di-neopentylbenzimidazolylidene[81] and phenylisothiocyanate, with stoichiometric 2,4,6-trideuterophenyl-isothiocyanate at 120 °C resulted in the formation of an equimolar mixture of the starting materials and expected products after 20 h.[82] The NHC–isothiocyanate dissociation process was found to be first order in adduct, zero order in isothiocyanate, and exhibited a positive $\Delta S^{\ddagger}$ (14 ± 3 cal/mol•K). These results lead us to believe that the aforementioned NHC–isothiocyanate exchange reaction proceeded via adduct dissociation followed by statistical recombination.

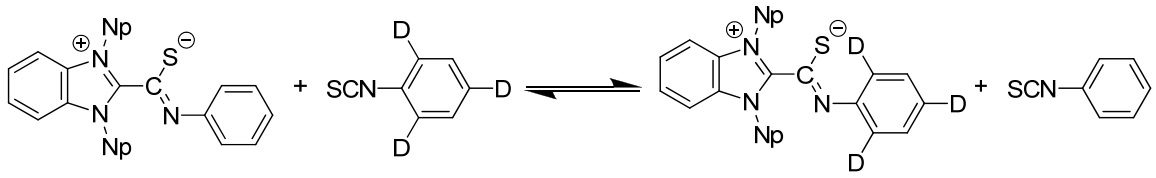

2.3 **2.4**

Figure 2.2 Exchange reaction of adduct **2.3** with deuterated phenyl isothiocyanate.

Building on these results, we next explored the feasibility of preparing structurally reversible polymers based on NHC–isothiocyanate coupling chemistry. Bis(NHC) **2.5** was selected as a suitable monomer because its reactive carbene moieties were connected via an extended π-system and it featured bulky alkyl N-substituents to enhance its solubility in organic solvents.[83] To form high polymer with electronically-delocalized structures, bis(isothiocyanate) fluorene derivative **2.6**,[84] which contains two n-hexyl chains at the 9-position to enhance solubility, was chosen as the complementary monomer.

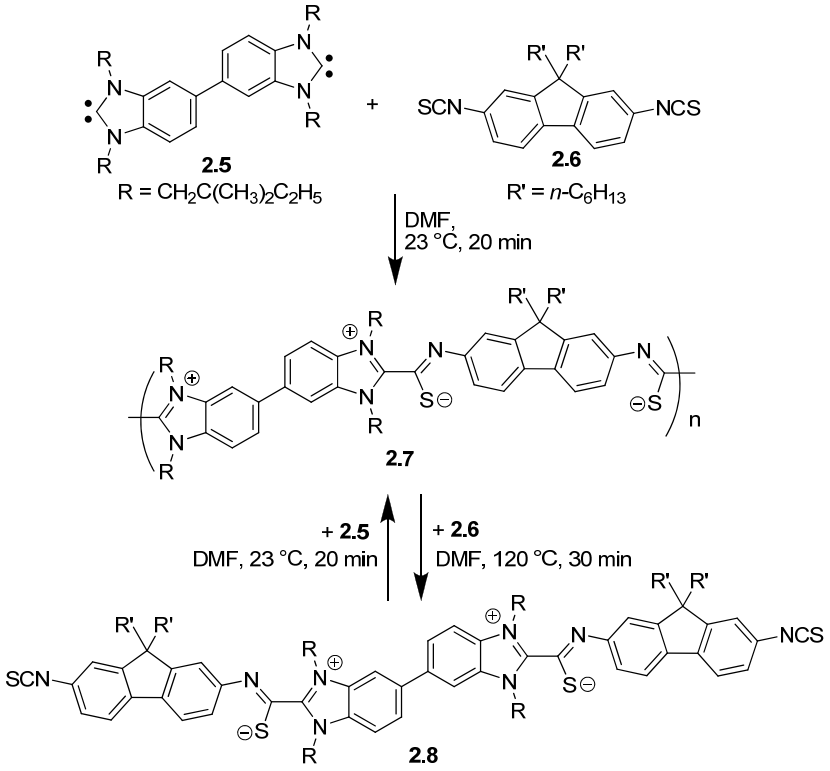

Scheme 2.1. Synthetic methodology used to form a structurally dynamic polymer derived from a bis(NHC) and various bis(isothiocyanate)s.

Addition of **2.5** to an equimolar quantity of **2.6** in DMF ($[\mathbf{2.5}]_0 + [\mathbf{2.6}]_0 = 0.2$ M) at ambient temperature resulted in the formation of a viscous solution within 20 min. Pouring the resulting mixture into excess diethyl ether caused polymer **2.7** to precipitate,

which was subsequently collected in 98% isolated yield via filtration. The polymer was found to be highly soluble in non-polar as well as polar organic solvents, which facilitated its characterization by NMR spectroscopy. Compared to its monomers, the diagnostic signals of **2.7** were shifted downfield and were in accord with the structure shown in Scheme 2.1. Analysis of **2.7** using gel permeation chromatography (GPC) (eluent = DMF with 0.1 M LiBr) revealed that this material exhibited a number average molecular weight85 (M_n) of 14.8 kDa and was polydisperse (PDI = 2.1), results typical for a step-growth polymerization. Relatively high molecular weight (MW) polymers (Mn values up to 29.0 kDa) were prepared by performing the aforementioned polymerization reactions at higher concentrations ([total monomer]$_0$ up to 0.8 M).

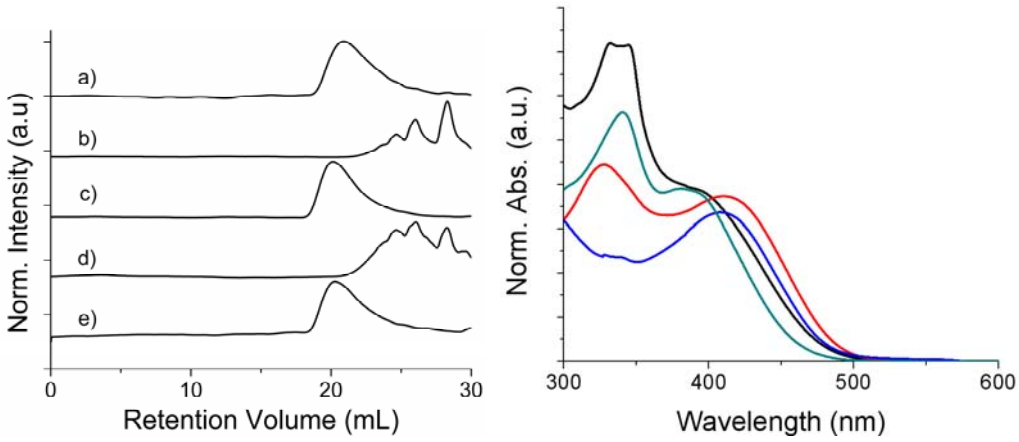

Figure 2.3. GPC and UV-vis of revesible polymerization (left) Gel permeation chromatograms (eluent:DMF containing 0.1 M LiBr; rate: 1.0 mL/min): a) polymer **2.7**; b) polymer **2.7** with 1.0 equiv of **2.6** (per repeat unit); c) solution obtained from (b) after the addition of 1.0 equiv. of **2.5** (per repeat unit); d) solution obtained from (c) after the addition of 1.0 equiv. of **2.6** (per repeat unit); e) solution obtained from (d) after the addition of 1 equiv. of **2.5** (per repeat unit). (right) UV-vis spectra of polymer **2.7** before (red) and after (black) the addition of 1.0 equiv of **2.6** (per repeat unit) as well as model compounds **2.8** (green) and **2.9** (blue) in DMF.

Next, the structurally dynamic characteristics of **2.7** were investigated.[86] Heating a DMF solution of this polymer (Mn = 14.8 kDa; PDI = 2.1) in the presence of 1.0 equiv of **2.6** (relative to the polymer's repeat unit) resulted in a significant decrease in the polymer's MW. Analysis of the crude reaction mixture by GPC reveaed a series of low MW peaks ranging from 1.5 to 6.1 kDa of which the predominant peak was attributed to **2.8** (isolated from the reaction mixture and compared to an authentic sample; see below). Subsequent addition of **2.5** to the aforementioned reaction mixture resulted in the reformation of polymer **2.7** with a M_n = 18.0 kDa (PDI = 2.9). Owing to the high fidelity of the NHC–isothiocyanate coupling reaction, these depolymerization / polymerization cycles were repeated multiple times on the same samples. Analogous results were obtained when **2.7** was depolymerized with **2.5** and then treated with **2.6** to re-established the formation of polymer.(see Figure 2.3)

In parallel with molecular weight measurements, the aforementioned depolymerization / polymerization reactions were monitored via UV–vis spectroscopy. Polymer **2.7** exhibited a λ_{max} = 410 nm (in DMF). However, upon depolymerization via treatment of **2.7** with excess **2.6**, as described above, this value shifted hypsochromically to 392 nm.(Figrue 2.3) Qualitatively, the longer λ_{max} of the polymer suggested that the effective conjugation length of these materials exceeded that of their lower MW analogues.

To gain additional insight into the electronic structure of this polymeric material, model compounds **2.8** and **2.9**, which approximate the two possible repeating units of **2.7**, were synthesized. The former was prepared by adding an excess (4.0 equiv) of **2.6** to a THF solution (14 mM) of **2.5**, followed by purification via column chromatography. As shown in Figure 2.4, compound **2.9** was prepared by treating 1,3-di(2,2-dimethylbutyl)benzimidazolium tetrafluoroborate with sodium tert-butoxide (to generate

the respective NHC in situ) in THF followed by the addition of 0.3 equiv of **2.6** in 30% overall yield. Analysis of **2.8** via UV-vis spectroscopy revealed a λmax at 382 nm (DMF), a result which indicated that its effective chromophore is shorter than that of **2.7** and was consistent with the aforementioned depolymerization experiments. In constrast, the UV-vis spectrum of **2.9** (λmax = 409 nm in DMF) was found to be similar to that of **2.7** which suggested to us that the polymer was effectively comprised of a series of these zwitterionic chromophores.

The relatively limited conjugation observed in **2.7** was attributed to the lack of planarity between the NCS and the NHC moieties. Indeed, the N–C–C–S dihedral angles found in known[87] X-ray crystal structures of NHC–isothiocyanate adducts range from 67.2 – 78.9°. Thus, although the structure of **2.7** is formally conjugated, limited π-overlap between monomer units that closely resemble model compound **2.9** constrain long-range electronic communication in this polymer. However, this restriction does not prohibit the materials' ability to conduct electrical charge. For example, while thin (5 μm) films of **2.7** were found to be non-conductive ($\sigma < 10^{-10}$ S/cm), exposure to iodine vapor increased the material's electrical conductivity to σ = 1.7 mS/cm, as determined using a four-point probe technique.[88] Currently we are investigating others dopants which could provide additional insight into the charge transfer mechanisms exhibited by these doped materials.[89]

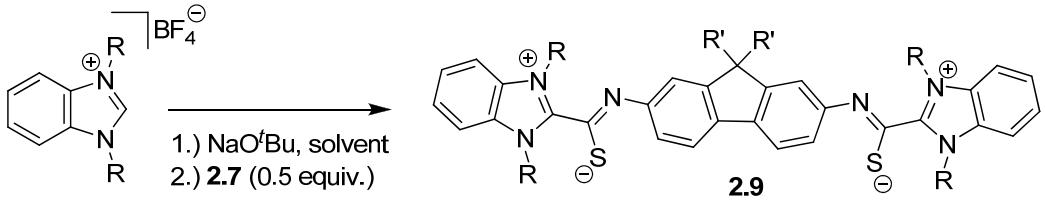

Figure 2.4. Syntheses of the model compound **2.9** used to evaluate the electronic structure of polymer **2.7**. R = $CH_2C(CH_3)_2C_2H_5$. R′ = n-C_6H_{13}.

CONCLUSION

In conclusion, we have developed a new class of aromatic polymers using NHC / isothiocyanate coupling chemistry. Simply combining bis(NHC)s with complementary bis(isothiocyanates)s produced polymers that were found to be structurally reversible. Moreover, these results effectively expand the utilities of free bis(NHC)s as polymer building blocks and creates a new design strategy for accessing polyelectrolytes with charges as integral components of their main chains.[90] Moreover, the polymerization reaction reported herein is one of the few examples where chemical unsaturation is maintained as monomer is converted to polymer and can be adapted into a system that will afford a structurally reversible, conjugated polymer. Efforts toward this goal will focus on increasing the effective conjugation length via planarization of the N–C–C–S dihedral angle in the aforementioned materials, principally via desymmetrization of the NHC's N-substituents, as well as through varying the electronic properties of the bis(NHC) and bis(isothiocyanate) monomers.

Chapter 3: N-Heterocyclic Carbene / Azide Coupling Chemistry as a New Polymerization Method: Access to a Novel Class of Aromatic Polytriazenes

INTRODUCTION

Aromatic polymers containing carbon-nitrogen double-bonds, such as poly(azomethine)s, have garnered tremendous interest across a range of scientific and engineering disciplines.[91] These polymers commonly exhibit high thermal stabilities[92] as well as good mechanical[93] and electronic properties, including second- and third-order nonlinear optical properties[94] and high electrical conductivities (upon doping).[95] Since these materials can also coordinate to a variety of transition metals and other electrophilic species, they are well-suited for use in applications ranging from catalysis to sensors.[92b, 96] In general, such polymers are prepared through condensation type polymerizations involving AA/BB monomers (typically: dialdehydes and diamines), although the high reactivity between primary amines and aldehydes often renders the polymerization reaction uncontrollable.[97] As a result, there is a need for the development of new polymerization methods, particularly those that are modular, for forming the aforementioned types of aromatic polymeric materials.

Recently, we reported a new method for forming C=N bonds that involves the combination of N-heterocyclic carbenes (NHCs)[45, 76, 98] with organic azides (see Figure 3.1 Eq. 1).[99] The reaction affords linear triazenes, tolerates wide variation of both of the NHC as well as azide coupling partners, and proceeds in nearly quantitative yield. Through a comprehensive study of the products of this reaction, it was determined that electronic delocalization across the triazene linkage was not only efficient, but tunable.[100] Furthermore, despite their relatively high nitrogen contents, the triazene products are thermally-stable. For example, derivatives possessing bulky N-substituents (e.g., tert-

butyl) were found to be stable in the solid-state to temperatures exceeding 150 °C. In many ways, the NHC / azide coupling reaction resembles the "click" cycloaddition reaction[101] which has found tremendous utility in the synthesis of macromolecular materials,[102] including conjugated polymers.[103] One clear distinction between the cycloaddition and the NHC/azide coupling reactions, however, is that the latter does not require the use of a catalyst which facilitates the isolation of pure products.

Collectively, the unique features of NHC/azide coupling reaction poise it for use in synthetic polymer chemistry,[104] particularly for accessing aromatic polymers containing C=N bonds. We envisioned combining difunctional NHCs (**3.1**) with complementary difunctional azides (**3.2**) to create polytriazenes (**3.3**) that exhibit electronically delocalized structures (see Figure 3.1 Eq. 2).

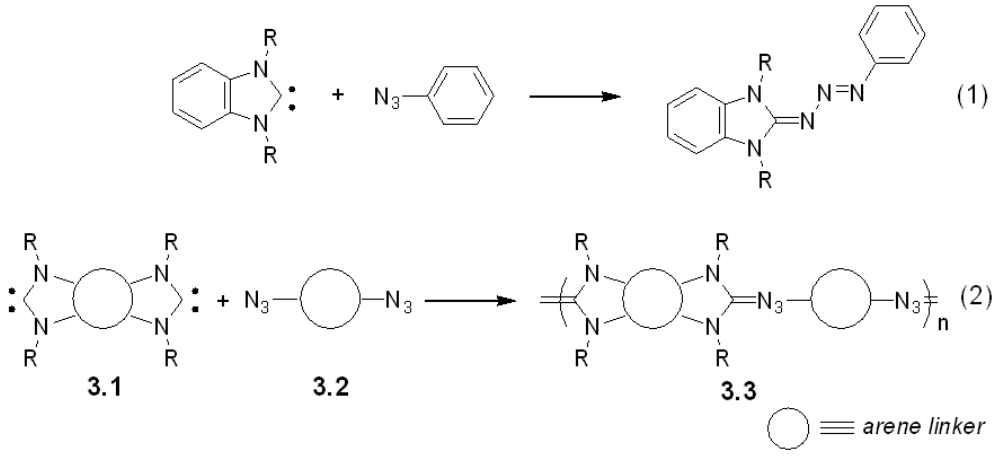

Figure 3.1 Triazene formation and polymerization with "bis"functional monomers

The structures of various bis(NHC)s (**3.1**) and bis(azide)s (**3.2**) that were studied as potential monomers are shown in Figure 3.1. The bis(NHC)s were prepared from their respective tetraamines followed by formylative cyclization and deprotonation, in accord with published procedures.[58, 80c] The N-substituents featured in these monomers were chosen to enhance the solubilities of the respective polymers as well as probe their effects

on the thermal properties exhibited by their respective polymers (see below).[105] To maximize the formation of conjugated bonds in their respective polymers, bis(aryl azide)s were studied exclusively. In particular, 1,4-diazidobenzene (**3.7**) as well as 4,4′-diazidobiphenyl (**3.8**) were synthesized. Considering CPs containing fluorene have found utility in display devices,[84] a 2,7-diazido derivative (**3.9**) which features two hexyl chains at the 9-position to enhance stability toward photooxidation as well as solubility was also studied.

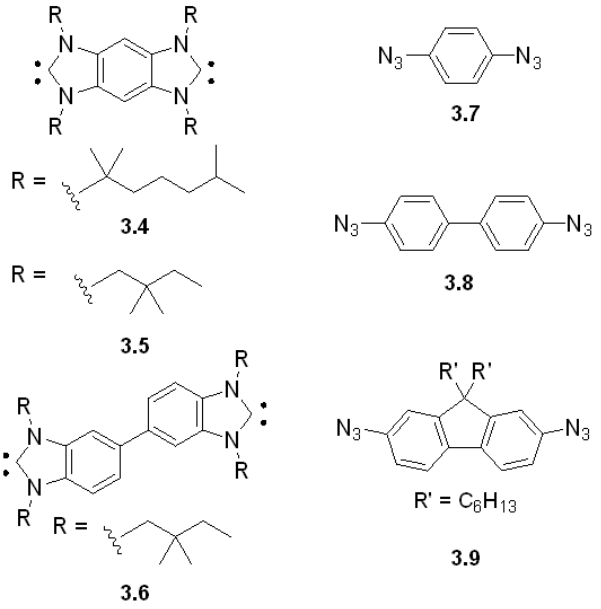

Figure 3.2. Structures of bis(NHCs)s **3.4**-**3.6** and bis(azide)s **3.7**-**3.9** explored in this study.

RESULTS AND DISCUSSION

In an initial experiment, bis(NHC) **3.4** was added to an equimolar quantity of bis(azide) **3.7** in $CDCl_3$ ($[\text{total monomer}]_0$ = 0.1 M) and then stirred at ambient temperature. Gratifyingly, the expected polymer **3.10** was observed by ^{1}H NMR spectroscopy shortly after the monomers were combined, as evidenced by the

development of broad signals that were shifted downfield. Polymer formation was monitored over time by integrating signals diagnostic of **3.7** (δ = 7.00 ppm) to its analogous signals found in the repeats units of **3.10** (7.58 ppm). Furthermore, by comparing signals attributed to the end-groups of **3.10** (terminal triazene Ar-H, δ = 7.05 ppm) to signals associated with its main chain, the number-average molecular weight (M_n) of the polymer was calculated. After 24 h, the reaction appeared to be complete, producing a polymer with a M_n = 29.4 kDa.[106]

Once the polymerization was complete, the reaction mixture was poured into an excess of pentanes which is a poor solvent for the polymer but a good solvent for its respective monomers. The precipitated solids were then collected and dried under high vacuum to afford **3.10** in 92% isolated yield. Analysis of the polymer by gel permeation chromatography revealed an absolute M_n = 31.8 kDa and a broad polydispersity (PDI = 1.8), as expected for a step-growth polymerization (see Figure 3.3). As a testament to its high purity, the elemental composition of **3.10** (72.95; H, 10.04; N, 17.01) was found to be in good agreement with its calculated values (C, 72.67; H, 10.24; N 17.09).

As summarized in Table 3.1, a series of analogous polymerizations were performed using various combinations of bis(NHC)s **3.1** and bis(azide)s **3.2**. Each of these reactions were run for 24 h in THF or $CHCl_3$ and then poured into pentanes, which caused the respective polymers to precipitate, facilitating their isolation. The structures of the polytriazenes obtained from these reactions were confirmed by NMR spectroscopy. Their NMR-derived M_ns ranged from 27.7 to 29.4 kDa and were similar with those obtained via GPC. In general, polymerizations involving **3.4** produced higher molecular

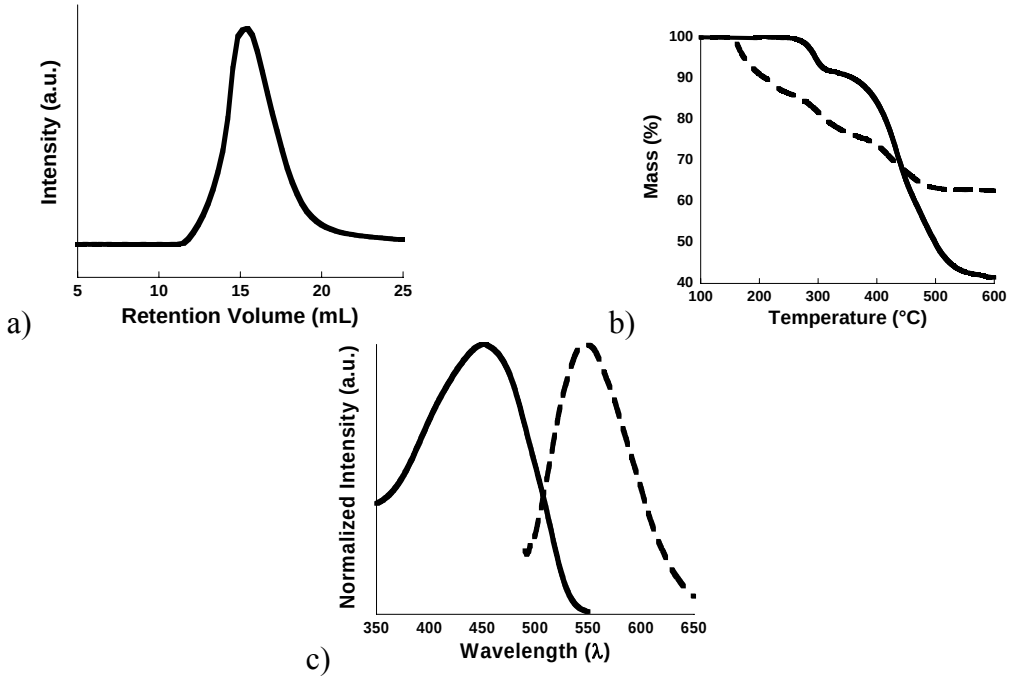

Figure 3.3. GPC and TGA of **3.10** and UV-vis/emission of **3.12**. (a)Gel permeation chromatogram of **3.10**. Conditions: 40 °C, THF / pyridine (9 : 1) as eluent, 1 mL/min. (b) Thermogravigrams of **3.10** (dotted line) and **3.10** (solid line). Conditions: 10 °C/min, nitrogen atmosphere. (c) Normalized absorption (solid line) and emission (dotted line) spectra for **3.12** in THF.

weight (MW) polymers than analogous reactions involving **3.5**. The difference may be explained by the reduced conformational freedom associated with the former monomer (and thus reducing chances for MW limiting cyclization and related side-reactions). Polymers **3.10-3.18** were of high purity, as determined by elemental analysis, and displayed good solubilities in common organic solvents.

Upon synthesis, the thermal stabilities of **3.10-3.18** were evaluated using thermogravimetric analysis (TGA). Despite the relatively large amount of nitrogen present in the main chains of these materials, they were found to be thermally-stable and exhibited decomposition temperatures (T_d) that were dependent on their structures. For example, the T_d of **3.10**, which features tertiary N-substitutents, was found to occur 154 °C (see Figure 2b); in contrast, **3.16** which features primary N-alkyl groups did not

decompose until 282 °C. In this latter material, the first decomposition proceeded with a mass loss equal to two units of molecular nitrogen (N_2) (~7%) as previously observed for analogous small molecules.[107] Likewise, the thermal decomposion of **3.10** presumably affords the respective polyguanidine which is stable to >300 °C.

Finally, efforts shifted toward examining the electronic and photophysical properties of **3.10-3.18**. In THF, their absorption λ_{max} ranged between = 379 and 485 nm depending on their structure. Polymers prepared from 1,4-diazidobenzene (**3.7**) absorbed at longer wavelengths compared to those prepared from **3.8** or **3.9**. Furthermore, the λ_{max} of a relatively low MW **3.10** (M_n = 5.0 kDa, λ_{max} = 450 nm)[108] was hypsochromically-shifted relative to a high MW analogue (M_n = 29.4 kDa, λ_{max} = 485 nm), indicating that the polymer's electronic properties was dependent on its size. Collectively, this data suggests that these polymers exhibit electronically-delocalized structures. Polymers **3.12** and **3.18**, which contain fluorenyl units in their main chains, exhibited λ_{em} = 546 nm in THF (ϕ = 0.2%) (see Figure 3.3). Polymer **3.10** was found to exhibit an irreversible oxidation at $E_{1/2}$ = +0.15 V (versus SCE) via cyclic voltammetry.[109] Prompted by this result, the polymer was spin-coated onto a glass slide and tested for electrical conductivity using a multi-point probe station.[110] Although virgin films were found to be insulating ($\sigma < 10^{-10}$ S/cm), they were rendered conductive ($\sigma = 4 \times 10^{-3}$ S/cm) after exposure to iodine vapor for 24 h.

CONCLUSION

In conclusion, we have developed a novel, efficient, and practical route to a new class of polymers using NHC / azide coupling chemistry. Simple combination of bis(NHC)s with complementary bis(aryl azide)s produced aromatic polytriazenes that exhibited good optical and electronic properties, high thermal stabilities, and high solubilities in common organic solvents. To the best of our knowledge, this is the

Table 3.1. Key properties of the polytriazenes prepared from the monomers indicated.

polymer	yield[b] (%)	Mn, NMR[c] (kDa)	Mn, GPC[d] (kDa)	PDI	Td[e] (°C)	λmax[f] (nm)
3.10 (3.4 + 2a)	98	29.4	34.8	1.8	154	485
3.11 (3.4 + 3.8)	95	24.6	27.5	1.6	157	434
3.12 (3.4 + 3.9)	76	21.5	23.9	1.8	160	450
3.15 (3.5 + 3.9)	81	8.3	17.6	1.6	262	476
3.16 (3.6 + 3.7)	96	22.1	27.6	2.3	282	437
3.17 (3.6 + 3.8)	95	20.3	22.7	2.3	282	379
3.18 (3.6 + 3.9)	72	17.7	19.9	1.9	278	436

All polymerization reactions were performed in either THF or $CHCl_3$ using equimolar quantities of monomers **3.1** and **3.2** (total initial concentration of monomer = 0.1 M). [b] Isolated yields of the products were obtained after precipitation into pentanes. Polymers containing **3.9** were partially soluble in pentanes which resulted lower isolated yields. Monomer conversion to polymer, as determined by ^{1}H NMR spectroscopy, was quantitative. [c] Determined via end-group analysis; see text. [d] Performed using THF : pyridine as the eluent (9 : 1) at 40 °C using light scattering, refractive index, and viscometry detectors. [e] Performed under an atmosphere of nitrogen at a scan rate = 10 °C/min. [f] UV/vis spectra were recorded in THF at ambient temperature.

first example of using free bis(NHC)s as polymer building blocks and effectively opens a new design strategy in synthetic polymer chemistry for accessing aromatic polymers containing carbon-nitrogen double-bonds. Considering the large number of methods known for modifying the structures and electronic properties of NHCs as well as organic azides, the method and polymers reported herein are well suited for adaptation and use in a variety of electronic and opto-electronic applications.

Chapter 4: Ionic Dithioester-Based RAFT Agents Derived From N-Heterocyclic Carbenes

INTRODUCTION

Over the past 15 years, controlled radical polymerizations (CRP),[111] such as atom transfer radical polymerization,[71] nitroxide mediated polymerization[Error! Bookmark not defined.] and reversible addition-fragmentation chain transfer (RAFT) polymerization,[112] have emerged as powerful methods for preparing polymeric materials with pre-determined molecular weights and low polydispersities.[113] Since initial reports[114] in the late 1990s, RAFT and related[115] polymerizations have experienced tremendous growth. As a result of their versatility and compatibility with a broad range of monomers and solvents, these techniques have found utility in many facets of macromolecular chemistry, including aqueous polymerizations and the synthesis of advanced materials with useful functions. [116,117]

RAFT polymerizations typically employ specialized chain transfer agents (CTAs)[118] that facilitate the transfer of relatively few propagating radical species amongst many growing polymer chains.[119] As a result, deleterious bimolecular termination pathways are effectively minimized, which enables all chains to grow in a uniform fashion. Of the various types of CTAs known, which include trithiocarbonates, dithiocarbamates, xanthates, and dithioesters, the latter have been used extensively. Effective dithioester-based RAFT agents with the general structure S=C(Z)-SR share two design features: (1) benzyl, cumyl, 2-cyanopropyl, or other R groups that afford a stable radical upon undergoing homolytic cleavage from the dithio moiety[120] while still retaining sufficient reactivity to facilitate polymerization and (2) a Z group that balances sufficient electrophilicity toward radical addition with efficient fragmentation, ultimately

governing polymerization activity.[121] In general, RAFT agents with electron-rich Z groups facilitate fragmentation but disfavor radical addition, a feature that has found utility in polymerizing vinyl acetate.[122] In contrast, electron-deficient Z groups favor radical addition but afford highly stable intermediates that resist fragmentation and/or termination, which often leads to relatively long polymerization reactions. Since the general features required to facilitate radical addition oppose those required for efficient fragmentation, the key to an active and broadly useful RAFT agent is to find a Z group that offers an optimal balance. Dithiobenzoates are excellent examples because aryl Z groups (particularly Z = phenyl) balance radical stability with propensity toward fragmentation; as such, they currently offer control over a wide range of monomers.[112,118,119]

As illustrated in Figure 4.1, we envisioned a 2-carbodithioimidazolium salt capable of intermittently delocalizing positive charge onto the dithioester moiety through conformational change. In particular, coplanarization of the dithioester and imidazolium moieties should result in a system with a low energy LUMO suitable for radical addition.

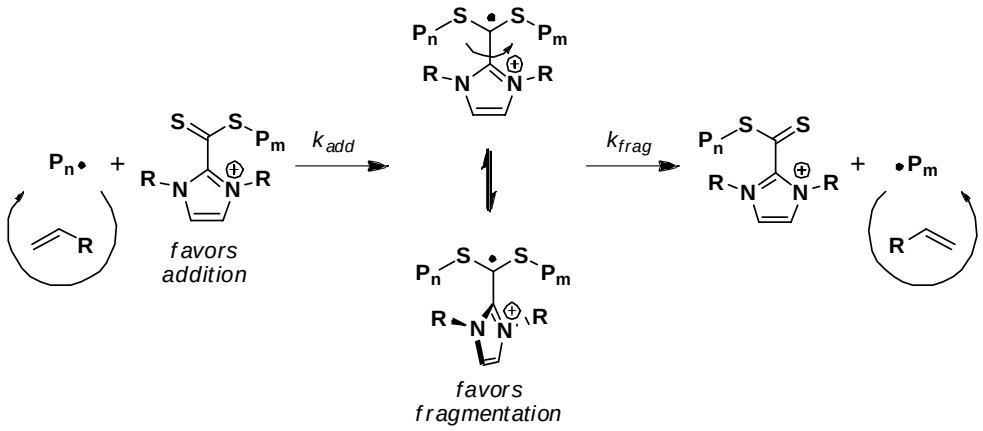

Figure 4.1 Proposed mechanism of cationic dithioesters to control radical transfer processes in RAFT polymerizations. Counter-anions have been omitted for clarity

Since the resulting radical species is pseudo-benzylic, it should be relatively stable. However, rotation about the imidazolium-dithioester bond should effectively diminish electronic communication between these two groups and afford a relatively destabilized radical species primed for fragmentation. Considering the rotational barrier will be influenced by sterics, we ultimately envision fine tuning these processes by varying the size of the N-substituents. Herein, we disclose our initial results toward realizing this concept. In particular, the synthesis of two new dithioester-based RAFT agents containing imidazolium Z groups and their potential in controlling free radical polymerizations are described. A fundamental corollary of our investigation was to explore the effect of placing a positive charge in close proximity to the dithioester moiety on polymerization activity which, to the best of our knowledge, has not been previously studied in detail.[123]

RESULTS AND DISCUSSION

Syntheses of the aforementioned imidazolium-based dithioesters are summarized in Scheme **4.2** and capitalize on the chemistry of N-heterocyclic carbenes,[76, 124] a versatile class of compounds finding tremendous utility in catalysis[125] and polymer synthesis.[54, 58, 104,126] Furthermore, a large number of synthetic methods are known that enable straightforward modulation of the N-substituents as well as other structural features of the N-heterocycle.[124] Treatment of commercially-available 1,3-dimesitylimidazolylidene (**4.1**) with excess carbon disulfide in tetrahydrofuran (THF) afforded inner salt **4.2** in 99% yield after 2 h at ambient temperature.[127] Subsequent alkylation of **4.2** with benzyl bromide at 85 °C in acetonitrile afforded benzyl 1,3-dimesitylimidazolium-2-carbodithioate bromide (4.3) in 93% yield.

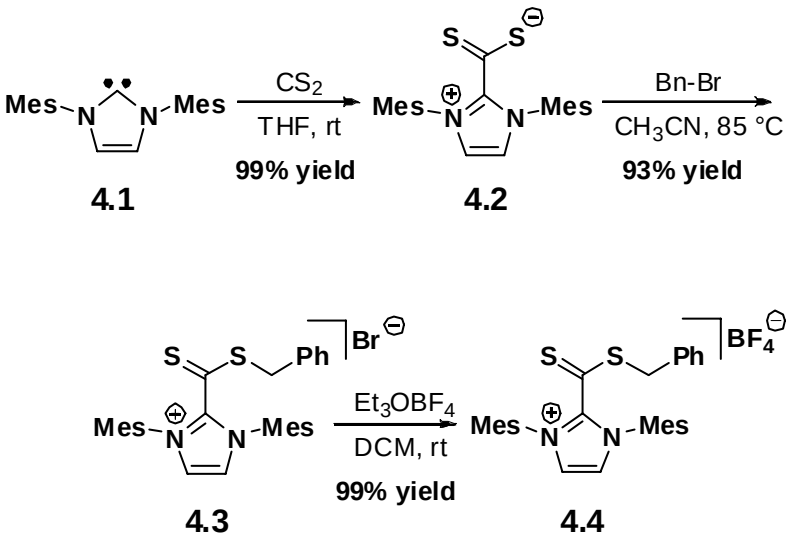

Scheme 4.1 Synthesis of ionic RAFT agents **4.3** and **4.4**. Mes = 2,4,6-trimethylphenyl. rt = room temperature

To confirm the molecular structure of **4.3**, a crystal was grown by slow evaporation of a saturated ethyl acetate solution and analyzed by X-ray diffraction. As shown in the ORTEP diagram in Figure 4.2, the dithioester moiety is nearly orthogonal to the plane of the imidazolium species (avg. abs. N-C-C-S ≈ 71°). This observation suggested to us that electronic communication between the dithioester and imidazolium moieties was restricted in the solid-state. However, the rotational barrier about the dithioester-imidazolium bond in **4.3** was calculated[128] to be less than 7 kcal/mol, suggesting that an appreciable population of the coplanar conformation should exist at room temperature in solution.

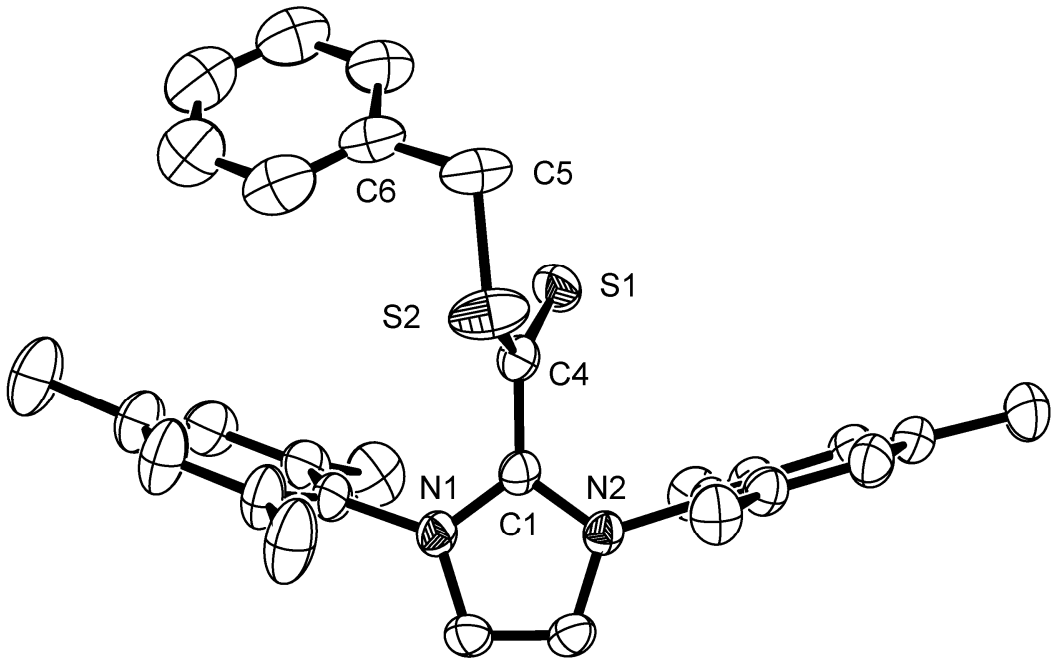

Figure 4.2 ORTEP diagram of **4.3**. Hydrogen atoms, solvent molecules, and counterions have been removed for clarity. Ellipsoids were drawn at the 50% probability level. Selected distances (Å) and angles (°): N1-C1, 1.339(4); N2-C1, 1.344(4); C1-C4, 1.484(4); S1-C4, 1.623(6); S2-C4, 1.703(5); S2-C5, 1.804(6); N1-C1-N2, 107.9(2); C1-C4-S1, 121.0(4); S1-C4-S2, 125.6(5); C4-S2-C5, 103.9(4); C6-C5-S2, 114.2(11); N1-C1-C4-S1, -114.5(7); N1-C1-C4-S2, 74.2(6); N2-C1-C4-S1, 68.7(7); N2-C1-C4-S2, -102.6(6); C1-C4-S2-C5, -173.0(10); C4-S2-C5-C6, 76.6(8)

Upon synthesis and characterization of **4.3**, efforts were directed toward exploring the ability of this compound to mediate the polymerization of styrene.[129] Initially, 0.96 mmol of **4.3** and 0.19 mmol of 2,2′-azobisisobutyronitrile (AIBN) were dissolved in 1.1 mL of degassed styrene (monomer : CTA : AIBN = 200 : 5 : 1). To monitor monomer conversion, a small amount of an internal standard (i.e., 1,2,3-trimethoxybenzene) was included in the reaction mixture. After heating at 110 °C under an atmosphere of nitrogen three days, no polymer was observed by ^{1}H NMR analysis of the crude reaction mixture which indicated to us that **4.3** was highly effective at limiting propagating radical species.[130] To facilitate polymerization, the CTA : AIBN ratio was reduced to 1 : 1 and

the aforementioned polymerization experiment was repeated. After 24 h at 110 °C, 87% of monomer was consumed and a polystyrene with a number average molecular weight (Mn) of 19.1 kDa, as determined by gel permeation chromatography,[131] was obtained and in good agreement with its theoretical molecular weight of 18.7 kDa.[132] Unfortunately, the chromatograms of these polymers showed significant tailing and bimodal distributions were observed at higher conversions. To circumvent these deleterious issues, polymerizations were attempted at lower temperatures but were ultimately hampered by the poor solubility of **4.3** in styrene.

Considering the complementary reactivity of the nucleophilic bromide anion and the eletrophilic benzyl group in **4.3**, we surmised that this compound most likely decomposed via an SN_2-type process over the course of the polymerization reaction. To investigate, solutions of **4.3** were heated to 100 °C in either DMSO-d_6 or chlorobenzene,[133] and monitored over time by ^{1}H NMR spectroscopy. Although **4.3** was found to decompose in both solvents, the relative decomposition rates were highly dependent on the solvent polarity. For example, in DMSO-d_6, **4.3** was found to fully decompose within 3 h, but required > 20 h in chlorobenzene to achieve complete decomposition. Extrapolating this reactivity, we suspect the decomposition of **4.3** would proceed even slower in bulk styrene, a relatively non-polar solvent that disfavors SN_2-type reactions. However, the limited solubility of this compound in less polar solvents (i.e., C_6D_6 or toluene-d_8) prevented verification of this hypothesis.

In an effort to minimize decomposition, the nucleophilic bromide counteranion was exchanged for a tetrafluoroborate via anion metathesis. This transformation was accomplished by treating a CH_2Cl_2 solution of **4.3** with a stoichiometric amount of triethyloxonium tetrafluoroborate at room temperature,[134] which afforded **4.4** as a pink powder in >99% yield. Gratifyingly, compound **4.4** showed improved solubilities in

non-polar organic solvents, including styrene, and exhibited no signs of decomposition in a variety of organic solvents (chlorobenzene, $CDCl_3$, or toluene) at 100 °C for at least 48 h. In DMSO, however, approximately 15% of **4.4** was found to decompose over the same period of time.

Encouraged by these favorable physical and thermal properties, CTA **4.4** was explored for its ability to mediate the polymerization of styrene. Using reaction conditions similar to those described above (i.e., styrene : **4.4** : AIBN = 200 : 1 : 1), a polystyrene with a number average molecular weight (M_n) of 19.6 kDa and a polydispersity index (PDI) of 1.26 was obtained in 84% yield after 22 h at 70 °C. The experimentally-determined M_n was in good agreement with its theoretical value of 18.7 kDa, which was based on monomer conversion and complete incorporation of **4.4** into growing polymer.[132] To gain support for the latter, we capitalized on the BF_4 counteranion associated with **4.4**, which presumably should also be associated with its respective polymer. Analysis of the aforementioned polymer by ^{19}F NMR spectroscopy revealed two distinct singlets at $\delta = -152.6$ and -152.7 ppm in a 1 : 4 ratio, respectively, which were in accord with the isotopic distribution of boron and at similar chemical shifts as those exhibited by **4.4**. A solution of this polymer was then spiked with a known quantity of 1,2,4,5-tetrafluorobenzene ($\delta = -138.7$ ppm), and the mixture was analyzed using ^{19}F NMR spectroscopy. Integrating the ^{19}F NMR signals attributed to the standard relative to those of derived from the BF_4 revealed that these two species were present a ratio of 55 : 45, respectively. Using the known concentration of the standard, the M_n of the polymer was calculated to be 16.6 kDa which is in good agreement with the value obtained by GPC. In other words, using this method, there appears to be approximately one unit of **4.4** on the terminus of each polymer chain.

An ability to prepare well-defined polymers with relatively low CTA : AIBN ratios was unusual since RAFT polymerizations typically employ ratios of up to 10 : 1 in order to maintain control. Despite this low ratio, key characteristics of a controlled/"living" polymerization were observed. For example, as shown in Figure 4.3, monitoring a bulk polymerization of styrene mediated by **4.4** using a CTA : AIBN = 1 : 1 revealed: (A) pseudo-first order kinetics with respect to monomer as evidenced by the linear correlation between the log monomer concentration and time, (B) a linear relationship between polymer molecular weight and monomer conversion whilst polydispersity remained low (< 1.3). Representative GPC chromatograms for this polymerization reaction are shown in Figure 4.3C.

Considering AIBN decomposes into two isobutyrylnitrile radicals, the aforementioned results suggested to us that a single unit of 5.4 is capable of mediating multiple radical species. This unique ability may be at least partially explained by highly favored radical addition to **4.4** coupled with efficient fragmentation. To gain additional insight into this process, the chain transfer constant (Ctr), which reflects the ability of the CTA to facilitate radical addition, was determined by ^{1}H NMR analysis to be 22 (Figure 4.3D).[120] This Ctr value is similar to that derived for dibenzyl trithiocarbonate,[121] an effective CTA for mediating RAFT polymerizations. Hence, to rationalize the results observed, we surmise that **4.4** exhibits higher absolute rates of addition and fragmentation than benzyl dithiobenzoate.

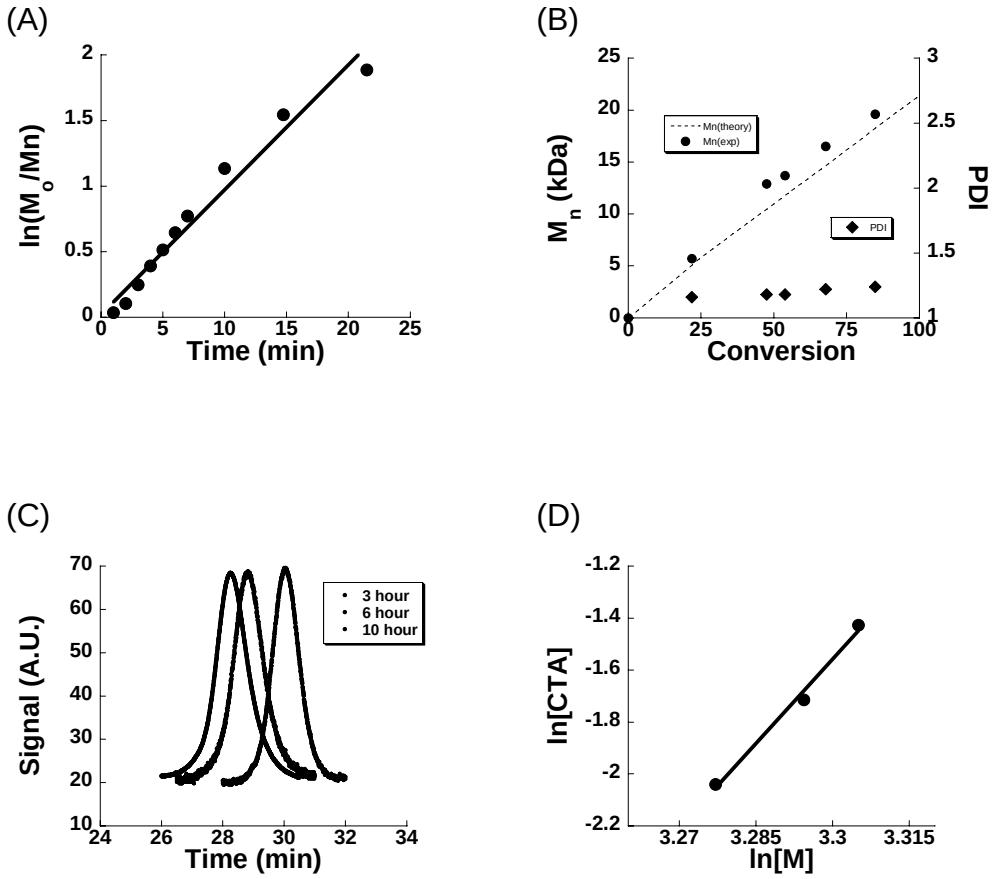

Figure 4.3 Kinetic measurments for the polymerization of styrene with **4.3**. (A) Plot of log monomer concentration versus time. (B) Plot of experimentally determined Mn, and PDI versus monomer conversion. (C) GPC chromatograms taken at 4, 7 and 10 h. (D) Double log plot of [RAFT agent] vs [Monomer] used for determination of Ctr (22) through calculation of slope. The slope value was found to be 22, which is also the Ctr. Conditions: $[\mathbf{4.3}]_0$ = 48 mM, $[AIBN]_0$ = 48 mM, $[mesitylene]_0$ = 20 mM (internal standard), bulk styrene, 70 °C (monomer : CTA : AIBN = 200 : 1 : 1).

CONCLUSIONS

In summary, we have synthesized two new ionic dithioester-based chain transfer agents (CTAs) and studied their abilities to mediate free radical polymerizations. Starting with a commercially-available N-heterocyclic carbene, the syntheses of these agents was accomplished in up to three high yielding steps that required only straightforward filtration techniques for isolation.[135] These compounds were found to be

effective for preparing well-defined polystyrenes at relatively low CTA loadings and temperatures. Considering the breadth of imidazole chemistry, the methodology reported herein should facilitate rapid access to RAFT agents that are highly functionalized or exhibit tunable activities through judicious N-substitution, electronic modulation of the N-heterocyclic carbene component, or variation of the counteranion. Efforts along these lines are in progress and will be reported in due course.

Chapter 5: Evaluating the Role of Additive pKa on the Proton Conductivities of Blended Sulfonated Poly(Ether Ether Ketone) Membranes

INTRODUCTION

Nafion is a sulfonated tetrafluorethylene copolymer that is commonly used in proton exchange membranes (PEMs) as a result of its remarkable proton conductivities (i.e., 5 x 10^{-2} S cm^{-1} at 23 °C), high thermal stabilities, and excellent mechanical properties.[136,137] Unfortunately, Nafion-based membranes suffer from a number of drawbacks that complicates its use as PEMs in fuel cells and in other applications. In particular, the operation of this material is dependent upon water for proton transport. This necessitates operating temperatures below 100 °C and, at this temperature, the platinum catalyst used as part of the anode in fuel cells is inevitably poisoned.[138,139,140,141,142,143144] Additionally, Nafion suffers from a high permeability of methanol which not only wastes fuel but also ultimately leads to poisoning of the cathode catalyst.

To overcome these limitations, a number of other polymeric materials have been explored as alternatives to Nafion, including polybenzimidazoles,[139] sulfonated polystyrene,[140] sulfonated polysulfones (sPSf),[141] and sulfonated poly(ether ether ketones) (sPEEK). While membranes based on these polymers generally exhibit relatively lower proton conductivities compared to Nafion, it has been shown that blending aromatic heterocycles, such as imidazole, with sPSf or sPEEK greatly enhances the proton conductivities of the respective blended membranes.[138] These increased proton conductivities are believed to be the result of acid-base interactions between the

acidic sulfonic groups appended to the polymer backbones and the basic imidazole functionalities, a process that ultimately facilitates proton transport through the membrane.[143] With these results in mind, we hypothesized that the pKa of the added heterocycle should significantly affect the proton conductivities of the aforementioned blended membranes, and therefore studying this relationship could provide unique fundamental insights into important equilibrium processes which affect the proton conductivity of membranes used in fuel cells and other applications.

In this study, a series of sPEEK membranes were blended with various heterocycles having pKa values ranging from 5.75 to 14.9 and characterized by various proton conductivity measurements as a function of temperature. We note that the studies presented here were designed to gain a fundamental understanding of the importance of acid-base interactions occurring between acidic polymers and the heterocycles, and were not meant to be replicated into fully functional fuel cells as it has been previously shown that imidazoles can poison the electrode catalyst.[145,146] However, information gained from these studies can be expected to guide the development of new membrane polymers that contain heterocycles appended to them.

RESULTS AND DISCUSSION

Measurement of the Ion Exchange Capacities (IEC) of sPEEK Membranes Blended with Various Heterocycles. Four different heterocycles, whose pKa values ranged from 5.75 to 14.9 (in water), were selected to be blended with sPEEK and studied for their abilities to modulate the proton conductivity exhibited by the resulting membrane. These heterocycles include: imidazole, benzimidazole, 4-nitroimidazole, and 4,5-dicyanoimidazole. Upon synthesis, the proton conductivities of the blended membranes were evaluated using an impedance analyzer under anhydrous conditions.

Table 1 compares the ion exchange capacities (IEC) of the blended membranes consisting of various quantities of the aforementioned heterocycles. Regardless of the quantity of the heterocycle added, the measured IEC values of the blended membranes were found to be lower than that of the plain sPEEK (IEC = 1.75). Furthermore, the measured IEC values (1) increased inversely with the pKa value of heterocycle added and (2) decreased as larger quantities of heterocycle were employed. These results are consistent with the occurrence of acid-base interactions in the blend membranes. Furthermore, these results also suggest that the concentration of proton ions can be modified by changing the quantity of heterocycle added to the membrane (see below).

molar ratio of SO_3H: heterocycle	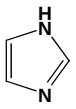	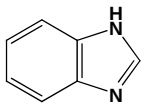	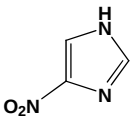	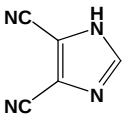
	pKa = 14.9	12.5	8.93	5.75
10.7	1.08	1.16	1.32	1.56
7.7	1.01	1.13	1.26	1.46
5.4	0.95	1.05	1.17	1.42

Table 5.1. Ion exchange capacities (IEC) of a range of sPEEK/heterocycle blend membranes with various [SO_3H]/[heterocycle] mole ratios. The IEC value for pure sPEEK is 1.75.

Proton conductivities of sPEEK membranes blended with various heterocycles at the same concentration. After measuring the IECs of the blended membranes, subsequent efforts focused on measuring their proton conductivities as a function of temperature. Shown in Figure 5.1 are plots of proton conductivity as a function of temperature for each membrane as well as plain sPEEK (with no added heterocycle) as a control. The data

shown indicates that proton conductivity of the plain sPEEK membrane decreases with increasing temperature, presumably due to the decreasing amount of water present in the membrane, which is the proton transfer medium. However, with the addition of a heterocycle, the proton conductivities of the blend membranes exhibit higher proton conductivities than plain sPEEK. A plausible explanation for this result is that the nitrogen atoms on the heterocycles can facilitate a proton transfer by acting as proton donors and acceptors between the sulfonic acid groups on the sPEEK[143] This is further supported by results presented below which show an increase in the membranes proton conductivity when the concentration of the heterocycle is increased.

In addition, it was found that the acidity of the imidazole plays an important role in the conductivity profile of the membranes. By closely studying the profiles (see Figure 5.1), several interesting trends emerge. First, all of the membranes containing a heterocycle showed an increase in proton conductivity at lower temperatures followed by a decreasing trend in proton conductivity at higher temperatures. Second, the relative temperature at which conductivity peaks can be correlated to the pKa of the heterocycle added to the membrane. Finally, the high temperature conductivity of the membranes exhibits a direct relationship to the pKa of the heterocycle.

Proton Conductivities of sPEEK Membranes Blended with Heterocycles at Different Concentrations. Since the amount of water present in membranes is often inversely related to temperature, we anticipated that the lack of water may be compensated by an increased concentration of heterocycle. Thus, proton conductivity of the aforementioned sPEEK membranes should scale with the concentration of heterocycle added. To explore this possibility, sPEEK membranes with different amounts of heterocycle were prepared. Using the procedure described above, three unique membranes containing polymer SO_3H : imidazole molar ratios = 5.5, 7.7, and

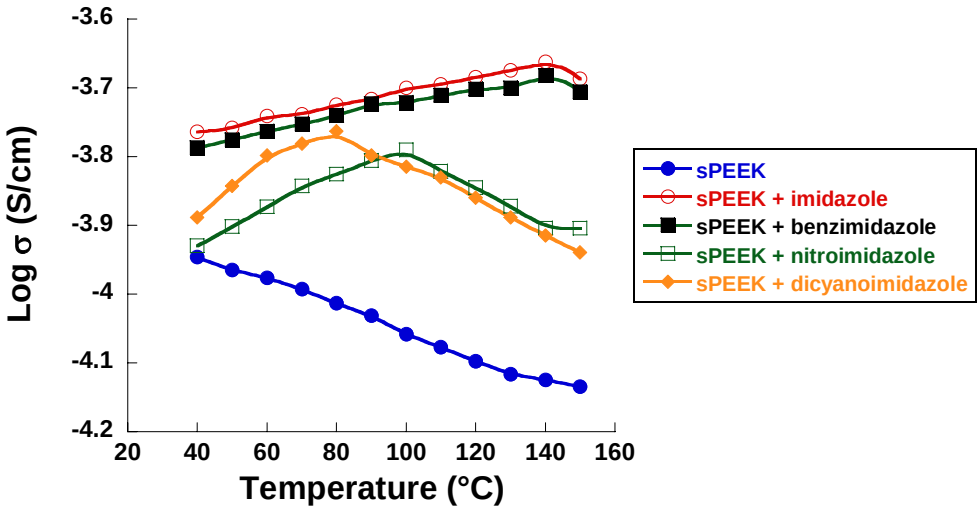

Figure 5.1. Proton conductivities exhibited by the sPEEK/heterocycle blend membranes as a function of temperature.

10.7 were prepared and their respective proton conductivities were measured as described above. As shown in Figure 5.2 (left), proton conductivities increased with the amount of heterocycle added, as expected for a membrane which transports protons via a vehicle mechanism. Similar results were observed when an analogous series of membranes were prepared using 4,5-dicyanoimidazole, a relatively acidic heterocycle, and tested (see Figure 5.2, right). While proton conductivities of the membranes containing imidazole as the additive increased as a function of temperature, membranes containing 4,5-dicyanoimidazole showed the opposite trends.

MECHANISTIC ORIGINS OF RESULTS. To explore the origin of the above results further, we considered a mechanistic model. In the dehumidified system of a polyacid doped with a small amount of mobile bases, we hypothesized that the primary contribution to proton transport would be through the diffusion of positively charged basic groups (vehicular mechanism).

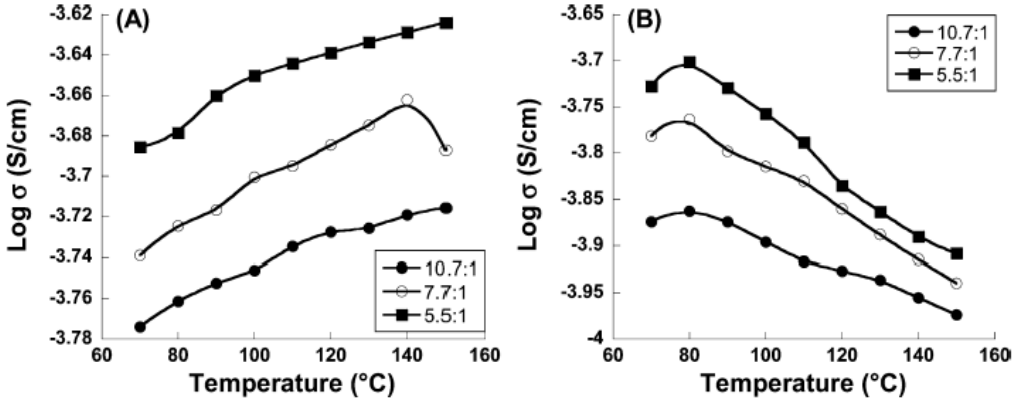

Figure 5.2. Variations of the proton conductivities of sPEEK/N-heterocycle; sPEEK/imidazole (A) and sPEEK/4,5-dicyanoimidazole (B) membranes with temperature at various volumes of the heterocycle. The ratio of $[SO_3H]$:[heterocycle] employed for each membrane studied are indicated in the embedded legends.

The conductivity σ(T) of such a system at low concentration of the base groups can then be expressed as:

$$\sigma(T) = \frac{eD_b^+(T)}{k_B T}\rho_b^+(T) \quad \text{eq. 5.2}$$

where e is the electron (proton) charge and D_b^+(T) represents the diffusion coefficient of charged base groups, ρ_b^+(T) denotes the density of the base groups. In the above system, D_b^+(T) is expected to be a weakly increasing function of temperature T, in which case the temperature dependence of the conductivity σ(T) noted in the aforementioned experiments can be expected to arise mainly from the temperature dependency of the charged base groups density ρ_b^+(T) .

The temperature dependence of ρ_b^+(T) arises from the interplay of two competing chemical reactions: proton exchange between the acid and base, and association of these same two components via hydrogen bonding (see Scheme 5.1):

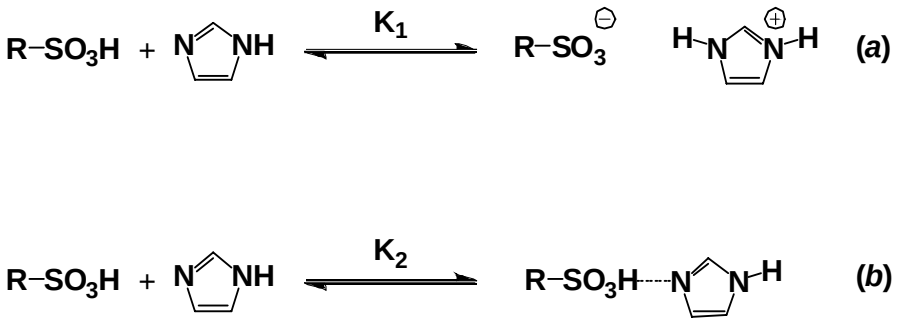

Scheme 5.1. Illustration of two competing equilibria which influence the blend membrane's proton conductivity.

In the following, we *A* and *B* to be the acid and base groups, and *AB* to be the complexes of the base group *B* bound to an acid group *A* via a hydrogen bond. To deduce an expression for $\rho_b^+(T)$ based on the above chemical reaction equilibria, we use the following notations: ρ_a,ρ_b -total number densities of acid and base groups ρ^o_a - number density of unassociated uncharged acid groups; ρ^-_a - number density of dissociated charged acid groups; ρ^o_a- number density of undissociated uncharged base groups; ρ_b^+ - number density of charged base groups; ρ_{ab} - number density of associated base groups. Therefore, we have:

$$\rho_a = \rho_a^0 + \rho_a^- + \rho_{ab}$$
$$\rho_b = \rho_b^0 + \rho_b^+ + \rho_{ab}$$
$$\rho_a^- = \rho_b^+$$

We denote

$$\varphi = \frac{\rho_b}{\rho_a};\ \alpha = \frac{\rho_a^-}{\rho_a};\beta = \frac{\rho_{ab}}{\rho_a}.$$

We note that the conductivity σ(T) is directly proportional to $\rho_b^+(T)$ through equation (5.1). The equilibrium constants can be expressed in the above notation as:

$$K_1 = \frac{\alpha^2}{(1 - \alpha - \beta)(\varphi - \alpha - \beta)}$$

$$\rho_a K_2 = \frac{\beta^2}{(1 - \alpha - \beta)(\varphi - \alpha - \beta)}$$

For K_1 and K_2, we adopted a simple Arrhenius type model:

$$K_i(T) = a_i \exp[\frac{-b_i T}{273(273+T)}]$$

(i=1,2) where T is the temperature measured in centigrade (C^o), a_1, b_1, a_2, and b_2 are phenomenological parameters quantifying the chemical kinetics.

The above model and the mechanistic proposal can be validated against the experimental data presented in the preceding sections. For this, we consider the results presented in Figure 5.2 (using the experimental values for the base concentrations), and fit the parameters a_1, b_1, a_2, and b_2 above. The results of such fits are presented in Figure 5.3a and 5.3b with plots of the temperature dependencies of the reaction constants K_1(T) and K_2(T) in Figures 3c and 3d. It is seen that we can indeed achieve semi-quantitative correspondence between the model predictions and the experimental results. Moreover, it is evident that in the situation where the conductivities display a monotonic temperature behavior (Figure 5.3a), the reaction constants K_1(T) and K_2(T) are such that K_1(T)<K_2(T) over the entire range of temperature (Figure 5.3c). In contrast, when the conductivities display a nonmonotonic temperature dependency (Figure 5.3b), it is observed that the reaction constants crosses over from K_1(T)<K_2(T) at lower temperatures to K_1(T)>K_2(T) at higher temperatures (Figure 5.3d).

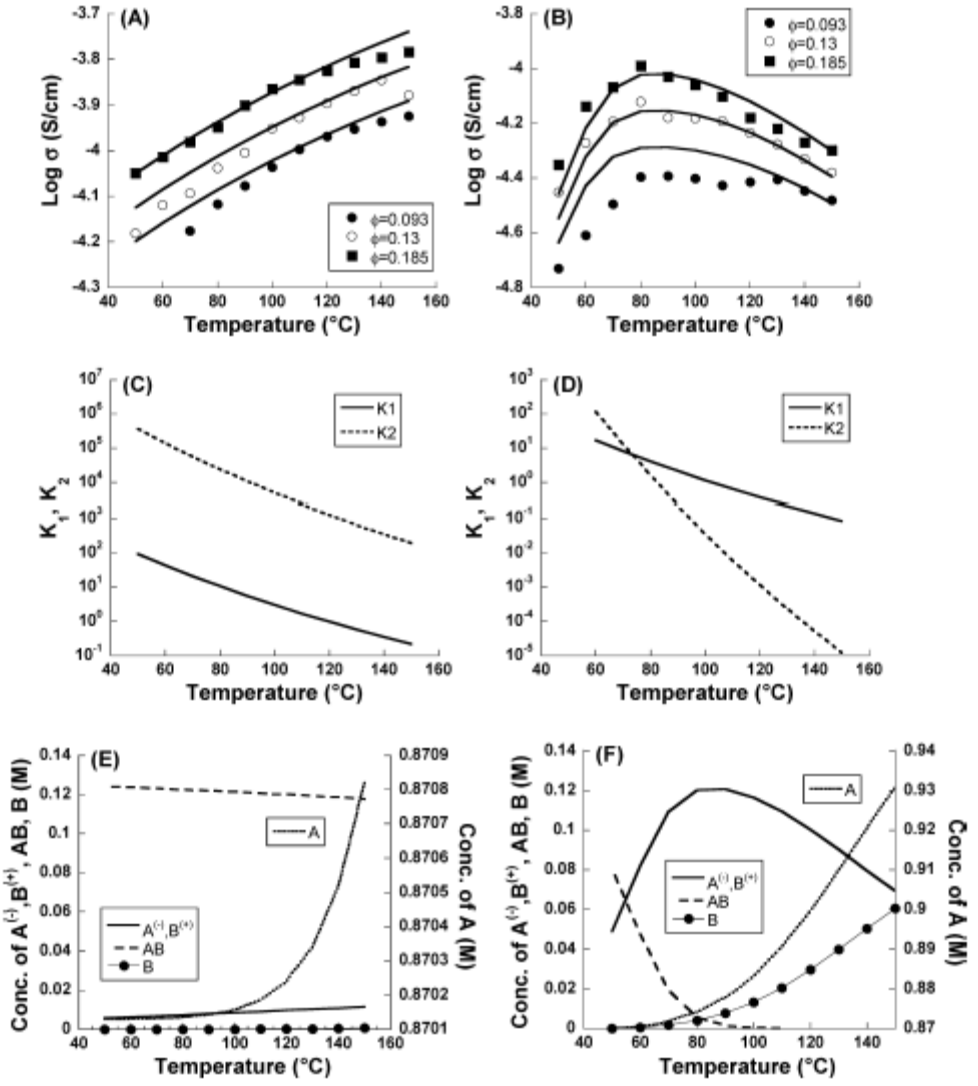

Figure 5.3. (A) and (B) Comparison of the experimental results of Fig. 5.2 (indicated by symbols) with the predictions of the mechanistic model (continuous lines). The conductivity of pure SPEEK has been subtracted from the experimental results to account for the residual water). (C) and (D) Comparison of the temperature dependence of the temperature dependence of the equilibrium constants K_1 and K_2 used for fitting the experimental results. (E) and (F) Results for the concentrations of the A, B, A^-,B^+ and AB components arising from our model fits.

The above results for the fit parameters K_1(T) and K_2(T) serve to provide a mechanistic basis for the experimental observations of the temperature dependence of

conductivity. We first consider the case of strong bases (imidazole) where the association reaction is expected to be the more dominant effect. For such situations, at low temperatures most of the acid and base groups are present in the associated form and hence the concentration of associated groups (*AB*) is high (Figure 5.3e). With an increase in temperature, the dissociation of the *AB* groups leads to an increasing concentration of *A* and *B* groups (Figure 5.3e). The latter in turn leads to an increased concentration of $B^{(+)}$ groups (through forward reaction a) and hence an increase of conductivity as a function of temperature.

In contrast, for weaker bases (dicyanoimidazole), we observe (Figure 3f) that the number of associated groups (*AB*) is much smaller at low temperatures and hence the dissociation induced increase in conductivity manifests only for a small range of temperatures (beyond which the number of *AB* groups become insignificant). Beyond this regime, due to the reverse of the first reaction (reaction a) we observe that the concentration of $B^{(+)}$ groups and conductivity decreases with increasing temperature.

In summary, the above results underscore the critical interplay between the association and the acid-base proton exchange reactions in determining the temperature dependence of the conductivity. This interelationship is expected to be applicable even in the context of other small molecule bases and influence the temperature dependence of the conductivity as a function of their basicity. Moreover, the semi-quantitative success of the model in fitting the experimental results provide a means to predict the temperature dependence of the conductivity for different base concentrations pending knowledge of the temperature dependence for a single base concentration. The latter can potentially be a valuable tool in modeling conductivity measurement experiments involving other small molecule bases.

CONCLUSIONS

Imidazole derivatives with varying pKa values were blended with sPEEK membranes and their respective proton conductivities were measured. The results show that the conductivity profiles are defined by the active equilibria in the membrane which regulate the concentration of charge carrier species. Theoretical modeling illustrates the effect of the acidity on these equilibra and therefore the conductivity profiles. Our model and the fit parameters suggested that in stronger bases the temperature-induced dissociation of AB groups concomitantly leads to an increase B^+ groups and the conductivity. In contrast, in weaker bases the above effect is followed by decrease in conductivity arising from the reverse of the proton exchange reaction. This knowledge of the key factors which influences the proton conductivities of the membranes described herein should facilitate the design and development of more efficient derivatives, particularly for fuel cell applications.

Chapter 6: 'Click'-Functionalization of Poly(sulfone)and Its Characterization in Direct Methanol Fuel Cells

INTRODUCTION

Direct methanol fuel cells (DMFC) provide a convenient source of power because (1) they do not require recharging with an electrical outlet, and (2) unlike hydrogen fuel cells, they use a relatively less volatile liquid fuel that is easy to store and transport.[147,148] Unfortunately, the DMFC technology is hampered by the sluggish methanol oxidation kinetics and the crossover of methanol fuel from the anode to the cathode through the membrane, which leads to fuel loss, cathode catalyst poisoning, and cell voltage drop.[149]

The most common electrolyte used in fuel cells, including DMFCs, is a sulfonated fluoropolymer called Nafion. This polymer is known to exhibit high proton conductivities (100 – 150 mS/cm) under operating conditions, but is expensive and suffers from high methanol permeability (1.2×10^{-6} cm^2/s).[150] Sulfonation of commercially-available polyaromatic materials, such as poly(sulfones)[141] and poly(ether ether ketones),[142a,c,143,151,] has been demonstrated to afford proton conductive membranes that exhibit reduced methanol permeability relative to Nafion ($1 – 9 \times 10^{-7}$ cm^2/s). One drawback, however, is that these sulfonated membranes often suffer from relatively low proton conductivities (11 – 17 mS/cm), particularly under low humidity conditions [142c] where there is not enough water present to act as a proton carrier.

To enhance conductivity, various N-heterocycles, such as imidazole or triazole, may be added to the aforementioned membranes.[138b,152] These N-heterocycles are believed to function as proton carriers and have been shown to improve the conductivity of membranes which contain them by threefold, even under low humidity conditions. However, the added N-heterocycles often leach from the polymer membrane when they

are operated at temperatures less than 100 ºC, where liquid water is present in the membrane, and some of them also poison the cathode catalyst.[153] To alleviate this issue, the nitrogen-containing bases were covalently linked to a polymer chain,[138a-c,154,155] but it involved complicated synthesis and/or additional post-polymerization modifications.

Another strategy to reduce methanol permeability while maintaining high proton conductivities has been to cross-link the polymer chains in the membrane.[156,157,158,159] It is believed that the cross-links limit membrane swelling and decreases the size of the proton conducting channels in the hydrated state. Smaller channels slow the diffusion of methanol and ultimately lower methanol crossover. However, the post-polymerization cross-linking reaction is practically challenging as it must be performed during or after membrane casting.

Herein we describe a method that overcomes many of these challenges and enables simultaneous installation of tethered N-heterocycles (to enhance proton transfer) and covalent crosslinking (to reducing swelling and methanol crossover).[160,161] The procedure utilizes the copper-catalyzed azide-alkyne 1,3-dipolar cycloaddition (CuCAAC) reaction between poly(sulfone)s containing pendant azides with alkyne additives. This "click" reaction[162,163] was selected because it not only proceeds to high conversions, but also is highly selective, tolerant to many functional groups and generates Brønsted basic 1,2,3-triazoles (pK_B: 0 – 1),[164] which we envisioned to serve as the N-heterocycles[165,166] in the proton shuttling processes described above.

RESULTS AND DISCUSSION

Sulfonation of Poly(sulfone)s Containing Pendant Azides via Click Chemistry. As a potentially suitable agent to modify poly(sulfone)s containing pendant

azides, alkyne sulfonate **6.1** features a flexible alkyl chain that was envisioned to distance the sulfonic acid from the main chain of the polymer to which it may be attached. As a result, the hydrophobic regions of the polymer backbone may be effectively separated from the hydrophilic regions and result in better swelling properties.[167] As shown in Scheme 6.1, **6.1** was synthesized by the nucleophilic ring-opening of 1,3-propanesultone with sodium propargylate under mild conditions and isolated in high yield (97%) following precipitation and collection via filtration. Although **6.1** was found to decompose over a period of days, forming an insoluble red powder, a solution of this compound in *N,N*-dimethylacetamide (DMAc) was found to be stable under ambient conditions for extended periods of time.

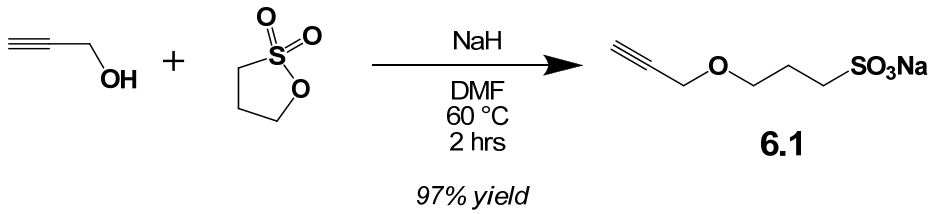

Scheme 6.1. Synthesis of alkyne sulfonate 6.1 via the ring-opening of 1,3-propanesultone with propargyl alcohol under basic conditions.

With 1 in hand, efforts shifted toward exploring the utility of this compound to modify azide-functionalized poly(sulfone)s. As shown in Scheme 6.2, polysulfone **6.2** (M_N = 22.7 kDa, PDI=2.01; prepared as described by Guiver[186]) was treated with **6.1** (2.0 equiv per repeat unit of **6.2**) under CuAAC conditions in DMAc. The progress of the cycloaddition reaction was monitored by the disappearance of the distinct IR absorption of the aryl azide (υ_{N3} = 2119 cm^{-1}; KBr; see Figure 1) as well as the appearance of a singlet at δ = 8.1 ppm, diagnostic of a triazole C-*H* proton, in the ^{1}H NMR spectrum (DMSO-d_6) (see Figure 6.2). The polymer was isolated in 75% by removal of the solvent

under reduced pressure at 60 ºC followed by washing with excess water and methanol and finally acidifying with 2M H_2SO_4. Gratifyingly the IEC (ion exchange capacity) of the polymer (2.1 meq/g) also corresponded well with the theoretical value (2.2 meq/g). The GPC of the resulting polymer exhibited a slightly lower molecular weight (M_N = 18.9 kDa, PDI = 1.43) compared to its starting material (M_N = 22.7 kDa, PDI = 2.01). We believe that the pendant sulfonate groups on the polymer are solvophobic relative to the eluent (DMF 0.1M LiBr) and the polymer assumes a more tightly packed conformation to minimize these solvent/sulfonate interactions. As a result, the polymer adopts a smaller hydrodynamic radius and, hence, an apparent reduction in molecular weight.

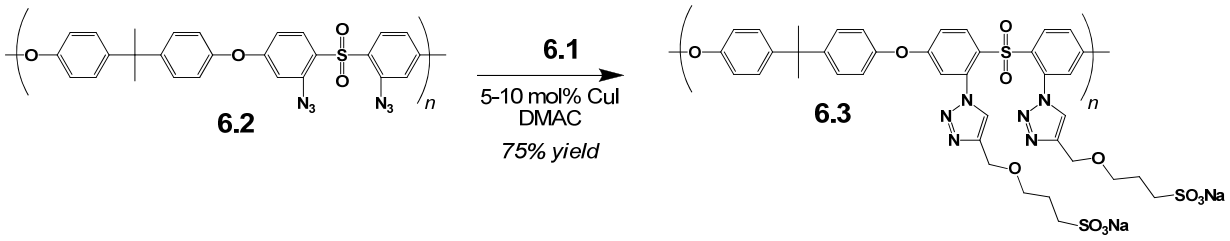

Scheme 6.2. Cu-catalyzed 1,3-dipolar cycloaddition of alkyne sulfonate **6.1** with an azide modified polysulfone **6.2**.

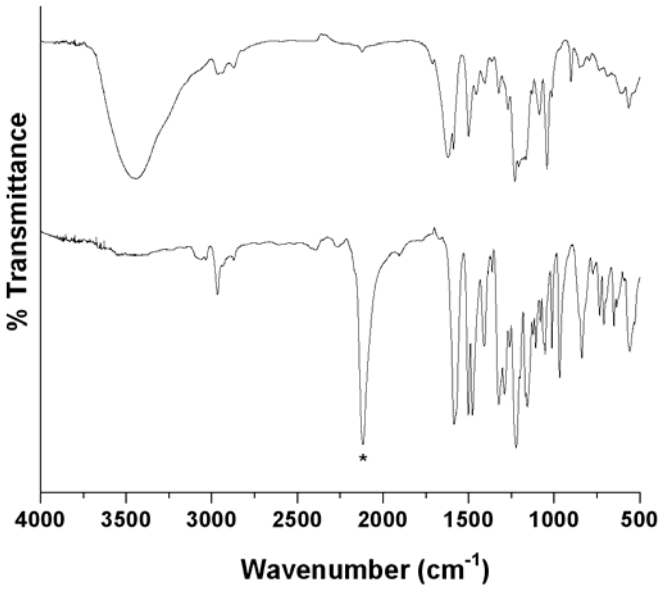

Figure 6.1. FT-IR spectrum (KBr) of polymer **6.2** (bottom) and polymer **6.3** (top). The asterisk denotes an azide stretching frequency.

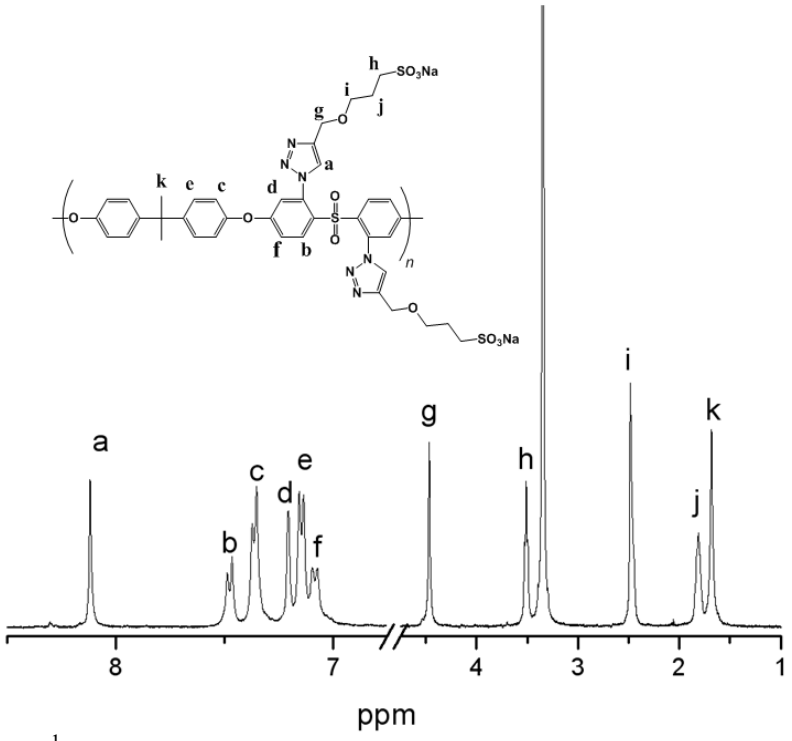

Figure 6.2. ^{1}H NMR spectrum of **6.3**. (DMSO-d_6) The diagnostic chemical shifts are labeled.

Synthesis and Study of Cross-linked Poly(sulfone) Membranes.

Once it was demonstrated that poly(sulfone) was successfully modified with **6.1** using the aforementioned cycloaddition chemistry, efforts shifted toward the synthesis of cross-linked polymers using a similar approach. Polymer **6.2** was dissolved in DMAc followed by the addition of various quantities of alkyne sulfonate **6.1**, 1,7-octadiyne as a cross-linker, and copper catalyst (10 mol%); see Table **6.1**. Each of these solutions were independently degassed and then heated at 60 °C for 12 h in an air-free petri dish. The solvent was then evaporated at 60 ºC to produce polymeric membranes that were released from the dish by addition of 2M H_2SO_4. As expected, the crosslinked polymeric materials obtained from these reactions were insoluble; hence, they could not be analyzed via NMR spectroscopy. However, as summarized in Table 6.1, a close correlation between the theoretical and the observed IECs was observed. In addition, the methanol permeabilities and proton conductivities of these membranes were measured. Low levels of sulfonation resulted in membranes that exhibited low methanol permeabilities and modest conductivities. For example membrane **6.3d** (which contained 30% crosslinker and an IEC of 1.3) displayed a 10-fold reduction in methanol crossover (1.03×10^{-7} cm^2/s) but exhibited only a modest reduction in proton conductivity (40 mS/cm) versus Nafion 117 (111 mS/cm). However, further increasing the IEC of the resulting materials (via incorporation of increasing amounts of **6.1**) resulted in membranes that were too mechanically unstable for further testing.

Table 6.1. Methanol permeabilities and proton conductivities (σ) for selected membranes.

Polymer	IEC Theory, meq/g	IEC Expt meq/g	mol % 1,7-octadiyne	MeOH perm (cm^2/s)	σ (mS/cm)
6.3a	0.82	0.74	0	4.76×10^{-9}	13
6.3b	1.3	1.2	0	6.85×10^{-7}	60
6.3c	1.3	1.3	20	3.10×10^{-7}	74
6.3d	1.3	1.3	30	1.03×10^{-7}	40
6.3e[b]	1.6	1.5	30	4.11×10^{-5}	111
6.3f[b]	1.8	1.8	0	[c]	[c]
6.3g[b]	1.8	1.7	20	3.90×10^{-6}	53
6.3h[b]	1.8	1.7	25	4.83×10^{-6}	50
Nafion 117	0.91	0.91	0	1.25×10^{-6}	120

[a]The impedance measurements were acquired at 65 ºC and 100% relative humidity. [b] These membranes formed mechanically weak gels upon acidification and were too fragile to incorporate into viable fuel cells. [c] These membranes proved to be too weak for further testing. The methanol permeability data was acquired at 25 ºC.

Synthesis and Study of Cross-linked Poly(sulfone) Copolymer Membranes. To enhance the mechanical properties of the aforementioned materials and to further separate the hydrophilic regions from the hydrophobic regions described above, a series of crosslinked copolymers comprised of polymer **6.2**, a partially-sulfonated polymer with varying degrees of sulfonation (polymer **6.4**) and crosslinker (1,7-octadiyne)were synthesized (see Scheme 6.3).[168,169] As summarized in Table 6.2, this method afforded polymers **6.5** which formed mechanically robust membranes that exhibited lower methanol permeabilities and similar conductivities as Nafion 117. Unfortunately, further sulfonation of the hydrophilic block led to poor quality films which we attributed to phase separation. We surmise that the difference in ionic strength of these polymer solutions became so large such that the ionic attraction of the sulfonate groups were not offset by the entropy gained from homogenization.

Table 6.2. Methanol permeability and conductivity data for copolymers **6.5a-b**.[a]

Polymer	DS of Sulfonated polymer	sulfonated/ unsulfonated wt/wt	IEC Theory, meq/g	IEC Expt meq/g	mol % 1,7-octadiyne	MeOH perm (cm^2/s)	σ (mS/cm) 65 ºC 100%RH
6.5a	1.2	4.01	1.3	1.2	30	3.57×10^{-7}	86
6.5b	1.6	3.8	1.5	1.4	30	1.87×10^{-6}	111

[a] Methanol permeability measurements were performed at ambient temperature (25 ºC).

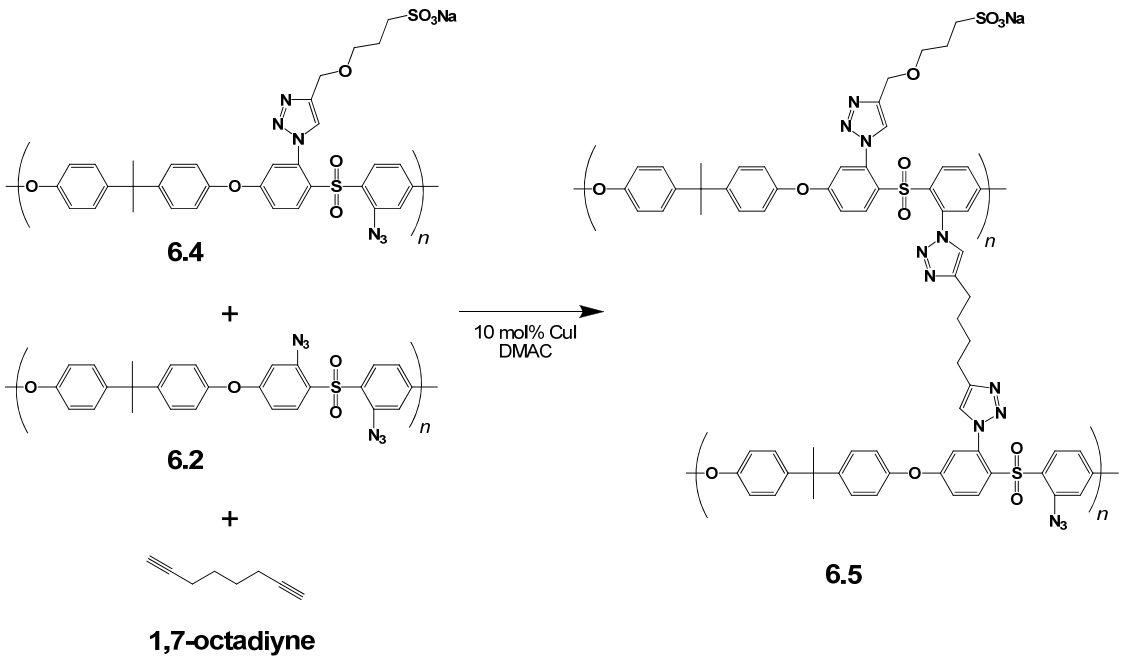

Scheme 6.3. Copolymer formation via crosslinking of two different polymer chains.

Membrane-Electrode Assembly (MEA): Preparation and Testing Performance.

MEAs containing Polymer **6.5a** as electrolyte were fabricated under two conditions, pressing under 100 °C and ambient temperature. As comparison, MEA comprising Nafion 117 were also fabricated as previously described.**Error! Bookmark not defined.** The electrochemical performance of MEAs was evaluated using a computer controlled fuel cell testing setup (Scribner 840) at 65 ºC with 1 M MeOH cycled through

the anode at rate of 2.5 mL/min and oxygen fed to the cathode at rate of 200 mL/min. Both **6.5a** and the Nafion MEA were prepared using commercial electrodes (BASF) with a catalyst loading of 5 mg/cm^2 Pt (cathode) and Pt:Ru (anode) treated with Nafion ionomers. The Nafion MEA was assembled by hot pressing at 120 ºC 1500 lbs. for 2 minutes and thirty seconds.

The performance of the fuel cell containing **6.5a** was found to be highly dependent on MEA assembly conditions. For the MEA of polymer 5a fabricated over 100 ^{o}C, the membrane became brittle when drying during the hot pressing and hard to handle, which has also been observed in other cross-linked polymers.[170] The brittleness of the membrane may also cause the higher interface resistance between electrode and membrane, which results a higher polarization loss in the polarization curve. However, when pressing at ambient temperature, the membrane remained hydrated and more flexible, resulting in a better contact between the electrode and membrane interface and a better performance compared to that fabricated at higher temperature as shown in Figure 6.3. The **6.5a-100C** MEA also shows higher maximum power density (130 mW/cm^2) which is comparable to that of Nafion 117 membrane (150 mW/cm^2) under the same conditions.

Although the **6.5a** polymer membrane (110 μm) is thinner than the Nafion 117 membrane (175 μm), it shows a bit lower performance due to lower proton conductivity compared to that of Nafion 117 and incompatibility between the aromatic polymer membrane and Nafion ionomer in the electrode on both sides. The open circuit voltage (OCV) of **6.5a** is higher than that of Nafion 117 membrane, which is due to the lower methanol permeability (as shown in Table 6.1) and the consequent smaller voltage loss at the cathode side. The lower methanol permeability could not only help to lower the Pt

catalyst loading at the cathode but also lead to a better long-term stability and performance in DMFC.

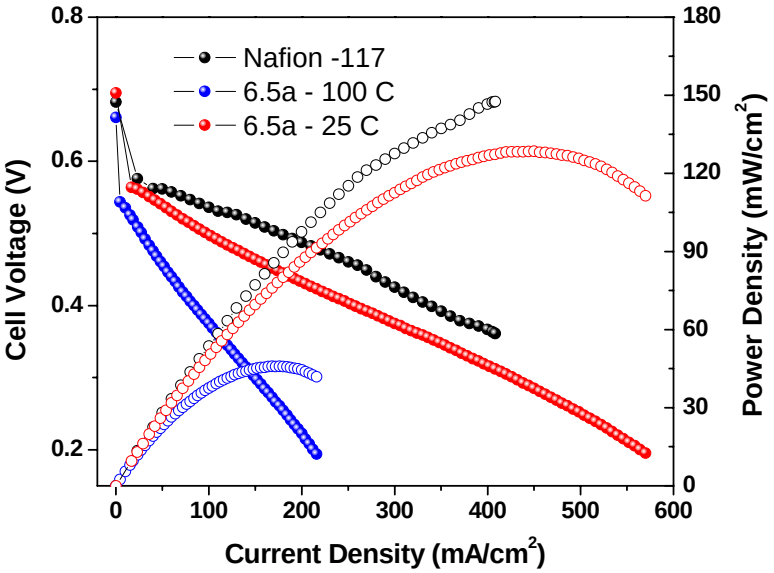

Figure 6.3. MEA tests of **6.5a** and Nafion 117. Filled circles show polarization curve; open circles show power density curve. A Pt-black catalyst was used at the cathode and a Pt:Ru black catalyst was used at the anode. Both of these loadings were 5 mg/cm^2. The active cell area is 5 cm^2. Sample **6.5a-100C** refers to a MEA that was assembled via hot pressing at 100 ºC. Sample **6.5a-25C** refers to a MEA that was assembled via pressing at ambient temperature.

CONCLUSIONS

A new method for modifying poly(sulfone)s containing pendant azides is reported. Using copper-catalyzed, 1,3-dipolar cycloaddition chemistry, Brønsted basic 1,2,3-triazoles and cross-links were successfully formed in a single step which was found to significantly decrease the methanol permeability while maintaining relatively high proton conductivity in the resulting membranes. The fuel cell performances were comparable to Nafion with a maximum power output of 130 mW/cm^2. The method

described herein effectively establishes a new and versatile route to functionalization of aromatic polymers; extension of this methodology to other proton conductive materials is currently underway.

Appendix

EXPERIMENTAL FOR REVERSIBLE POLYMERS

General Considerations: Unless otherwise noted, all reactions were performed under an atmosphere of nitrogen using standard Schlenk techniques or inside a nitrogen-filled drybox. Toluene and tetrahydrofuran (THF) were distilled from calcium hydride or sodium and benzophenone under an atmosphere of nitrogen prior to use. The following compounds were prepared as previously described: 2,7-dinitrofluorene,[171] N,N′-di-neo-pentylbenzimidazolinylidene,[172] and 1,1′,3,3′-tetra(2,2-dimethylbutyl)-5,5′-bibenz-imidazolylidene (**2.5**).[173] 2,4,6-Trideuteroaniline was also prepared as previously described[174] and the level of deuteration was analyzed by 1H NMR spectroscopy using an internal standard (mesitylene). All other compounds were purchased from commercial sources and used without additional purification. 1H NMR spectra were recorded using a Varian Gemini (300 MHz or 400 MHz) spectrometer. Chemical shifts are reported in delta (δ) units and expressed in parts per million (ppm) downfield from tetramethylsilane using the residual protio solvent as an internal standard ($CDCl_3$, 7.24 ppm; C_6D_6, 7.15 ppm; CD_2Cl_2, 5.32 ppm; DMSO-d_6, 2.49 ppm). ^{13}C NMR spectra were recorded using a Varian Gemini (75 or 100 MHz) spectrometer. Chemical shifts are reported in delta (δ) units and expressed in parts per million (ppm) downfield from tetramethylsilane using the solvent as an internal standard ($CDCl_3$, 77.0 ppm; C_6D_6, 128.0 ppm; CD_2Cl_2, 53.8 ppm, DMSO-d_6, 39.5 ppm). ^{13}C NMR spectra were routinely run with broadband decoupling. Elemental analyses were performed by Midwest Microlabs, LLC (Indianapolis, IN). Molecular weights were determined by gel permeation chromatography (GPC) using a Waters HPLC system consisting of three Viscotek I-series columns (2 × GMHHRH and 1 × G3000HHR) arranged in series, a 1515 pump, and a 2414 RI detector and are reported

relative to polystyrene standards in DMF (0.1 M LiBr) at 40 °C (column temperature). IR spectra were recorded using Perkin-Elmer Spectrum BX FT-IR system. High-resolution mass spectra (HRMS) were obtained with a VG analytical ZAB2-E or a Karatos MS9 instrument and are reported as m/z (relative intensity). UV–visible absorption spectra were recorded on a Perkin-Elmer Lambda 35 spectrophotometer. All measurements were made with matching 6Q Spectrosil quartz cuvettes (Starna) with 1.0 cm path lengths and 3.0 mL sample solution volumes. Beer's law measurements were performed using 10, 20, 30 and 40 μM sample concentrations. Thermogravimetric analyses were performed on a Mettler Toledo TGA/SDTA851e. Differential scanning calorimetry analyses were performed on a Mettler Toledo DSC 823e. Mechanical analyses were performed using a TA Instruments Q800 DMA configured in tensile geometry. Polymer film conductivities were measured on an Agilent 4156C precision semiconductor parameter analyzer equipped with a four-point probe with a probe spacing of 1.59 mm. Melting points were obtained with a Mel-Temp apparatus and are uncorrected.

Compound 2.3. A 40 mL flask was charged with N,N′-di-neo-pentylbenzimidazolium tetrafluoroborate (638 mg 1.84 mmol), 10 mL of THF, and a stir bar. After adding solid sodium tert-butoxide (195 mg, 2.02 mmol) to the resulting suspension, the reaction mixture was stirred for 2 h at ambient temperature. Phenyl isothiocyanate (311 mg, 2.02 mmol) was then added and the reaction mixture was stirred for an additional 20 min at ambient temperature. The resulting mixture was then diluted with CH_2Cl_2 (20 mL) and filtered through a short column of Celite. Removal of the residual solvent under reduced pressure afforded a solid material that was washed with hexanes. Collection of the residue followed by drying under reduced pressure afforded

the desired product in 78% yield (634 mg) as a yellow solid. m.p. 203–205 ºC. ^{1}H NMR (400 MHz, $CDCl_3$): δ 7.63 (dd, J = 3.1, 3.3 Hz, 2H), 7.50 (dd, J = 3.1, 3.1 Hz, 2H), 7.33-7.40 (m, 4H), 7.05-7.09 (m, 2H), 4.773 (b, 4H), 1.12 (s, 18H). ^{13}C NMR (100 MHz, $CDCl_3$): δ 167.2, 150.8, 150.5, 131.8, 128.6, 125.8, 123.6, 121.9, 113.9, 56.6, 34.3, 29.0. HRMS: [M+1] calcd for $C_{24}H_{32}N_3S$: 394.2317; Found: 394.2311. IR (KBr): ν 996, 1463, 1493, 1519, 2964 cm-1. Anal. calcd (%) for $C_{24}H_{31}N_3S$: C, 73.24; H, 7.94; N, 10.68; S, 8.15; Found: C, 73.23; H, 7.72; N, 10.69; S, 8.17.

2,4,6-Trideuterophenylisothiocyanate. A 500 mL round bottom flask equipped with a stir bar was charged with 2,4,6-trideuteroaniline (3.1 g, 32.2 mmol) and water (200 mL). Under rapid stirring, thiophosgene (3.7 mL, 48.3 mmol) was injected into the reaction vessel and the resulting mixture was stirred for 2 h at ambient temperature The aqueous layer was then extracted with CH_2Cl_2 (2 × 50 mL). Removal of the residual organic solvent under reduced pressure afforded the desired product in 60% yield (2.63 g) as a light yellow liquid. m.p. –22.17 ºC (determined by DSC). ^{1}H NMR (400 MHz, $CDCl_3$): δ 7.36 (s, 2H). ^{13}C NMR (100 MHz, $CDCl_3$): δ 135.2, 131.1, 129.3, 127.0 (t, C-D, J = 27.3 Hz), 125.5, (t, C-D, J = 25.0 Hz). HRMS: [M+1] calcd for $C_7H_3D_3NS$: 139.0409; Found: 139.0406. Anal. calcd (%) for C_7H_5NS: C, 60.83; H, 3.73; N, 10.13; S, 23.20; Found: C, 60.58; H, 3.83; N, 10.13; S, 22.91. IR (KBr): ν 549, 922, 1435, 1573, 2088 (NCS), 3059 cm^{-1}.

Compound 2.4. A 5 mL flask was charged with *N,N′*-di-*neo*-pentylbenzimidazolium tetrafluoroborate (349 mg 1.01 mmol), 2 mL of THF, and a stir bar. After adding solid sodium *tert*-butoxide (107 mg, 1.11 mmol) to the resulting suspension, the mixture was stirred for 2 h at room temperature. A precipitate formed

which was subsequently removed using a 0.2 μm syringe filter. The filtrate was treated with 2,4,6-trideuterophenylisothiocyanate (153 mg, 1.11 mmol) and the resulting mixture was stirred for an additional 20 min. Subsequent removal of solvent under reduced pressure afforded a residue that was later washed with hexanes to afford a yellow solid. Purification of this solid via column chromatography (eluent: 10% acetone / 90% hexanes (v/v); stationary phase: silica gel) afforded 350 mg (88% yield) of the desired product as a yellow solid. mp 214–216 ºC. ^{1}H NMR (400 MHz, $CDCl_3$): δ 7.62 (dd, J = 3.1, 2H), 7.48 (dd, J = 3.1, 2H), 7.36 (s, 2H), 4.75 (b, 4H), 1.11 (s, 18H). ^{13}C NMR (100 MHz, $CDCl_3$): δ 167.16, 150.79, 150.37, 131.78, 128.40, 125.80, 123.38 (t, C-D, J = 26 Hz), 121.57 (t, C-D, J = 24 Hz), 113.89, 56.62, 34.29, 29.00. HRMS: [M+1^{+}] calcd for $C_{24}H_{29}D_3N_3S$: 397.2505; Found: 397.2503. IR (KBr): ν 1000, 1467, 1492, 1518, 2963 cm^{-1}. Anal. calcd (%) for $C_{24}H_{31}N_3S$: C, 72.68; H, 7.94; N, 10.59; S, 8.08; Found: C, 72.89; H, 7.79; N, 10.44; S, 8.07.

2,7-Diamino-9,9-dihexylfluorene. Using a modified literature procedure,[3] a 100 mL round bottom flask was charged with 1.18 g (2.77 mmol) of 2,7-dinitrofluorene, 50 mL of ethanol, 400 mg of Pd on carbon (10% w/w), 4.0 mL (130 mmol) of hydrazine monohydrate, and a stir bar. The flask was then equipped with a condenser and the resulting reaction mixture was stirred at reflux for 8 h. After cooling to ambient temperature, the mixture was filtered through Celite to remove the residual inorganic materials. Subsequent removal of solvent under reduced pressure afforded 960 mg (96% yield) of the desired product as a colorless syrup which crystallized after several days. ^{1}H NMR (400 MHz, $CDCl_3$): δ 7.31 (dd, J_1 = 5.5Hz, J_2 = 1.6 Hz, 2H), 6.59 (m, 4H), 3.60 (br s, 4H), 1.80 (m, 4H), 1.1 (m, 12H), 0.75 (t, J = 7.1 Hz, 6H), 0.63 (m, 4H). ^{13}C NMR (100 MHz, $CDCl_3$): δ 151.6, 144.5, 133.1, 119.0, 113.8, 110.0, 54.59, 40.92, 31.59, 29.87,

23.69, 22.69, 14.04. HRMS: [M^+] calcd for $C_{25}H_{37}N_2$: 365.2951; Found: 365.2951. Spectral data matched literature values.[3]

2,7-Diisothiocyanato-9,9-dihexylfluorene (2.6). A 250 mL round bottom flask was charged with 2,7-diamino-9,9-dihexylfluorene (0.961 g, 2.77 mmol), deionized water (50 mL), thiophosgene (0.637 mL, 8.31 mmol), and a stir bar. After stirring the resulting mixture at ambient temperature for 1 h, CH_2Cl_2 (50 mL) was added. Separation of the organic layer followed by concentration under reduced pressure afforded a dark colored syrup. The residue was then dissolved in hexanes, filtered through a short column of silica gel and then concentrated under vacuum to afford 1.11 g (89% yield) of the desired product as colorless crystals. mp 67–68 ºC. ^{1}H NMR (400 MHz, $CDCl_3$): δ 7.6 (d, J = 7.8 Hz, 2H), 7.1 (m, 4H), 1.9 (m, 4H), 1.1 (m, 12H), 0.76 (t, J = 7.2 Hz, 6H), 0.51 (m, 4H). ^{13}C NMR (100 MHz, $CDCl_3$): δ 152.5, 139.0, 134.8, 130.2, 124.9, 120.8, 120.4, 55.7, 40.2, 31.5, 29.5, 23.7, 22.6, 14.0. HRMS: [M^+] calcd for $C_{27}H_{32}N_2S_2$ 448.2007; Found: 448.2014. IR (KBr): ν 818, 1439, 1461, 2110 (NCS), 2927 cm^{-1}. Anal. Calcd (%) for $C_{27}H_{32}N_2S_2$: C, 72.28; H, 7.19; N, 6.24; S, 14.29; Found: C, 72.42; H, 7.26; N, 6.40; S, 13.89.

Polymer 2.7. A 5 mL vial was charged with **2.6** (269 mg, 0.598 mmol) and a stir bar. A separate 5 mL vial was charged with 1,1′,3,3′-tetra(2,2-dimethylbutyl)-5,5′-bibenzimidazolylidene (342 mg, 0.598 mmol), and a stir bar. After dissolving each substrate in THF (2 mL), the vials were combined and stirred at ambient temperature. After 20 min, the resulting solution was poured dropwise into an excess of diethyl ether (200 mL), which caused solids to precipitate. The solids were collected by filtration and then dried under reduced pressure to afford 443 mg (92% yield) of the desired product as

a yellow to red powder. ^{1}H NMR (400 MHz, $CDCl_3$): δ 7.8 (br, 8H), 7.4 (br s, 2H), 7.2 (end group m, 4H), 4.9 (br, 8H), 1.9 (m, 4H), 1.8 (m, 8H), 1.0 (m, 66 H). ^{13}C NMR (100 MHz, $CDCl_3$): δ 165.3, 151.5, 148.1, 138.1, 137.7, 132.7, 131.9, 125.6, 121.0, 119.0, 118.0, 114.6, 112.6, 56.3, 56.1, 54.8, 40.5, 36.9, 36.9, 34.1, 34.1, 31.6, 30.0, 25.79, 25.69, 24.0, 22.7, 14.0. 8.48, 8.44. Anal. Calcd. (%) for $C_{65}H_{90}N_6S_2$: C, 76.57; H, 8.90; N, 8.24; S, 6.29. Found: C, 75.97; H, 8.89; N, 8.09; S, 6.28;

Compound 2.8. A 40 mL vial was charged with **2.6** (317 mg, 707 mmol), THF (5 mL), and a stir bar. A separate 5 mL vial was charged with 1,1′,3,3′-tetra(2,2-dimethylbutyl)-5,5′-bibenzimidazolylidene (100 mg, 175 mmol), THF (5 mL) and a stirbar. The solution of the latter was then added dropwise to the solution of the former. After stirring the resulting mixture at ambient temperature for 20 min, the residual solvent was removed under reduced pressure. The residue was then washed with excess hexanes to afford a yellow precipitate which was isolated by centrifugation and dried under vacuum. Purification via column chromatography (eluent: 20% acetone / 80% hexanes (v/v); stationary phase: silica gel) afforded 71 mg (57% yield) of the desired product as a orange solid. mp 214–216 ºC. ^{1}H NMR (400 MHz, $CDCl_3$): δ 7.66-7.80 (m, 10H), 7.60 (d, J = 8.6 Hz, 2H), 7.40 (br s, 2H), 7.16-7.18 (m, 4H), 4.8-4.9 (br, 8H), 1.9 (m, 8H), 1.6 (m, 8H), 1.0 (bm, 88 H). ^{13}C NMR (100 MHz, $CDCl_3$): δ 165.9, 151.9, 150.8. 149.1, 140.6, 137.9, 135.4, 133.4, 132.5, 131.7, 128.2, 125.6, 124.6, 121.3, 120.4, 120.0, 117.7, 114.8, 112.9, 57.8, 56.7, 42.2, 38.8, 36.1, 33.6, 27.9, 26.0. 24.9, 16.4, 11.0. HRMS: [M^{2+}] calcd for $C_{92}H_{122}N_8S_4$ 734.4410; Found: 734.4410. IR (KBr): ν 818, 1008, 1467, 2108 (NCS), 2857, 2930, 2961 cm^{-1}. Anal. Calcd. (%) for $C_{92}H_{122}N_8S_4$: C, 75.26; H, 8.38; N, 7.63; S, 8.74; Found: C, 75.33; H, 8.49; N, 7.54; S, 8.63. UV–vis (DMF): λ_{max} =337, 380 nm (ε = 4.3 × 10^4 M^{-1} cm^{-1}).

Isolation of 2.8 from the Reaction of 2.7 with 2.6. A 5 mL vial equipped with a stir bar was charged with 0.7 mL solution of **2.7** (0.2 M in DMF; 0.14 mmol of the polymer's repeat units), and **2.6** (159 mg, 0.354 mmol). The vial was then capped and placed in an oil bath at 120 ºC for 12 h. Subsequent analysis of the reaction mixture by GPC revealed that only low molecular weight materials were present. The mixture was poured into excess methanol, which caused solids to precipitate. The solids were collected via filtration, redissolved in a minimal amount of chloroform and then purified by column chromatography (eluent: 10% acetone / 90% hexanes (v/v); stationary phase: silica gel) to afford 15 mg (7.3% yield) of the desired product. Spectral data were consistent with the values listed above.

1,2-bis(2,2-dimethylbutyrylamido)benzene. A 1 L round bottom flask equipped with a stir bar was charged with 1,2-phenylenediamine (5.00 g, 46.2 mmol), dichloromethane (500 mL), and 2,2-dimethylbutryl chloride (13.3 mL, 97.1 mmol). After stirring the mixture for 5 min, triethylamine (14.0 mL, 97.1 mmol) was added in a single portion. The resulting mixture was then stirred for an additional 12 h at ambient temperature. Subsequent removal of the residual solvent under reduced pressure afforded a solid that washed with excess water (500 mL) and then dried under vacuum at 80 ºC to afford the desired product (13.6 g) in 97% yield as a tan powder. mp 126–128 ºC. ^{1}H NMR (400 MHz, $CDCl_3$): δ 8.23 (s, 2H), 7.28 (dd, J = 2.3, 3.6 Hz, 2H), 7.07 (dd, J = 3.5, 2.5 Hz, 2H), 1.59 (q, J = 7.5 Hz, 4H), 1.19 (s, 12H), 8.6 (t, J = 7.4 Hz, 6H). ^{13}C NMR (100 MHz, $CDCl_3$): δ 177.4, 131.0, 125.8, 125.6, 43.0, 33.9, 24.9, 9.3. HRMS: [M+H$^+$] calcd for $C_{18}H_{29}N_2O_2$: 305.2229; Found: 305.2225. Anal. Calcd. (%) for $C_{18}H_{28}N_2O_2$: C, 71.02; H, 9.27; N, 9.20; Found: C, 70.98; H, 9.02; N, 9.23.

***N,N′*-Bis(2,2′-dimethylbutyl)benzimidazolium tetrafluoroborate.** In a 1 L round bottom flask equipped with a stir bar and a reflux condenser, 1,2-bis(2,2-dimethylbutyrylamido)benzene (5.07 g, 16.6 mmol) was dissolved in dry tetrahydrofuran (200 mL) and placed under an atmosphere of nitrogen. A suspension of $LiAlH_4$ (2.46 g, 66.5 mmol) in tetrahydrofuran (40 mL) was then injected through the reflux condenser and the reaction was heated to reflux for 48 h. The reaction mixture then cooled in an ice bath and the residual $LiAlH_4$ was quenched by slow addition of water (3 mL) followed by an aqueous solution of NaOH (10% w/v, 3 mL) and finally water (12 mL). The resulting mixture was then warmed to ambient temperature and dried over sodium sulfate (20 g) with continous stirring for 30 min. The mixture was then filtered and the residual solvent was removed under reduced pressure. The residual solvent was then treated with an aquous solution of HBF_4 and trimethylorthoformate (previously prepared by combining 8.5 mL of 48% (w/w) aqueous HBF_4 to 100 mL of trimethylorthoformate). After heating the resulting mixture to 80 C for 3 h, excess diethyl ether (100 mL) was added, which caused solids to precipitate. The solids were collection via filtration and dried under vacuum at 80 ºC to afford the desired product (5.0 g) in 80% yield as a white crystalline solid. mp 203–204 ºC. ^{1}H NMR (400 MHz, DMSO-d_6): δ 9.62 (s, 1H), 8.14 (dd, J = 3.1, 3.2 Hz, 2H), 7.68 (dd, J = 3.1, 3.2Hz, 2H), 4.40 (s, 4H), 1.35 (q, J = 7.5Hz, 4H), 0.9-0.8 (m, 18H). ^{13}C NMR (100 MHz, DMSO-d_6): δ 144.1, 132.6, 126.8, 114.7, 56.6, 36.1, 32.2, 24.2, 8.5. HRMS: [M^+] calcd for $C_{19}H_{31}N_2$: 287.2487; Found: 287.2487. Anal. Calcd. (%) for $C_{19}H_{31}BF_4N_2$: C, 60.97; H, 8.35; B, 2.89; F, 20.30; N, 7.48; Found: C, 60.61; H, 8.13; N, 7.43.

Compound 2.9. A 30 mL vial equipped with a stir bar was charged with *N,N′*-bis(2,2′-dimethylbutyl)benzimidazolium tetrafluoroborate (500 mg, 1.33 mmol),

tetrahydrofuran (3 mL), and sodium *tert*-butoxide (127 mg, 1.33 mmol). The vial was then capped and stirred at ambient temperature for 4 h. The vial was then opened and then charged with 2,7-diisothiocyanato-9,9-dihexylfluorene (**2.6**) (200 mg, 0.445 mmol), re-sealed, and then stirred at ambient temperature for an additional 4 h. The residual solvent was then removed under reduced pressure and the product was purified by column chromatography (using silica gel as the stationary phase and 0→40% acetone in hexanes (v/v) as the mobile phase) to afford the desired product (414 mg) in 30% yield as an orange solid. mp 216–218 ºC. ^{1}H NMR (400 MHz, $CDCl_3$): δ 7.75 (d, *J* = 8.0 Hz, 2H), 7.64 (d, *J* = 8.0 Hz, 2H), 7.59 (dd, *J* = 2.9,3.3 Hz, 4H), 7.45, (dd, *J* = 3.1, 3.1 Hz, 2H), 7.37 (s, 2H), 4.78 (b, 8H, 1.89 (m, 4H), 1.46 (q, *J* = 7.4Hz, 8H), 1.2-0.8 (m, 60H), 0.669 (t, *J* = 7.0 Hz, 6H). ^{13}C NMR (100 MHz, $CDCl_3$): δ 165.8, 151.4, 150.8, 148.2, 137.6, 131.9, 125.7, 120.9, 118.8, 118.0, 113.8, 55.9, 54.7, 40.5, 36.8, 34.0, 31.6, 30.0, 25.6, 24.0, 22.7, 14.1, 8.4. HRMS: [M+H$^+$] calcd for $C_{65}H_{93}N_6S_2$: 1021.6903; Found; 1021.6882. Anal. Calcd. (%) for $C_{65}H_{92}N_6S_2$: C, 76.42; H, 9.08; N, 8.23; S, 6.28; Found: C, 76.44; H, 9.03; N, 8.33; S, 6.21. UV–vis (DMF): λ_{max} = 338, 409 nm (ε = 1.3 × 10^6 M^{-1} cm^{-1}).

2,4,6-Trideuterophenylisothiocyanate. A 500 mL round bottom flask equipped with a stir bar was charged with 2,4,6-trideuteroaniline (3.1 g, 32.2 mmol) and water (200 mL). Under rapid stirring, thiophosgene (3.7 mL, 48.3 mmol) was injected into the reaction vessel and the resulting mixture was stirred for 2 h at ambient temperature The aqueous layer was then extracted with CH_2Cl_2 (2 x 50 mL). Removal of the residual organic solvent under reduced pressure afforded 2.63 g (60% yield) of the desired product as a light yellow liquid. mp –22.17 ºC (determined by DSC). ^{1}H NMR (400 MHz, $CDCl_3$): δ 7.36 (s, 2H). ^{13}C NMR (100 MHz, $CDCl_3$): δ 135.2, 131.1, 129.3, 127.0

(t, C-D, J = 27.3 Hz), 125.5, (t, C-D, J = 25.0 Hz). HRMS: [M+H$^+$] calcd for $C_7H_3D_3NS$: 139.0409; Found: 139.0406. Anal. calcd (%) for C_7H_5NS: C, 60.83; H, 3.73; N, 10.13; S, 23.20; Found: C, 60.58; H, 3.83; N, 10.13; S, 22.91. IR (KBr): ν 549, 922, 1435, 1573, 2088 cm^{-1}.

Exchange Reaction: Determination of Reaction Rate of the and Reaction Order. As summarized in Table 2.1, a series of vials were charged with various quantities of **2.3**, 2,4,6-trideuterophenylisothiocyanate and toluene-d_8. Each reaction mixture was then transferred to an NMR tube and sealed with a Teflon coated screw cap. After acquiring an initial ^{1}H NMR spectrum, the tube was heated in an oil bath thermostated to 392 K. The tube was periodically removed from the oil bath and analyzed by ^{1}H NMR spectroscopy. The concentration of **2.3** was determined by integrating the arene signals derived from phenylisothiocyanate versus the arene signals derived from 1,3-di-neopentylbenzimidazolylidene and plotted over time. The rate of the exchange reaction was estimated from the linear portion of the corresponding graph (i.e., the early stages of the exchange reaction). Based on the results shown in Table A1, the exchange process was determined to be first order with respect to **2.3** and zeroth order with respect to PhNCS-d_3.

Table A1. Summary of the exchange rate data for **2.3**→**2.4**.[a]

entry	[**2.3**]$_0$ (mM)	[PhNCS-d_3]$_0$ (mM)	rate of exchange (M s^{-1})
1	28.0	74.3	1.62×10^{-6}
2	24.3	148	1.39×10^{-6}
3	11.2	70.0	7.06×10^{-7}

[a] The rates of exchange were measured at 392 K in toluene-d_8.

Activation Parameters. Given that the formation of NHC–isothiocyanate adducts was observed to occur instantaneously and that free NHC was not observed in any of the exchange reactions described above, adduct dissociation was considered to be the rate limiting step of the exchange process. Under this assumption, the aforementioned exchange reaction was repeated at various temperatures using the conditions described in Table 2.1 (entry 2). As summarized in Figure 2.5, linear regression was applied to the data obtained and the $\Delta H^{\ddagger}$ and $\Delta S^{\ddagger}$ of the adduct dissociation process was determined using Eqs. 2.1 and 2.2, where k' is Boltzmann's constant and h is Planck's constant.

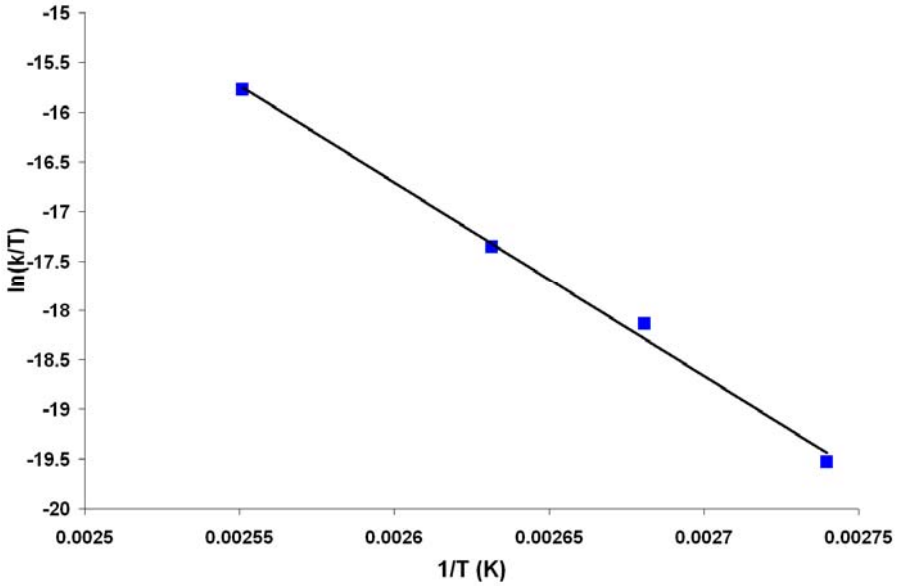

Figure A1. Eyring Plot of of **2.3**→ **2.4**, where k is the first-order rate constant (min^{-1}) and T is the temperature (K). The data was fitted to a linear regression (y = –19574x + 34.184, R2 = 0.9954) which was used to calculate the activation parameters using Eqs. **2.1** and **2.2**, where k′ is Boltzmann's constant and h is Planck's constant.

$$slope = \frac{-\Delta H^{\ddagger}}{R} \qquad \text{(eq.2.1)}$$

$$intercept = \ln\left(\frac{k'}{h}\right) + \frac{\Delta S^{\ddagger}}{R} \qquad \text{(eq2.2)}$$

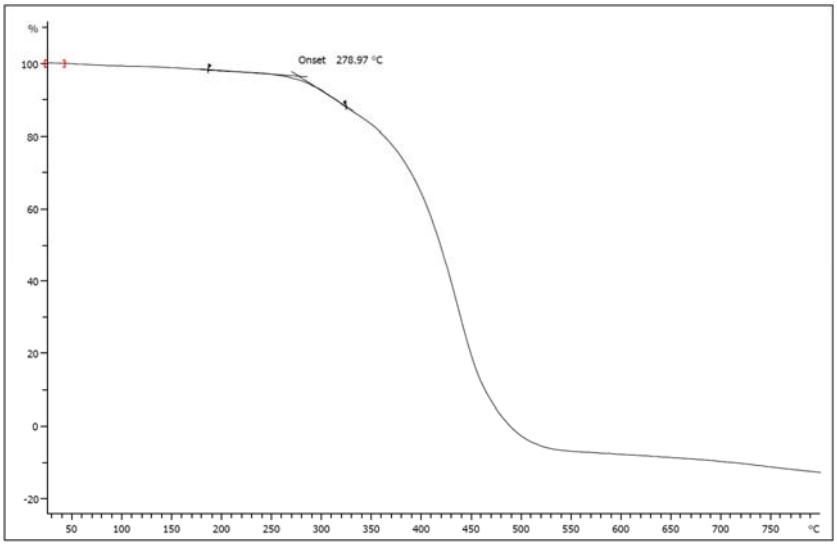

Figure A2. Thermogravigram of **2.7**. Conditions: N_2 atmosphere, ramp rate = 10 °C/min.

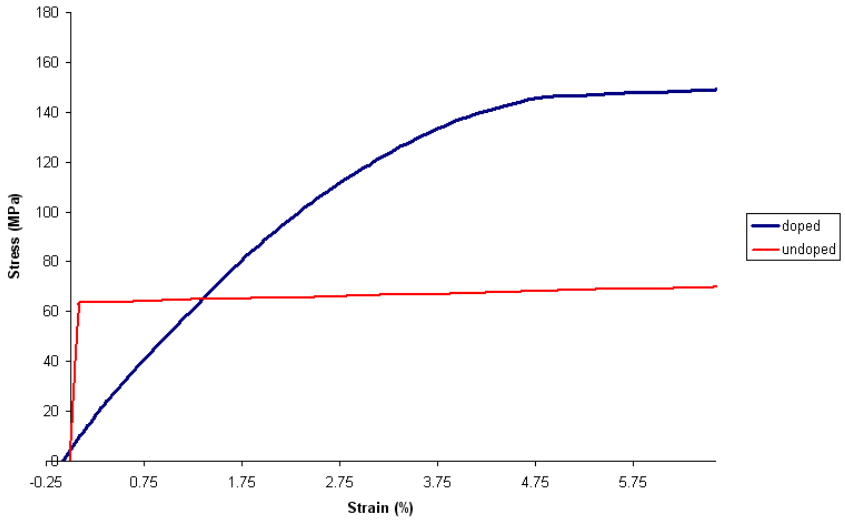

Figure A3. Tensile testing data of a polymer **2.7**. virgin sheet (red line) and after exposure to iodine vapor for 24 hours (blue line).

EXPERMENTAL FOR POLY(TRIAZENE)S

General Considerations. Unless otherwise noted, all reactions were performed under an atmosphere of nitrogen using standard Schlenk techniques or in a nitrogen filled glove-box. Dichloromethane was distilled from calcium hydride and degassed by two freeze-pump-thaw cycles. Tetrahydrofuran and toluene were distilled from Na/benzophenone and degassed by two freeze-pump-thaw cycles. All reagents were purchased from Aldrich or Acros and were used without further purification. 1,4-diazidobenzene[175] (**2a**), 4,4′-diazidobiphenyl[176] (**2b**), 2,7-diamino-9,9-dihexylfluorene,[177] and 1,1,5-trimethylhexylamine[178] were synthesized by known literature procedures. ^{1}H NMR spectra were recorded using a Varian Gemini (300 MHz or 400 MHz) spectrometer. Chemical shifts are reported in delta (δ) units and expressed in parts per million (ppm)

downfield from tetramethylsilane using the residual protio solvent as an internal standard ($CDCl_3$, 7.24 ppm; C_6D_6, 7.15 ppm; CD_2Cl_2, 5.32 ppm; DMSO-*d*$_6$, 2.49 ppm). ^{13}C NMR spectra were recorded using a Varian Gemini (100 MHz) spectrometer. Chemical shifts are reported in delta (δ) units and expressed in parts per million (ppm) downfield from tetramethylsilane using the solvent as an internal standard ($CDCl_3$, 77.0 ppm; C_6D_6, 128.0 ppm; CD_2Cl_2, 53.8 ppm, DMSO-*d*$_6$, 39.5 ppm). ^{13}C NMR spectra were routinely run with broadband decoupling. Gel permeation chromatography (GPC) was performed on a Viscotek system equipped with a VE 1122 pump, a VE 7510 degasser, two fluorinated polystyrene columns (I-MBHW-3078 and I-MBLMW-3078) thermostatted to 30 °C (using a ELDEX CH 150 column heater) and arranged in series, a Viscotek 270 Dual Detector (light scattering detector and differential viscometer), and a VE 3580 refractive index detector. IR spectra were record using Perkin-Elmer Spectrum BX FT-IR system. High-resolution mass spectra (HRMS) were obtained with a VG analytical ZAB2-E or a Karatos MS9 instrument and are reported as m/z (relative intensity). The cyclic voltammetry experiment was conducted using a CH Instruments Electrochemical Workstation (series 700B). The electrochemical cell contained Pt working and counter electrodes and a Ag wire as a quasi reference electrode and the analysis was performed in CH_2Cl_2 using 1 mM analyte and 0.1 M $(Bu_4N)(PF_6)$ as electrolyte, and referenced to $Fe(Cp^*)_2/Fe(Cp^*)_2^+$ at -0.13 V versus SCE at a scan rate = 0.1 V s^{-1}. UV-visible absorption and fluorescence emission spectra were recorded on a Perkin-Elmer Lambda 35 spectrophotometer and a PTI QuantaMaster 4L fluorimeter, respectively. All measurements were made with matched 6Q Spectrosil quartz cuvettes (Starna) with 1 cm path lengths and 3.0 mL sample solution volumes. Beer's law measurements were

performed using 10, 20, 30 and 40 μM sample concentrations. Emission spectra were acquired using 1.0 μM solutions of fluorophore. Quantum yields were determined relative to 1.0 μM quinine sulfate in 0.1 *N* H_2SO_4.[179] All measurements were performed in THF under ambient conditions.

Tetrakis-*N*-(1,1,5-trimethylhexyl)benzobis(imidazolium) bis(tetrafluoroborate). A two-step, one-pot procedure was used to synthesize this compund. Following a previously reported procedure,[180] a 100 mL pressure tube was charged with $Pd(OAc)_2$ (0.171g, 0.76 mmol), *t*BuONa (0.146 g, 1.52 mmol), 1,3-bis(2,6-diisopropylphenyl)imidazolium chloride (0.65 g, 1.5 mmol) and toluene (20 mL). The suspension was stirred for 10 min at ambient temperature until nearly all of the material dissolved. To the resulting orange mixture, 1,2,4,5-tetrabromobenzene (10.0 g, 25.4 mmol), 1,1,5-trimethylhexylamine (14.6 g, 102 mmol), and *t*BuONa (10.0 g, 104 mmol) were added. The reaction was heated to 140 °C for 12 h. After removing precipitated solids *via* filtration, the residual solvent and amine were evaporated under reduced pressure at 65 °C to obtain dark oil, which was sufficiently pure to use without additional purification. ^{1}H NMR (C_6D_6): δ 6.68 (s, 2H), 3.60 (br, 4H), 1.63-0.95 (m, 76H). ^{13}C NMR (C_6D_6): δ 132.0, 114.9, 54.3, 43.5, 40.1, 28.3, 28.1, 22.9, 22.6. HRMS calcd. for $C_{42}H_{82}N_4$: 642.6539; Found: 642.6534. The crude 1,2,4,5-tetrakis-*N*-(1,1,5-trimethylhexyl)benzene was added to degassed $HC(OMe)_3$ (150 mL), followed by HBF_4 (7.3 mL, 50 wt% in Et_2O). The mixture was then stirred for 1 h. The resulting precipitate was collected *via* filtration, washed with excess Et_2O (100 mL) and then dried

at 45 °C under high vacuum to afford 12.5 g (59% yield over two steps) of the desired product as tan solid. ^{1}H NMR (DMSO-d_6): δ 9.06 (s, 2H), 8.6 (s, 2H), 2.22 (br, 8H), 1.92 (s, 24 H), 1.37 (septet, J = 6.8 Hz, 4H), 1.03-0.96 (br, 16 H), 0.65 (d, J = 6.8 Hz, 24H). ^{13}C NMR (DMSO-d_6): δ 144.0, 128.9, 102.5, 65.3, 38.7, 38.1, 26.9, 26.5, 22.1, 20.8. HRMS: [M+] calcd. for $C_{44}H_{80}N_4$: 664.6383; Found: 664.6387.

Tetrakis-*N*-(1,1,5-trimethylhexyl)benzobis(imidazolylidene) (1a). A 250 mL flask was charged with tetrakis-*N*-(1,1,5-trimethylhexyl)benzobis(imidazolium) bis(tetrafluoroborate) (10.0 g, 11.9 mmol), THF (125 mL), and sodium hexamethyldisilazide (4.45 g, 24 mmol). After stirring the resulting mixture at ambient temperature for 2 h, it was filtered through Celite. The residual solvent then removed under reduced pressure to obtain 7.9 g (100% yield) of the desired product as tan solid. ^{1}H NMR (C_6D_6): δ 7.93 (s, 2H), 2.16-2.11 (br, 8H), 1.90 (s, 24H), 1.41-1.07 (br, 20H), 0.76 (d, J = 8.4 Hz, 24H). ^{13}C NMR (C_6D_6): δ 229.9, 131.1, 96.9, 59.9, 41.4, 40.0, 29.5, 27.8, 22.7, 21.9. HRMS: [M+] calcd. for $C_{44}H_{79}N_4$: 662.6248; Found: 662.6254.

3,3',4,4'-Tetra(2,2-dimethylbutyrylamido)biphenyl. A flask was charged with 3,3′-diaminobenzidine tetrahydrochloride (5.00 g, 0.0139 mol) and a stir bar, and then fitted with a rubber septum. The flask was then evacuated and back-filled with dry nitrogen followed by the addition of CH_2Cl_2 (250 mL) and 2,2-dimethylbutyryl chloride (8.01 mL, 0.0583 mol). After stirring the resulting mixture for 5 min, triethylamine (15.8 mL, 0.114 mol) was slowly added. The reaction mixture was then stirred for 18 h at ambient

temperature. Removal of the solvent produced a brown solid that was washed with excess water and then dried under vacuum at 70 °C to afford 7.92 g (99% yield) of the desired compound. ^{1}H NMR ($CDCl_3$): δ 8.86 (s, 2H), 8.68 (s, 2H), 7.60 (s, 2H), 7.207 (d, J = 8.4 Hz, 2H), 6.93 (d, J = 7.8, 2H), 1.71 (m, 8H, CH_2), 1.31 (s, 12H), 1.28 (s, 12H), 0.92 (q, J = 7.1, 12H). ^{13}C NMR ($CDCl_3$): δ 177.9, 177.3, 135.8, 130.8, 129.7, 125.3, 122.8, 121.7, 43.4, 43.3, 33.9, 33.7, 25.2, 25.1, 9.3. HRMS: [M^+] calcd. for $C_{36}H_{54}N_4O_4$: 606.4145; Found: 606.4150.

1,1′,3,3′-Tetra(2,2-dimethylbutyl)-5,5′-bibenzimidazolium bis(tetrafluoroborate). After charging a flask equipped with a reflux condenser and a stir bar with 3,3',4,4'-tetra(2,2-dimethylbutyrylamido)biphenyl (7.00 g, 0.0115 mol), it was evacuated and back-filled with nitrogen followed by THF (250 mL). In a separate flask, $LiAlH_4$ (3.50 g, 0.092 mol) was dispersed in THF (50 mL) and then slowly added to the aforementioned reaction vessel over a period of 5 min. After refluxing the mixture for 18 h, the solvent was removed under reduced pressure. The crude product was then dissolved in degassed Et_2O (200 mL) and cooled to 0 °C. Residual $LiAlH_4$ was quenched through slow addition of degassed 10% (aq) sodium hydroxide (4 mL) followed by degassed water (12 mL). The organic layer was then dried over sodium sulfate, which was later removed through filtration. The solvent was then removed under reduced pressure. A solution of 48% (aq) tetrafluoroboric acid (8.40 mL, 0.0461 mol) in trimethylorthoformate (150 mL) was then added, and the resulting mixture was heated to 90 °C. After 30 min, the solvent was removed and the off white solid was washed with copious THF to afforded 8.34 g

(97% yield) of desired product as a white powder. ^{1}H NMR (DMSO-d_6): δ 9.71 (s, 2H), 8.55 (s, 2H), 8.31 (d, J = 8.8, 2H), 8.13 (d, J = 8.8, 2H), 4.51 (s, 4H), 4.46 (s, 4H), 1.41 (m, 8H), 0.96 (24H), 0.92 (m, 12H). ^{13}C NMR (DMSO-d_6): δ 145.0, 137.9, 133.4, 132.5, 126.7, 115.5, 113.2, 56.8, 56.6, 36.2, 32.2, 32.1, 24.2, 8.5. HRMS m/z calcd for $C_{38}H_{60}N_4F_4B$ [M+]: 659.4839; Found: 659.4842.

1,1′,3,3′-Tetra(2,2-dimethylbutyl)-5,5′-bibenzimidazolylidene (1c). A 30 mL vial was charged with 1,1′,3,3′-tetra(2,2-dimethylbutyl)-5,5′-bibenzimidazolium bis(tetrafluoroborate) (1.00 g, 1.33 mmol), a stir bar, and THF (10 mL). Sodium hydride (0.081 g, 3.3 mmol) was then added followed by sodium *tert*-butoxide (0.012 g, 0.113 mmol). After stirring the resulting reaction mixture for 12 h at ambient temperature, it was filtered using a 0.45 μm PTFE filter. Residual solvent was then removed under vacuum to afford 0.713 g (94 % yield) of the desired product as a white powder. ^{1}H NMR (C_6D_6): δ 7.63 (s, 2H), 7.49 (d, J = 8.2, 2H), 7.20 (d, J = 8.2, 2H), 4.12 (s, 4H), 4.073 (s, 4H), 1.42 (m, 8H), 0.99 (24H), 0.94 (m, 8H). ^{13}C NMR (C_6D_6): δ 137.4, 136.0, 135.9, 121.3, 111.0, 110.2, 57.4, 57.3, 37.6, 36.5, 33.2, 25.7, 25.6, 22.7, 18.4, 14.2, 8.6. HRMS m/z calcd for $C_{38}H_{62}N_4$ [M+]: 574.4974; found: 574.4962

2,7-Diazido-9,9-dihexylfluorene (2c). 2,7-Diamino-9,9-dihexylfluorene (5.0 g, 13.7 mmol) was added in small portions to a solution of sodium tetrafluoroborate (3.3 g, 30.1 mmol) in water (30 mL) and HCl (30 mL, 12.1 N) at 0 °C. A solution of sodium nitrite (2.84 g, 41.1 mmol) in water (12 mL) was then slowly added while maintaining the

internal temperature of the reaction below 5 ºC. After 2 h, the precipitated solids were collected by filtration and washed with cold water (40 mL). The wet precipitate was then placed in a flask, suspended in water (60 mL) and then cooled to 0 °C. A solution of sodium azide (2.67 g, 41.1 mmol) in water (10 mL) was then added dropwise to the suspension. After the addition was complete, the reaction was allowed to warm to ambient temperature and then stirred for an additional 1 h. The resulting precipitate was collected by filtration, washed with water (200 mL) and dried under vacuum to afford 5.21 g (91% yield) of the desired product as a yellow powder. ^{1}H NMR (C_6D_6): δ 7.26 (d, *J* = 7.9 Hz, 2H), 7.00 (s, 2H), 6.79 (d, *J* = 5.8 Hz, 2H), 1.76 (m, 4H), 1.05-0.83 (br, 12H) 0.79-0.60 (br, 10H). ^{13}C NMR (C_6D_6): δ 152.9, 139.3, 137.9, 120.9, 118.0, 113.8, 55.6, 40.4, 31.6, 29.8, 23.9, 22.8, 14.0. HRMS calcd. for $C_{25}H_{32}N_6$: 416.2688; Found: 416.2694. FTIR (KBr): ν_{N3} = 2105 cm^{-1}.

1,2,4,5-Tetra(2,2-dimethylbutyrylamido)benzene A flask was charged with 1,2,4,5-tetraaminobenzene tetrahydrochloride (4.05 g, 0.0143 mol) and a stir bar, and then fitted with a rubber septum. The flask was then evacuated and back-filled with dry nitrogen followed by the addition of CH_2Cl_2 (90 mL) and 2,2-dimethylbutyryl chloride (8.24 mL, 0.0599 mol). After stirring the resulting mixture for 5 min, triethylamine (16.32 mL, 0.117 mol) was slowly added. The reaction mixture was then stirred for 18 h at ambient temperature. Removal of the solvent produced a brown solid that was washed with excess water and then dried under vacuum at 70 °C to afford 7.35 g (97% yield) of the desired compound. ^{1}H NMR (DMSO d_6): δ 9.04 (s, 4H), 7.528 (s, 2H), 1.57 (q, J= 7.5

Hz, 8H), 1.15 (s, 24H), 0.807 (t, *J* =7.5 Hz, 12H), ^{13}C NMR (DMSO d_6): δ 176.17, 128.1, 121.5, 42.6, 33.0, 24.7, 9.1. HRMS [M^+] calcd. for $C_{30}H_{50}N_4O_4$: 530.3832, found 530.3835.

Tetrakis-*N*-(2,2-dimethylbutyl)benzobis(imidazolium) bis(tetrafluoroborate) After charging a flask equipped with a reflux condenser and a stir bar with 3,3',4,4'-tetra(2,2-dimethylbutyrylamido)biphenyl (2.00 g, 0.00377 mol), it was evacuated and back-filled with nitrogen followed by THF (200 mL). In a separate flask, $LiAlH_4$ (1.11 g, 0.0300 mol) was dispersed in THF (20 mL) and then slowly added to the aforementioned reaction vessel over a period of 5 min. After refluxing the mixture for 18 h the reaction was cooled to 0 °C. Residual $LiAlH_4$ was quenched through slow addition of degassed 10% (aq) sodium hydroxide (4 mL) followed by degassed water (12 mL). The organic layer was then dried over sodium sulfate, which was later removed through filtration. The solvent was then removed under reduced pressure. A solution of 48% (aq) tetrafluoroboric acid (1.035 mL, 0.00792 mol) in trimethylorthoformate (25 mL) was then added, and the resulting mixture was allowed to stand at room temperature. After 30 min, the precipitate was collected by filtration and washed with THF which afforded 1.56 g (74% yield) of desired product as a light green powder. ^{1}H NMR (DMSO-d_6): δ 9.89 (s, 2H), 8.90 (s, 2H), 4.5 (s, 8H), 1.41 (q, *J* = 7.4 Hz, 8H), 0.94 (s, 24H), 0.882 (t, J= 7.5 Hz 12H), 1.41 (m, 8H), 0.96 (24H), 0.92 (m, 12H). ^{13}C NMR (DMSO-d_6): δ 147.6, 131.7, 100.1, 57.3, 36.3, 32.2, 23.9, 8.5.

Tetrakis-*N*-(2,2-dimethylbutyl)benzobis(imidazolylidene) (1b)). A 30 mL vial was charged with 1 Tetrakis-*N*-(2,2-dimethylbutyl)benzobis(imidazolium) bis(tetrafluoroborate (.503 g, 0.905 mmol), a stir bar, and THF (10 mL). Sodium hydride (0.0481 g, 1.90 mmol) was then added followed by sodium *tert*-butoxide (0.0868 g, 0.905 mmol). After stirring the resulting reaction mixture for 6 h at ambient temperature, it was filtered using a 0.45 μm PTFE filter. Residual solvent was then removed under vacuum to afford 0.250 g (52 % yield) of the desired product as a light orange powder. ^{1}H NMR (C_6D_6): δ 7.13 (s, 2H), 4.15 (s, 8H), 1.45 (q, *J* = 7.5 Hz, 8H), 1.02 (s, 24H), 0.94 (t, J=7.5 Hz, 12H). ^{13}C NMR (C_6D_6): δ 234.6, 132.7, 91.2, 57.4 36.3 33.0, 25.4, 8.3 HRMS m/z calcd for $C_{32}H_{57}N_4$ [M+]: 497.4580; found: 497.4577

Typical Polymerization: In a glove box a 5 ml vial was charged with a stir bar and 138 mg (0.296 mmol) of **1b** and then dissolved in 1.3 ml of dry/degassed THF. In a separated 5 vial 123 mg (0.296 mmol) of **2c** was issolved in 1.3 ml of dry/degassed THF. The solution of **2c** was then added to the solution of **1b** and the contents were then transferred back and forth between the two vials to assure good mixing and correct stoichiometry. The reaction was then capped with a Teflon coated lid and stirred at room temperature for 24 hrs. The product was collected by precipitating into 200 ml of pentane and filtered to yield 211 mg (81%) of **3d**.

Polymer (3a). Isolated yield: 98%. ^{1}H NMR ($CDCl_3$): δ 7.82 (s, 2H), 7.58 (s, 4H), 7.05 (end-group (2H), 0.05H), 2.22-0.65 (br, 72H). ^{13}C NMR (CD_2Cl_2): δ 162.3, 150.4, 128.0,

121.7, 99.4, 64.9, 41.9, 38.9, 29.9, 27.8, 22.3, 22.0. GPC: M_n = 34.8 kDa, PDI = 1.8. TGA: T_d = 154 ºC. UV-Vis: λ_{max} = 485 nm, ε = 49700 $M^{-1}cm^{-1}$. Anal. calcd (%) for $C_{50}H_{82}N_{10}$: C, 72.95; H, 10.04; N, 17.01; found: C, 72.67; H, 10.24; N, 17.09.

Polymer (3b). Isolated yield: 95%. ^{1}H NMR ($CDCl_3$): δ 7.82 (s, 2H), 7.77-7.54 (br, 8H), 7.13-7.10 (end-group (4H), 0.11H), 2.16-0.75 (br, 72H). ^{13}C NMR ($CDCl_3$): δ 162.4, 151.0, 128.3, 127.8, 127.0, 121.7, 119.3, 99.4, 77.2, 65.0, 41.9, 38.8, 30.1, 29.5, 28.5, 27.8, 27.6, 22.7, 22.5, 21.9, 14.0. GPC: M_n = 27.5 kDa, PDI = 1.6. TGA: T_d = 157 ºC. UV-Vis: λ_{max} = 434 nm, ε = 36700 $M^{-1}cm^{-1}$. Anal. calcd (%) for $C_{56}H_{86}N_{10}$: C, 74.79; H, 9.64; N, 15.57; found: C, 74.91; H, 9.51; N, 15.48.

Polymer (3c). Isolated yield: 76%. ^{1}H NMR ($CDCl_3$): δ 7.83 (s, 2H), 7.58 (s, 6H), 7.09-6.95 (end-group (3H), 0.10H), 2.21-0.68 (br, 72H). ^{13}C NMR (CD_2Cl_2): δ 162.2, 151.8, 150.9, 139.5, 127.8, 67.9, 64.7, 55.0, 41.8, 40.8, 3.8.8, 31.6, 30.1, 29.8, 27.6, 25.6, 23.7, 22.6, 22.4, 21.8, 17.2, 17.2, 14.0. GPC: M_n = 23.9 kDa, PDI = 1.8. TGA: T_d = 160 ºC. UV-Vis: λ_{max} = 450 nm, ε = 33800 $M^{-1}cm^{-1}$. Fluorescence: λ_{em} = 546 nm (ϕ = 0.2%); λ_{em} = 372 nm (ϕ = 6.4%). Anal. calcd (%) for $C_{69}H_{110}N_{10}$: C, 76.76; H, 10.27; N, 12.97; found: C, 76.51; H, 10.44; N, 13.03.

Polymer (3d). Isolated yield: 65%. ^{1}H NMR (CD_2Cl_2): δ 7.8–7.6 (m br, 6H), 7.04 (br, 2H), 6.9 (s, endgroup(1H), 0.29H), 4.4 (br, 8H), 2.05 (br, 4H), 1.5 (br, 8H), 1.2-0.7 (m br, 58H) ^{13}C NMR

($CDCl_3$):δ 155.8,152.1, 150.9, 139.8, 128.9, 119.7, 92.1, 55.2, 40.8, 37.8, 33.9, 31.6, 31.6 , 29.8, 29.7, 25.0, 24.8, 23.9, 22.6, 22.6, 13.8, 8.1 GPC: M_n = 17.6 kDa, PDI = 1.2. T_d = 262 ºC. UV-Vis: λ_{max} = 476 nm, ε = 43800 $M^{-1}cm^{-1}$. Fluorescence: λ_{em} = 547 nm (ϕ = 0.1%). Anal. calcd (%) for $C_{57}H_{86}N_{10}$: C, 75.12; H, 9.51; N, 15.37; found: C, 72.56; H, 9.30; N, 14.44.

Polymer (3e). Isolated yield: 96%. ^{1}H NMR ($CDCl_3$): δ 7.79-7.57 (br, 6 H), 7.43-7.17 (br, 4H), 7.06 (end-group (2H), 0.06H), 4.65-4.23 (br, 8H), 1.56-1.40 (br, 8H), 1.17-0.74 (br, 36H). ^{13}C NMR ($CDCl_3$): δ 155.8, 150.2, 135.3, 133.4, 132.3, 122.1, 121.1, 108.5, 77.2, 67.9, 53.8, 37.9, 33.6, 31.1, 25.5, 25.3, 25.2, 8.3. GPC: M_n = 27.6 kDa, PDI = 2.3. T_d = 282 ºC. UV-Vis: λ_{max} = 437 nm, ε = 35900 $M^{-1}cm^{-1}$. Anal. calcd (%) for $C_{44}H_{62}N_{10}$: C, 72.29; H, 8.55; N, 19.16; found: C, 72.39; H, 8.48; N, 18.95.

Polymer (3f). Isolated yield: 95%. ^{1}H NMR ($CDCl_3$): δ 7.79-7.17 (br, 14H), 7.06 (br, end-group (4h), 0.15H), 4.65-4.23 (br, 8H), 1.56-1.40 (br, 8H), 1.17-0.74 (br, 36H). ^{13}C NMR ($CDCl_3$): δ 156.0, 150.6, 138.9, 135.4, 133.4, 132.3, 128.6, 127.1, 122.0, 110.2, 106.6, 107.7, 77.2, 53.8, 38.0, 33.7, 25.3, 25.2, 8.4, 8.3. GPC: M_n = 22.7 kDa, PDI = 2.3. T_d = 282 ºC. UV-Vis: λ_{max} = 379 nm, ε = 47900 $M^{-1}cm^{-1}$. Anal. calcd (%) for $C_{50}H_{66}N_{10}$: C, 74.40; H, 8.24; N, 17.35; found: C, 74.49; H, 8.38; N, 17.09.

Polymer (3g). Isolated yield: 72%. ^{1}H NMR ($CDCl_3$): δ 7.8-7.12 (br, 12H), 7.07 (br, end-group (3H), 0.13H), 4.65-4.23 (br, 8H), 1.56-1.40 (br, 8H), 1.17-0.74 (br, 36H). ^{13}C NMR ($CDCl_3$): δ 156.0, 151.9, 146.8, 139.9, 135.3, 133.5, 132.3, 121.0, 119.7, 117.0, 110.1, 108.5, 85.3, 77.2, 55.1, 53.6, 40.8, 38.0, 37.2, 34.0, 33.6, 31.6, 29.8, 25.3, 25.2, 23.8, 22.6, 22.3, 16.9, 14.0, 14.0, 8.4, 8.3. GPC: M_n = 19.9 kDa, PDI = 1.9. T_d = 278 ºC. UV-Vis: λ_{max} = 436 nm, ε = 37400 $M^{-1}cm^{-1}$. Fluorescence: λ_{em} = 375 nm (ϕ = 4.9%). Anal. calcd (%) for $C_{63}H_{90}N_{10}$: C, 76.63; H, 9.19; N, 14.18; found: C, 76.69; H, 9.23; N, 14.01.

EXPERIMENTAL FOR RAFT

General Considerations: THF was distilled from CaH_2 under an atmosphere of nitrogen prior to use. All other solvents were used as received without further purification. Styrene was filtered through a short plug of alumina to remove radical inhibitor and then degassed by performing three consecutive freeze-pump-thaw cycles. All other chemicals were purchased from Aldrich, Alfa Aesar, or Fisher and were used without further purification. The 1,3-dimesitylimidazol-2-ylidene (**4.1**) was synthesized using known[181] procedures, however it is commercially-available from Strem Chemicals. Likewise, the precursor to this N-heterocyclic carbene, 1,3-dimesitylimidazolium chloride, is also available from Strem Chemicals. ^{1}H NMR spectra were recorded using a Varian Unity Plus 400 spectrometer. Chemical shifts are reported in delta (δ) units, expressed in parts per million (ppm) downfield from tetramethylsilane using the residual protio solvent as an internal standard ($CDCl_3$, 7.26 ppm; C_6D_6, 7.15 ppm; DMSO-d_6, 2.50 ppm). ^{13}C NMR spectra were recorded using a Varian Gemini 300 spectrometer. Chemical shifts are reported in delta (δ) units, expressed in parts per million (ppm)

downfield from tetramethylsilane using the solvent as an internal standard ($CDCl_3$, 77.0 ppm; C_6D_6, 128.0 ppm; DMSO-d_6, 39.5 ppm). ^{13}C NMR spectra were routinely run with broadband decoupling. ^{19}F NMR spectra were recorded using a Varian Inova 500 spectrometer. Chemical shifts are reported in delta (δ) units, expressed in parts per million (ppm) downfield from Freon 11 ($CFCl_3$, 0 ppm; external standard). High-resolution mass spectra (HRMS) were obtained with a VG analytical ZAB2-E or a Karatos MS9 instrument and are reported as m/z (relative intensity). Gel permeation chromatography (GPC) was performed on either a Viscotek system equipped with a VE 1122 pump, a VE 7510 degasser, two fluorinated polystyrene columns (I-MBHW-3078 and I-MBLMW-3078) thermostatted to 30 °C (using a ELDEX CH 150 column heater) and arranged in series, a Viscotek 270 Dual Detector (light scattering detector and differential viscometer), and a VE 3580 refractive index detector, or a Waters HPLC system consisting of HR-1, HR-3, and HR-5E Styragel® columns arranged in series, a 1515 pump, and a 2414 RI detector. Molecular weight and polydispersity data are reported relative to polystyrene standards in THF (Viscotek system) or DMF/LiBr (Waters system). X-ray crystal structure data was collected for **4.3** (CCDC 653951) and deposited with the Cambridge Crystallographic Data Centre, 12 Union Road, Cambridge CB2 1EZ, UK.

1,3-Dimesitylimidazolium-2-carbodithioate (4.2): In a nitrogen-filled drybox, 1,3-dimesitylimidazol-2-ylidene (**4.1**) (340 mg, 1.12 mmol) was dissolved in dry THF (15 mL) in a 20 dram vial. After adding excess CS_2 (2.0 mL, 21 mmol), the reaction was stirred for 2 h at ambient temperature. Subsequent concentration of the reaction mixture under reduced pressure afforded 419 mg (99% yield) of the desired compound as a brown solid. ^1H NMR (DMSO-d_6): δ 7.83 (s, 2H, N-CH=C), 7.02 (s, 4H, Ar-H), 2.27 (s, 6H, p-

CH3), 2.22 (s, 12H, o-CH3). ^{13}C NMR (DMSO-d_6): δ 139.8, 135.4, 129.0, 109.3, 81.6, 48.5, 18.1. HRMS: [M+] calcd for $C_{22}H_{24}N_2S_2$: 381.1381; found: 381.1380.

Benzyl 1,3-Dimesitylimidazolium-2-carbodithioate Bromide (4.3): After dissolving **4.2** (419 mg, 1.10 mmol) in acetonitrile (25 mL), benzyl bromide (0.261 mL, 220 mmol) was added. The reaction was then sealed and heated to 85 °C for 24 h. Subsequent removal of solvent under reduced pressure afforded dark purple oil which was later dissolved in ethanol and triturated with excess hexanes. Collection of the resulting pale pink precipitate via filtration afforded 562 mg (93% yield) of the desired compound. ^{1}H NMR (DMSO-d_6): δ 8.55 (s, 2H, N-CH=C), 7.26 – 7.07 (m, 8H, Ar-H), 6.80 (d, 2H, J = 7.2 Hz, Ar-H), 4.58 (s, 2H, Ar-CH2-S), 2.33 (s, 6H, p-CH3), 2.08 (s, 12H, o-CH_3). ^{13}C NMR (DMSO-d_6): δ 141.8, 141.4, 135.4, 133.8, 130.5, 130.3, 129.1, 120.0, 126.9, 21.3, 18.1. HRMS: [M+] calcd for $C_{29}H_{31}N_2S_2$: 471.1923; found: 471.1929. An alternative, high-yielding synthesis of **4.3** that utilized a commercially-available imidazolium salt and did not require the use of a drybox was also developed: A flask was charged with 1,3-dimesitylimidazolium chloride (0.200 g, 0.586 mmol), NaH (0.020 g, 0.833 mmol), t-BuOK (0.002 g, 0.018 mmol) and a stir bar. Dry THF (50 mL) was then added and the resulting mixture was stirred at 50 °C for 3 h under an atmosphere of N_2. The mixture was then taken up into a syringe and filtered through a PTFE 0.45 μm syringe filter into stirred CS_2 (10 mL). After 1 h at room temperature, the resulting mixture was concentrated to 20 mL and then diluted with CH_3CN (30 mL). Benzyl bromide (1.00 g, 5.85 mmol) was then added in one portion which resulted in a color change from brown to dark purple. After stirring the reaction mixture at 50 °C for 2 h, solvent was evaporated under reduced pressure. The resulting dark pink oil was taken up into CH_2Cl_2 (4 mL) and then poured into excess hexanes (200 mL), which caused solids to precipitate. The solids were collected via filtration and dried to afford

0.290 g (96%) of **4.3** as a pale pink powder. Crystals suitable for X-ray analysis were obtained by slow evaporation of a saturated ethyl acetate solution. Crystal data for **4.3** ($C_{29}H_{33}N_2OS_2Br$): M = 569.60, T = 200(2) K, λ = 0.71073 Å, triclinic, space group P-1, a = 9.5660(2) Å, b = 11.5100(2) Å, c = 14.3890(3) Å, α = 100.183(1)°, β = 97.3290(12)°, γ = 100.406(1)°, V = 1430.41(5) Å3 , Z = 2, Dx (calcd) = 1.322 mg m-3, μ = 1.607 mm-1, F(000) = 592, Crystal size: 0.24 x 0.20 x 0.10 mm (red prisms), θrange = 1.94 to 27.48°, 17286 measured reflections, 6491 independent reflections [R(int) = 0.0382]), 340 restraints, 414 parameters, GOF = 1.026, Final R indices [I>2σ(I)]: R1 = 0.0552, wR2 = 0.1247; R indices (all data): R1 = 0.081, wR2 = 0.1389. Crystallographic data for this structure has been deposited with the Cambridge Crystallographic Data Centre (12 Union Road, Cambridge CB2 1EZ, UK) as CCDC 667711.

Benzyl 1,3-Dimesitylimidazolium-2-carbodithioate Tetrafluoroborate (**4.4**): In a nitrogen-filled drybox, a 20 dram vial was charged **4.3** (500 mg, 0.906 mmol), dry CH_2Cl_2 (3 mL), triethyloxonium tetrafluoroborate (207 mg, 1.09 mmol) and a stir bar. The vial was then sealed and stirred at room temperature for 24 h. Excess triethyloxonium tetrafluoroborate was quenched by adding methanol (1 mL) followed by stirring for an additional 2 h. Afterward, the resulting solution was poured into excess ether which caused solids to precipitate. The solids were subsequently collected by vacuum filtration and dried to afford 501 mg (99% yield) of the desired compound as a pale pink powder. ^{1}H NMR ($CDCl_3$): δ 7.82 (s, 2H, N-CH=C), 7.24 – 7.21 (m, 1H, Ar-H), 7.14 (t, 2H, J = 7.6 Hz, Ar-H), 6.95 (s, 4H, Ar-H), 6.81 (d, 2H, J = 7.9 Hz, Ar-H), 4.39 (s, 2H, Ar-CH2-S), 2.33 (s, 6H, p-CH3), 2.09 (s, 12H, o-CH3). ^{13}C NMR ($CDCl_3$): δ 141.8, 134.7, 132.2, 129.9, 129.7, 128.6, 128.2, 126.2, 41.0, 21.1, 17.8. ^{19}F NMR ($CDCl_3$): δ –152.7, –152.8.

Representative Polymerization Procedure: In a nitrogen filled drybox, a vial was charged with **4.4** (53.0 mg, 0.096 mmol), 1,2,3-trimethoxybenzene (100 mg, 0.59 mmol), azobisisobutyronitrile (16.0 mg, 0.096 mmol), and a stirbar. After styrene (2.00 g, 19.2 mmol) was added, the vial was placed into a 70 °C oil bath. To monitor the polymerization reaction, aliquots were periodically removed from the reaction mixture over time and analyzed by either gas chromatography or NMR spectroscopy. After 15 h (77% conversion), the vial was opened to air and diluted with THF (1.0 mL). The diluted reaction mixture was then poured slowly into excess MeOH (100 mL), which caused solids to precipitate. The solids were collected by vacuum filtration and dried under vacuum. Based on monomer conversion, the theoretical M_n (16.6 kDa) was found to be consistent with the GPC-determined M_n of 15.9 kDa (PDI = 1.22).

End-group Analysis Using ^{19}F NMR Spectroscopy: A polystyrene (139 mg, 0.71 μmol) with a M_n = 19.6 kDa (determined by GPC) previously prepared using **4.4** as described above was dissolved in 0.8 mL of $CDCl_3$. Analysis of this solution using ^{19}F NMR spectroscopy revealed two distinct BF_4 signals at δ –152.6 and –152.7 ppm in a 4 : 1 ratio, respectively, which is in accord with the isotopic distribution of boron. 1,2,4,5-Tetrafluorobenzene (0.88 μL, 0.84 μmol) was then added as an internal standard, and the resulting polymer solution was analyzed using ^{19}F NMR spectroscopy. Integrating the ^{19}F NMR signals attributed to the standard (δ –138.7 ppm) relative to those of derived from the BF_4 revealed that these two compounds were present a ratio of 55 : 45, respectively. Using the known concentration of the standard, the M_n of the polymer was calculated to be 16.6 kDa.

EXPERIMENTAL FOR BLEND MEMBRANES

Materials. Toluene, tetrahydrofuran (THF), dimethylformamide (DMF), dimethylsulfoxide (DMSO), dimethylacetamide (DMAc), and sulfuric acid were

purchased from Fisher Scientific. Imidazole was purchased from ICN Biomaterials. 4-Nitroimidazole was purchased from TCI Japan. 4,5-Dicyanoimidazole was purchased from TCI America. Benzimidazole was purchased from Acros Organics. sPEEK samples were prepared by the sulfonation of poly(ether ether ketone) (PEEK 450 PF; Victrex) via treatment with concentrated sulfuric acid in accord with literature procedures.[142d] In particular, 5 g of PEEK was dissolved in 150 mL of concentrated sulfuric acid (95.9 %) and then vigorously stirred at ambient temperature for up to 40 h. The reaction mixture was then poured into cold water, causing sPEEK to precipitate. The precipitate was collected via filtration, thoroughly rinsed with de-ionized water and then dried at 60 °C for 24 h. The degree of sulfonation (DS) in this material was determined to be 58% using known protocols. [142d]

Equipment. Proton conductivity values of the membranes were collected with a computer interfaced HP 4192 ALF Impedance Analyzer (Agilent Technologies, Inc., Santa Clara, CA, USA). Molecular weights were determined via gel permeation chromatography system composed of a Waters 1515 isocratic pump, 3 Viscotek I-series columns (2 x GMHHRH and 1 x G3000HHR) arranged in series, and a Waters 2414 detector and calibrated with a series of polystyrene standards in DMF.

Determination of heterocycle pKa. A series of 125 mL Erlenmeyer flasks were independently charged with either imidazole, benzimidazole, 4-nitroimidazole, or 4,5-dicyanoimidazole and dissolved in water to create a 0.05 M solutions of the heterocycle. The solutions were then acidified to pH = 2 using a 0.10 M aqueous solutions of HCl. The pH of the solutions were measured as they were titrated with 0.10 M aqueous solution of NaOH using a Symphony SP70P pH meter. The pKa was calculated by interpolation of the titration curve to find the pH at half the volume of base added to reach the equivalence point. The experimentally-determined pKa values of the conjugate

acid of various heterocycles at 23 °C were as follows: imidazole, 14.9; benzimidazole, 12.5; 4-nitroimidazole, 8.0 [93]; 4,5-dicyanoimidazole, 5.75, and were found to be consistent with values reported in the literature.[182,183]

Synthesis of Blended sPEEK Membranes. A series of 10 mL vials were charged with 0.150 g of sPEEK (M_n = 42.1 kDa, degree of sulfonation = 58%) and 0.50, 0.70, or 1.0 mL of 0.05 M solutions of either imidazole, benzimidazole, 4-nitroimidazole, or 4,5-dicyanoimidazole in DMAc. The resulting solutions were then poured into separate 6 cm diameter Petri dishes and dried in an oven thermostatted to 90 °C for 15 h. The resulting membranes were soaked in water to release them from the Petri dishes and then dried for an additional 2 h at 90 °C. This procedure produced robust membranes that could be handled and evaluated as described below.

Ion-exchange Capacity (IEC) and Measurements. IEC values was determined by suspending 0.1 – 0.2 g sPEEK and sPEEK/heterocycle blend membranes in 2.0 M NaCl solution (30 mL) for 24 h followed by titration with a standardized 0.05 N NaOH solution using phenolphthalein as the indicator.

Determination of Proton Conductivities. Membrane impedances were measured by assembling a cell consisting of a 1.5 cm x 1.5 cm piece of the membrane (thickness 40-50 μm) sandwiched between two circular stainless steel electrodes (1 cm2 area) and then analyzed using an HP 4192A LF impedance analyzer in the frequency range of 5 Hz to 13 MHz with an applied voltage of 10 mV. The cell was then placed in a furnace and was stabilized for 20 min at a series of temperatures before the impedence of the cell was measured. The temperature was then slowly increased from 25 °C to 150 °C, and then twice repeated with a fresh membrane. Error values were calculated by the measurement's standard deviation. Membrane thickness was measured by using a micrometer and the proton conductivity was calculated using the following equation:

$$\sigma = \frac{L}{A \times R} \qquad \text{eq. 5.1}$$

where L is the thickness of the membrane in cm, A is the area of the electrode in cm^2 and R is the impedance of the membrane in Ohms (Ω).

EXPERIMENTAL FOR CROSSLINKED MEMBRANES

General Considerations: *N,N*-Dimethylacetamide (DMAc) was purchased from Fisher Scientific, 1,3-propane sultone was purchased from MP Biomedicals LLC, and propargyl alcohol and 1,7-octadiyne were purchased from Acros Organics. Udel® P-1700 was purchased from Solvay Advanced Polymers. Nafion® 117 was purchased from DuPont. All reagents were used as received. Membranes were cast from solution in a 10 cm diameter custom-made flat-bottom sealed vessel under an atmosphere of nitrogen. Infrared (IR) spectra were recorded on a Perkin Elmer Spectrum BX FTIR spectrophotometer. High resolution mass spectra (HRMS) were obtained with a VG analytical ZAB2-E instrument (CI). NMR spectra were recorded on Varian UNITY+ 300, Varian Mercury 400, and Varian INOVA 500 spectrometers. Chemical shifts (δ) are given in ppm and are referenced downfield from residual protiated solvent (^{1}H: DMSO-d_6, 2.49 ppm; ^{13}C: DMSO-d_6, 39.5 ppm). Molecular weights were determined by gel permeation chromatography (GPC) using a Waters HPLC system consisting of three Viscotek I-series columns (2 × GMH$_{HR}$H and 1 × G3000H$_{HR}$) arranged in series, a 1515 pump, and a 2414 RI detector and are reported relative to polystyrene standards in DMF (0.1 M LiBr) at 40 °C (column temperature).

Melting points were obtained using a Mel-Temp apparatus and are uncorrected. The IEC (ion exchange capacity) was measured by drying the polymer in a vacuum oven at 70 ºC and then stirring in a 2M NaCl solution for 1 h. The resulting polymers were

then titrated with an 8 mM solution of NaOH using phenolphthalein as an endpoint indicator.

Methanol Permeability Measurements

Methanol permeability measurements were conducted in a glass cell consisting of two chambers, each with a total volume of 100 mL.[184] Magnetic stir bars were added to each chamber. The membrane was sandwiched between two rubber circular gaskets (internal diameter of 3 cm) and then clamped together. One side of the cell was filled with 80 mL of 1 M methanol and 0.01 M ethanol as an internal standard. The other side (analyte) was filled with 80 mL of 0.01 M ethanol. The chambers were then sealed with septa and each side was stirred with a magnetic stir bar. The concentration of methanol in the analyte side was measured by gas chromatography and integrated against the ethanol internal standard over time. The methanol permeability was calculated according to equation 6.1, where C_a and C_b refer to the methanol concentration in the feed and the permeate, respectively, V_b refers to the solution volume of permeate, and L, A, and t refer, respectively, to the membrane thickness, membrane area, and time.[185]

$$P = \frac{C_b V_b L}{A C_a t} \qquad \text{(Eq. A1)}$$

Syntheses

Polysulfone Containing Pendant Azides (6.2). The azide-functionalized poly(sulfone) **6.2** was synthesized using a modified literature procedure.[186] A 1 L flask was charged with poly(sulfone) (Udel® P-1700) (6.0 g, 13.5 mmol based on its repeat unit, M_N = 20.2 kDa, PDI = 2.12), a Teflon coated magnetic stir bar and THF (400 mL) under nitrogen. After cooling the reaction mixture to –78 ºC, *n*-butyl lithium (2.5 M; 2 equiv, 10.8 mL, 27.0 mmol) was added dropwise over a period of 2 h. In a separate flask,

a solution of *p*-toluensulfonyl azide (7.99 g, 40.5 mmol) in THF (20 mL) was cooled to –40 ºC and then added to the aforementioned polymer solution which caused solids to precipitate. The reaction mixture was then slowly warmed to –30 ºC at which point it became homogeneous. A 4:3 v/v mixture of water:ethanol (800 mL) was then added. The precipitated solids were collected by filtration to afford the desired polymer (6.7 g, 95% yield) as a white powder. Spectroscopic data were consistent with literature values. ^{1}H NMR (400 MHz, $CDCl_3$): δ 8.16 (d, J = 8.8 Hz, 2H), 7.26 (d, J = 8.9 Hz, 4H), 6.98 (d, J = 8.5 Hz, 4H), 6.76 (dd, J = 8.9, 2.3 Hz, 2H), 6.71 (d, J = 2.3 Hz, 2H), 1.71 (s, 6H). GPC (DMF with 0.1 M LiBr, 40 °C): M_N = 22.7 kDa, PDI = 2.01. IR (KBr): υ_{N3} = 2119 cm^{-1}.

Sodium 3-(prop-2-ynyloxy)propane-1-sulfonate (6.1). A 200 mL round bottom flask was charged with a magnetic stir bar, sodium hydride (95%; 1.033 g, 40.9 mmol) and *N,N*-dimethylformamide (DMF) (30 mL). The flask was cooled in an ice bath and a solution of propargyl alcohol (2.39 mL, 40.9 mmol) in DMF (30 mL) was slowly added under continuous stirring over 10 min. A solution of 1,3-propanesultone (5.00 g, 40.9 mmol) DMF (30 mL) was then added slowly. The resulting mixture was stirred on ice for 10 min, warmed to 60 °C and then stirred for an additional 2 h. The reaction was then concentrated under reduced pressure (with the aid of a rotary evaporator) at 60 ºC and diethyl ether (500 mL) was added which caused the product to precipitate. The desired product (7.9 g, 97% yield) was collected via filtration as a white powder. NOTE: in the solid state, the isolated material was found to develop a reddish color and become insoluble over time. However, the material was found to be stable under ambient conditions when dissolved in *N,N*-dimethylacetamide (DMAc) ([**6.1**]$_0$ = 0.503 M). m.p. 120–150 °C (the material turned from white to dark red). ^{1}H NMR (400 MHz, DMSO-d_6): δ 4.05 (d, J = 2.4 Hz, 2H), 3.4 (t, 2H, overlaps with H_2O), 3.35 (t, J = 2.4 Hz, 1H),

2.47 (2H, m, overlaps with DMSO), 1.78 (2H, m). ^{13}C NMR (100 MHz, D_2O) referenced to internal MeOH standard (49.50 ppm): δ 80.1, 76.5, 69.0, 58.2, 48.5, 24.8. HRMS [M-] calcd. for $C_6H_9O_4S$ 177.02215 found 177.02282 IR (KBr): ν = 3478 (broad), 3290, 2945, 2870, 2112, 1638, 1199, 1066, 630 cm^{-1}.

Representative Membrane Casting Procedure (for Homopolymer 6.3d). A 25 mL flask was charged with polymer **6.2** (700 mg, 1.29 mmol based on the molecular weight of its repeat unit), DMAc (5 mL), and a magnetic stir bar. The solution was stirred until the polymer was completely dissolved. After adding a DMAc solution of **6.1** ($[\mathbf{6.1}]_0$ = 0.503 M; 2.44 mL, 1.23 mmol), the reaction vessel was sealed with a septum. After degassing the vessel under reduced pressure, CuI (38.3 mg, 200 μmol) and 1,7-octadiyne (51.0 μL, 0.387 mmol) were added. The resulting mixture was stirred for 30 min at ambient temperature and then filtered through a cotton plug into a custom-built, air-free petri dish as it was continuously purged with nitrogen. The purging was stopped upon completion of the transfer. The chamber was then sealed and heated at 60 ºC in an oven for 12 h. The chamber was then removed from the oven and allowed to cool to ambient temperature. To allow the residual solvent to evaporate, the top of the chamber was removed and the chamber was heated at 60 °C in the oven for an additional 6 h followed by heating at 80 ºC for 12 h. The membrane was released from the cell by adding 100 mL of H_2SO_4 (2 M; 100 mL). Upon removal of the membrane, it was acidified by heating at 80 ºC for 2 h in the presence of H_2SO_4 (2 M; 400 mL) in a 1 L Erlenmeyer flask. Finally, the membrane was washed with 400 mL of de-ionized water at 80 ºC for 2 h before testing.

Representative Membrane Casting Procedure (for Copolymer 6.5a*).* A 50 mL flask was charged with a magnetic stir bar, polymer **6.2** (550 mg, 1.05 mmol based on the molecular weight of the repeat unit), and DMAc (5 mL). The polymer was allowed to completely dissolve before adding a solution of **6.1** in DMAc (($[\mathbf{6.1}]_0$ = 0.503 M; 2.49 mL, 1.25 mmol), and CuI (23 mg, 0.121 mmol). The flask was then sealed with a septum, degassed under reduced pressure for 10 min and then backfilled with nitrogen. The resulting reaction mixture was stirred at ambient temperature for 8 h to generate polymer **6.4**. In a separate vial, polymer **6.2** (200 mg, 0.452 mmol based on the molecular weight of the repeat unit) was dissolved in DMAc (3 mL) and added to the reaction vessel followed by a solution of DMAc (1 mL) containing 1,7-octadiyne (56 µL, 0.43 mmol). The resulting mixture was degassed for 10 min under reduced pressure, backfilled with nitrogen, and then filtered through a cotton plug into a custom-built, air-free chamber as it was purging with nitrogen. After the purging was ceased, the chamber was sealed and heated at 60 ºC in an oven for 12 h. The chamber was then removed from the oven and allowed to cool to ambient temperature. To allow the residual solvent to evaporate, the top of the chamber was removed and the chamber was reheated at 60 ºC for 6 h with the aid of small circulation fan to facilitate drying. Finally, the membrane was dried at 80 ºC for 12 h. The membrane was released from the cell by adding 100 mL of H_2SO_4 (2 M; 100 mL). Upon removal of the membrane, it was acidified by heating at 80 ºC for 2 h in the presence of H_2SO_4 (2 M; 400 mL) in a 1 L Erlenmeyer flask. Finally, the membrane was washed with 400 mL of de-ionized water at 80 ºC for 2 h before testing.

References

[1] The term "conjugated polymer" signifies a macromolecule that exhibits formal chemical unsaturation along its main chain / backbone.

[2] Schwartz, B. J. *Nature Materials* **2008**, *7*, 427–427.

[3] Duan, X.; Liu, L.; Feng, F.; Wang, S. *Acc. Chem. Res.* **2010**, *43*, 260–270.

[4] McQuade, D. T.; Pullen, A. E.; Swager, T. M. *Chem. Rev.* **2000**, *100*, 2537–2574.

[5] Cheng, Y.-J.; Yang, S.-H.; Hsu, C.-S. *Chem. Rev.* **2009**, *109*, 5868–5923.

[6] Günes, S.; Neugebauer, H.; Sariciftci, N. S. *Chem. Rev.* **2007**, *107*, 1324–1338.

[7] Beaujuge, P. M.; Reynolds, J. R. *Chem. Rev.* **2010**, *110*, 268–320.

[8] Yoo, J. E.; Lee, K. S.; Garcia, A.; Tarver, J.; Gomez, E. D.; Baldwin, K.; Sun, Y.; Meng, H.; Nguyen, T.-Q.; Loo, Y.-L. *Proc. Natl Acad. Sci. USA* **2010**, *107*, 5712–5717.

[9] Zotti, G.; Vercelli, B.; Berlin, A. *Acc. Chem. Res.* **2008**, *41*, 1098–1109.

[10] Chabinyc, M. L.; Loo, Y.-L. *Polymer Rev.* **2006**, *46*, 1–5.

[11] Hellström, S.; Zhang, F.; Inganäs, O.; Andersson, M. R. *Dalton Trans.* **2009**, 10032–10039.

[12] Goodson III, T. G. *Acc. Chem. Res.* **2005**, *38*, 99–107.

[13] Schindler, F.; Lupton, J. M.; Feldmann, J.; Scherf, U. *Proc. Natl Acad. Sci. USA* **2004**, *101*, 14695–14700.

[14] Zheng, M.; Sarker, A. M.; Gürel, E. E.; Lahti, P. M.; Karasz, F. E. *Macromolecules* **2000**, *33*, 7426–7430.

[15] Gorman, C. B.; Ginsburg, E. J.; Grubbs, R. H. *J. Am. Chem. Soc.* **1993**, *115*, 1397–1409.

[16] Ciardelli, F.; Lanzillo, S.; Pieroni, O. *Macromolecules* **1974**, *7*, 174–179.

[17] Meyer, C. D.; Joiner, S.; Stoddart, J. F. *Chem. Soc. Rev.* **2007**, *36*, 1705–1723.

[18] Goodwin, J. T.; Lynn, D. G. *J. Am. Chem. Soc.* **1992**, *114*, 9197–9198.

[19] Zhao, D.; Moore, J. S. *J. Am. Chem. Soc.* **2002**, *124*, 9996–9997.

[20] Oh, K.; Jeong, K.-S.; Moore, J. S. *Nature* **2001**, *414*, 889–893.

[21] Giuseppone, N.; Lehn, J.-M. *J. Am. Chem. Soc.* **2004**, *126*, 11448–11449.

[22] Giuseppone, N.; Fuks, G.; Lehn, J.-M. *Chem. Eur. J.* **2006**, *12*, 1723–1735.

[23] McLoughlin, C.; Clyburne, J. A. C.; Weinberg, N. *J. Mater. Chem.* **2007**, *17*, 4304–4308.

[24] Glaser, R.; Chen, N.; Wu, H.; Knotts, N.; Kaupp, M. *J. Am. Chem. Soc.* **2004**, *126*, 4412–4419.

[25] Tezuka, Y.; Komiya, R. *Macromolecules* **2002**, *35*, 8667–8669.

[26] Krouse, S. A.; Schrock, R. R. *Macromolecules* **1989**, *22*, 2569–2576.

[27] Monfette, S.; Fogg, D. E. *Chem. Rev.* **2009**, *109*, 3783–3816.

[28] Zhang, W.; Moore, J. S. *Adv. Synth. Catal.* **2007**, *349*, 93–120.

[29] Mortreux, A.; Coutelier, O. *J. Mol. Cat. A: Chemical* **2006**, *254*, 96–104.

[30] Zhang, W.; Moore, J. S. *J. Am. Chem. Soc.* **2005**, *127*, 11863–11870.

[31] Hwang, C.; Sinskey, A. J.; Lodish, H. F. *Science* **1992**, *257*, 1496–1502.

[32] Kemp, M.; Go, Y.-M.; Jones, D. P. *Free Radic. Biol. Med.* **2008**, *44*, 921–937.

[33] Leichert, L. I.; Jakob, U. *Antiox. Redox Signaling* **2006**, *8*, 763–772.

[34] Nabeshima, T. *Coord. Chem. Rev.* **1996**, *148*, 151–169.

[35] Herranz, M. A.; Colonna, B.; Echegoyen, L. *Proc. Natl Acad. Sci. USA* **2002**, *99*, 5040–5047.

[36] Bauhuber, S.; Hozsa, C.; Breunig, M.; Göpferich, A. *Adv. Mater.* **2009**, *21*, 3286–3306.

[37] Su, Y.-Z.; Niu, Y.-P.; Xiao, Y.-Z.; Xiao, M.; Liang, Z.-X.; Gong, K.-C. *J. Polym. Sci. Part A: Polym. Chem.* **2004**, *42*, 2329–2339.

[38] Gomberg, M. *J. Am. Chem. Soc.* **1900**, *22*, 757–771.

[39] Allemand, J.; Gerdil, R. *Acta Cryst. B* **1978**, *34*, 2214–2220.

[40] Wanzlick, H. W.; Esser, F.; Kleiner, H. J. *Chem. Ber.* **1963**, *96*, 1208–1212.

[41] Maeda, T.; Otsuka, H.; Takahara, A. *Prog. Polym. Sci.* **2009**, *34*, 581–604.

[42] Rowan, S. J.; Cantrill, S. J.; Cousins, G. R. L.; Sanders, J. K. M.; Stoddart, J. F. *Angew. Chem. Int. Ed.* **2002**, *41*, 898–952.

[43] Chikaoka, S.; Takata, T.; Endo, T. *Macromolecules* **1991**, *24*, 331–332.

[44] Marsella, M. J.; Maynard, H. D.; Grubbs, R. H. *Angew. Chem. Int. Ed.* **1997**, *36*, 1101–1103.

[45] Arduengo III, A. J.; Harlow, R. L.; Kline, M. *J. Am. Chem. Soc.* **1991**, *113*, 361–363.

[46] Jones, W. D. *J. Am. Chem. Soc.* **2009**, *131*, 15075–15077.

[47] Delaude, L. *Eur. J. Inorg. Chem.* **2009**, 1681–1699.

[48] Nair, V.; Bindu, S.; Sreekumar, V. *Angew. Chem. Int. Ed.* **2004**, *43*, 5130–5135.

[49] Khramov, D. M.; Bielawski, C. W. *Chem. Commun.* **2005**, 4958–4960.

[50] Díez-González, S.; Marion, N.; Nolan, S. P. *Chem. Rev.* **2009**, *109*, 3612–3676.

[51] Hahn, F. E.; Jahnke, M. C. *Angew. Chem. Int. Ed.* **2008**, *47*, 3122–3172.

[52] Sommer, W. J.; Weck, M. *Coord. Chem. Rev.* **2007**, *251*, 860–873.

[53] Cowley, A. H. *J. Organomet. Chem.* **2001**, *617–618*, 105–109.

[54] Kamplain, J. W.; Bielawski, C. W. *Chem. Commun.* **2006**, 1727–1729.

[55] Scott, N. M.; Clavier, H.; Mahjoor, P.; Stevens, E. D.; Nolan, S. P. *Organometallics* **2008**, *27*, 3181–3186.

[56] Jafarpour, L.; Stevens, E. D.; Nolan, S. P. *J. Organomet. Chem.* **2000**, *606*, 49–54.

[57] Herrmann, W. A.; Schwarz, J.; Gardiner, M. G. *Organometallics* **1999**, *18*, 4082–4089.

[58] Boydston, A. J.; Williams, K. A.; Bielawski, C. W. *J. Am. Chem. Soc.* **2005**, *127*, 12496–12497.

[59] Louie, J.; Gibby, J. E.; Farnworth, M. V.; Tekavec, T. N. *J. Am. Chem. Soc.* **2002**, *124*, 15188–15189.

[60] Boydston, A. J.; Rice, J. D.; Sanderson, M. D.; Dykhno, O. L.; Bielawski, C. W. *Organometallics* **2006**, *25*, 6087–6098.

[61] Karimi, B.; Akhavan, P. F. *Chem. Commun.* **2009**, 3750–3752.

[62] Radloff, C.; Hahn, F. E.; Pape, T.; Fröhlich, R. *Dalton Trans.* **2009**, 7215–7222.

[63] Williams, K. A.; Boydston, A. J.; Bielawski, C. W. *J. R. Soc. Interface* **2007**, *4*, 359–362.

[64] Williams, K. A.; Bielawski, C. W. *Chem. Commun.* **2010**, accepted.

[65] Winberg, H. E.; Coffman, D. D. *J. Am. Chem. Soc.* **1965**, *87*, 2776–2777.

[66] Wycliff, C.; Samuelson, A. G.; Nethaji, M. *Inorg. Chem.* **1996**, *35*, 5427–5434.

[67] Bianchini, C.; Meli, A.; Vizza, F. *Angew. Chem.* **1987**, *99*, 821–822.

[68] Norris, B. C.; Bielawski, C. W. *Macromolecules* **2010**, *43*, 3591–3593.

[69] Khramov, D. M.; Bielawski, C. W. *Chem. Commun.* **2005**, *39*, 4958-4960.

[70] Khramov, D. M.; Bielawski, C. W. *J. Org. Chem.*, **2007**, *72*, 9407 -9417

[71] Matyjaszewski, K.; Xia, J. *Chem. Rev.* **2001**, *101*, 2921-2990.

[72] (a) White, S. R.; Sottos, N. R.; Geubelle, P. H.; Moore, J. S.; Kessler, M. R.; Sriram, S. R.; Brown, E. N.; Viswanathan, S. *Nature* **2001**, *409*, 794. (b) Chen, X.; Dam,

M. A.; Ono, K.; Mal, A.; Shen, H.; Nutt, S. R.; Sheran, K.; Wudl, F. *Science* **2002**, *295*, 1698.

[73] Miaudet, P.; Derré, A.; Maugey, M.; Zakri, C.; Piccione, P. M.; Inoubli, R.; Poulin, P. *Science* **2007**, *318*, 1294.

[74] (a) Nair, K. P.; Breedveld V.; Weck M. *Macromolecules* **2008**, *41*, 3429. (b) Scott, T. F.; Schneider, A. D.; Cook, W. D.; Bowman, C. N. *Science* **2005**, *308*, 1615. (c) Skene, W. G.; Lehn, J.–M. *Proc. Natl. Acad. Sci.* **2004**, *101*, 8270. (d) Otsuka, H.; Aotani, K.; Higaki, Y.; Takahara, A. *J. Am. Chem. Soc.* **2003**, *125*, 4064. (e) Rowan, S. J.; Cantrill, S. J.; Cousins, G. R. L.; Sanders, J. K. M.; Stoddart, J. F. *Angew. Chem. Int. Ed.* **2002**, *41*, 898. (f) Bell, S. A.; Meyer, T. Y.; Geib, S. J. *J. Am. Chem. Soc.* **2002**, *124*, 10698.

[75] Williams, K. A.; Dreyer, D. R.; Bielawski, C. W. *MRS Bull.* **2008**, *33*, 759.

[76] (a) Arduengo, III, A. J. *Acc. Chem. Res.* **1999**, *32*, 913. (b) Herrmann, W. A.; Köcher, C. *Angew. Chem., Int. Ed. Engl.* **1997**, *36*, 2162. (c) Bourissou, D.; Guerret, O.; Gabbaï, F.; Bertrand, G. *Chem. Rev.* **2000**, *100*, 39. (d) Wanzlick, H. W.; Buchler, J. W. *Chem. Ber.* **1964**, *97*, 2447.

[77] (a) Alder, R. W.; Blake, M. E.; Chaker, L.; Harvey, J. N.; Paolini, F.; Schütz, J. *Angew. Chem. Int. Ed.* **2004**, *43*, 5896. (b) Duong, H. A.; Tekavec, T. N.; Arif, A. M.; Louie, J. *Chem. Commun.* **2004**, 112. (c) Garrison, J. C.; Youngs, W. J. *Chem. Rev.* **2005**, 3978.

[78] (a) Liu, M.-F.; Wang, B.; Cheng, Y. *Chem Commun.* **2006**, 1215. (b) Xue, J.; Yang, Y.; Huang, X. *Synlett* **2007**, 1533. (d) Regitz, M.; Hocker, J.; Schössler, W.; Weber, B.; Liedhegener, A. *Liebigs Ann. Chem.* **1971**, *748*, 1.

[79] Poater, A.; Ragone, F.; Giudice, S.; Costabile, C.; Dorta, R.; Nolan, S. P.; Cavallo, L. *Organometallics* **2008**, *27*, 2679.

[80] (a) Coady, D. J.; Norris, B. C.; Tennyson, A. G.; Bielawski, C. W. *Angew. Chem. Int. Ed.* **2009**, *48*, 5187. (b) Hahn, F. E.; Radloff, C.; Pape, T.; Hepp, A. *Organometallics* **2008**, *27*, 6408. (c) Khramov, D. M.; Boydston, A. J.; Bielawski, C. W. *Angew. Chem. Int. Ed.* **2006**, *45*, 6186.

[81] Hahn, F. E.; Wittenbecher, L.; Boese, R.; Bläser, D. *Chem. Eur. J.* **1999**, *5*, 1931.

[82] The rate constant for this bimolecular reaction was determined to be $k = 60 \pm 3\ s^{-1}$ at 120 °C.

[83] Bis(NHC)s featuring less sophisticated *N*-substituents (e.g., ethyl, *n*-butyl, *tert*-butyl, etc.) are either prone to polymerization *via* NHC dimerization or produced

insoluble materials upon combination with **2.6**. As a result, such bis(NHC)s were not extensively examined.

[84] Scherf, U.; List, E. J. W. *Adv. Mater.* **2002**, *14*, 477.

[85] Molecular weights are reported relative to polystyrene standards

[86] The thermal stability of polymer **2.7** was evaluated using thermogravimetric analysis and found to lose approximately 10% of its mass at 300 °C under nitrogen.

[87] Akkurt, M.; Karaca, S.; Küçükbay, H.; Sireci, N.; Büyükgüngör, O. *Acta Cryst.* **2008**, *E64*, o809. (b) Akkurt, M.; Karaca, S.; Küçükbay, H.; Yilmaz, U.; Büyükgüngör, O. *Acta. Cryst.* **2005**, E61, o2875.

[88] Films of **2.7** exhibited a Young's modulus (E) of 65 GPa and a yield strength of 60 MPa. Upon doping with iodine, the resulting material exhibited a larger yield strength (140 MPa) and as well increased compliance (E = 3.3 GPa).

[89] Unfortunately, the iodine doped polymer materials did not exhibit structurally dynamic properties.

[90] Tennyson, A. G.; Kamplain, J. W.; Bielawski, C. W. *Chem. Commun.* **2009**, 2124.

[91] A. Iwan, D. Sek, Prog. Polym. Sci. 2008, 33, 289–345; (b) A. Pron, P. Rannou, *Prog. Polym. Sci.* **2001**, *27*, 135–190.

[92] (a) C. S. Marvel, W. S. Hill, J. Am. Chem. Soc. 1950, 72, 4819–4820; (b) C. J. Yang, S. A. Jenekhe, *Chem. Mater*. **1991**, *3*, 878–887.

[93] (a) P. W. Morgan, S. L. Kwolek, T. C. Pletcher, *Macromolecules* **1987**, *20*, 729–739; (b) P. W. Wojtkowski, *Macromolecules* **1987**, *20*, 740–748.

[94] (a) J. McElvain, S. Tatsuura, F. Wudl, A. J. Heeger, *Synth. Met.* **1998**, *95*, 101–105; (b) S. Di Bella, I. Fragala, I. Ledoux, M. A. Diaz-Garcia, T. J. Marks, *J. Am. Chem. Soc.* **1997**, *119*, 9550–9557; (c) P. K. Dutta, P. Jain, P. Sen, R. Trivedi, P. K. Sen, J. Dutta, *Eur. Polym. J.* **2003**, *39*, 1007–1011; (d) S. A. Jenekhe, C. J. Yang, H. Vanherzeele, J. S. Meth, *Chem. Mater.* **1991**, *3*, 985–987.

[95] (a) W. Fischer, F. Stelzer, F. Meghdadi, G. Leising, *Synth. Met*. **1996**, *76*, 201–204; (b) M. S. Weaver, D. D. C. Bradley, *Synth. Met*. **1996***, 83*, 61–66; (c) J.-S. Cho, K. Takanashi, M. Higuchi, K. Yamamoto, *Synth. Met*. **2005**, *150*, 79–82.

[96] I. Manners, H. R. Allcock, G. Renner, O. Nuyken, *J. Am. Chem. Soc*. **1989,** *111*, 5478–5480.

[97] (a) S. B. Park, H. Kim, W. C. Zin, J. C. Jung, *Macromolecules* **1993**, *26*, 1627–1632; (b) C. J. Yang, S. A. Jenekhe, *Macromolecules* **1995**, *28,* 1180–1196; (c) T. Matsumoto, F. Yamada, T. Kurosaki, *Macromolecules* **1997**, *30*, 3547–3552; (d) O. Thomas, O. Inganaes, M. R. Andersson, *Macromolecules* **1998**, *31*, 2676–2678; (e) S. Destri, M. Pasini, C. Pelizzi, W. Porzio, G. Predieri, C. Vignali, *Macromolecules* **1999,** *32,* 353–360; (f) D. Nepal, S. Samal, K. E. Geckeler, *Macromolecules* **2003**, *36*, 3800–3802; (g) E.-J. Choi, J.-C. Ahn, L.-C. Chien, C.-K. Lee, W.-C. Zin, D.-C. Kim, S.-T. Shin, *Macromolecules* **2004,** *37*, 71–78; (h) Y. Liu, Y.-L. Zhao, H.-Y. Zhang, X.-Y. Li, P. Liang, X.-Z. Zhang, J.-J. Xu, *Macromolecules* **2004**, *37*, 6362–6369; (i) Y. Takihana, M. Shiotsuki, F. Sanda, T. Masuda, *Macromolecules* **2004**, *37*, 7578–7583; (j) F.-C. Tsai, C.-C. Chang, C.-L. Liu, W.-C. Chen, S. A. Jenekhe, *Macromolecules* **2005**, *38*, 1958–1966; (k) Y. Liu, P. Liang, Y. Chen, Y.-M. Zhang, J.-Y. Zheng, H. Yue, *Macromolecules* **2005,** *38,* 9095–9099.

[98] For excellent reviews on stable NHCs, see: (a) W. A. Herrmann, K. Kocher, *Angew. Chem. Int. Ed.* **1997**, *36,* 2162;

[99] (b) D. M. Khramov, C. W. Bielawski, *J. Org. Chem*. **2007**, *72*, 9407.

[100] (a) E. Kleinpeter, B. A. Stamboliyska, *J. Org. Chem***. 2008,** *73*, 8250; (b) J. Preat, C. Michaux, A. Lewalle, E. A. Perpete, D. Jacquemin, *Chem. Phys. Lett*. **2008,** *451,* 37.

[101] (a) V. V. Rostovtsev, L. G. Green, V. V. Fokin, K. B. Sharpless, *Angew. Chem. Int. Ed.* **2002,** *41,* 2596; (b) C. W. Tomøe, C. Christensen, M. Meldal, *J. Org. Chem*. **2002,** *67*, 3075.

[102] (a) P. Wu, A. K. Feldman, A. K. Nugent, C. J. Hawker, A. Scheel, B. I. Voit, J. Pyun, J. M. J. Fréchet, K. B. Sharpless, V. V. Fokin, *Angew. Chem., Int. Ed.* **2004**, *43,* 3928; (b) B. Helms, J. L. Mynar, C. J. Hawker, J. M. J. Fréchet, *J. Am. Chem. Soc.* **2004**, *126*, 15020; (c) J. Scheel, H. Komber, B. I. Voit, B. I. *Macromol. Rapid Commun.* **2004**, *25*, 1175.

[103] D. J. V. C. van Steenis, O. R. P. David, G. P. F. van Strijdonck, J. H. van Maarseveen, J. N. H. Reek, *Chem. Commun*. **2005**, *34*, 4333.

[104] D. J. Coady, C. W. Bielawski, *Macromolecules* **2006**, *39*, 8895.

[105] Bis(NHC)s featuring less sophisticated N-substituents (e.g., ethyl, n-butyl, tert-butyl, etc.) are either prone to polymerization via NHC dimerization (see: ref. 54) or produced insoluble materials upon combination with **3.7-3.9**. As a result, these bis(NHC)s were not extensively examined.

[106] This M_n is a lower limit as it assumes no cyclic polymer formation.

[107] This result was consistent with previous studies showing that the decomposition products of certain triazenes are molecular nitrogen and its respective guanidine; see ref. [99 b].

[108] This polymer was prepared from **3.4** and **3.7** using a 10% molar excess of the latter monomer.

[109] $E_{1/2}$ = +0.15, +0.40 and +0.72 V. Conditions: CH_2Cl_2 as solvent, 0.1 M $(nBu)_4N•PF_6$ as electrolyte, 1 mM **3.10**, scan rate = 0.1 V/s, referenced to Fc/Fc+ (Fc = ferrocene; $E_{1/2}$ = 0.45 V vs. standard calomel electrode).

[110] Polymers were spin-coated from CH_2Cl_2 onto glass slides containing gold electrodes spaced at 1 mm, 2 mm, and 5 mm intervals. Film thickness was measured using a surface profiler and were found to be ~10 kÅ. Conductivity measurements of the polymer films were measured by two-point probe linear sweep voltammetry.

[111] Matyjaszewski, K.; Davis, T. P. Handbook of Radical Polymerization; Wiley: New York, **2002**.

[112] (a) Moad, G.; Rizzardo, E.; Thang, S. H. *Aust. J. Chem.* **2005**, *58*, 379-410. (b) Perrier, S.; Takolpuckdee, P. *J. Polym. Sci., Part A: Polym. Chem*. **2005**, *43*, 5347-5393.

[113] Braunecker, W. A.; Matyjaszewski, K. *Prog. Polym. Sci*. **2007**, *32*, 93-146.

[114] (a) Chiefari, J.; Chong, Y. K.; Ercole, F.; Krstina, J.; Jeffery, J.; Le, T. P. T.; Mayadunne, R. T. A.; Meijs, G. F.; Moad, C. L.; Moad, G.; Rizzardo, E.; Thang, S. H. *Macromolecules* **1998**, *31*, 5559-5562. (b) Charmot, D.; Corpart, P.; Adam, H.; Zard, S. Z.; Biadatti, T.; Bouhadir, G. *Macromol. Symp*. **2000**, *150*, 23-32.

[115] Macromolecular Design by Interchange of Xanthates (MADIX) polymerizations operate via a similar mechanism as RAFT polymerization.

[116] For excellent reviews, see: (a) Lowe, A. B.; McCormick, C. L. *Prog. Polym. Sci*. **2007**, *32*, 283-351. (b) Barner, L.; Davis, T. P.; Stenzel, M. H.; Barner-Kowollik, C. *Macromol. Rapid Commun.* **2007**, 28, 539-559.

[117] For selected examples, see: (a) Quinn, J. F.; Chaplin, R. P.; Davis, T. P.; *J. Polym. Sci. Polym. Chem*. **2002**, *40*, 2956-2966. (b) Skaff, H.; Emrick, T. *Angew. Chem. Int. Ed.* **2004**, *43*, 5383-5386. (c) Schilli, C. M.; Zhang, M. F.; Rizzardo, E.; Thang, S. H.; Chong, Y. K.; Edwards, K.; Karlsson, G.; Muller, A. H. E. *Macromolecules* **2004**, 37*,* 7861-7866. (d) O'Reilly, R. K.; Joralemon, M. J.;

Hawker, C. J.; Wooley, K. L. *Chem. Eur. J.* **2006**, *12*, 6776-6786. (e) Cambre, J. N.; Roy, D.; Gondi, S. R.; Sumerlin, B. S. *J. Am. Chem. Soc*. **2007**, *129*, 10348-10349.

[118] Favier, A.; Charreyre, M.-T. *Macromol. Rapid. Commun*. **2006**, *27*, 653-692.

[119] For leading discussions of the mechanism of RAFT polymerizations, see: (a) Moad, G.; Rizzardo, E.; Thang, S. H. *Polymer*. **2008**, *49*, 1079-1131. (b) Barner-Kowollik, C.; Buback, M.; Charleux, B.; Coote, M. L.; Drache, M.; Fukuda, T.; Goto, A.; Klumperman, B.; Lowe, A. B.; Mcleary, J. B.; Moad, G.; Monteiro, M. J.; Sanderson, R. D.; Tonge, M. P.; Vana, P. *J. Polym. Sci., Part A: Polym. Chem*. **2006**, 44, 5809-5831.

[120] Chong, Y. K.; Krstina, J.; Le, T. P. T.; Moad, G.; Postma, A.; Rizzardo, E.; Thang, S. H. *Macromolecules* **2003**, *36*, 2256.

[121] Chiefari, J.; Mayadunne, R. T. A.; Moad, C. L.; Moad, G.; Rizzardo, E.; Postma, A.; Skidmore, M. A.; Thang, S. H. *Macromolecules* **2003**, *36*, 2273-2283.

[122] Stenzel, M.; Cummins, L.; Roberts, G. E.; Davis, T. P.; Vana, P.; Barner-Kowollik, C. *Macromol. Chem. Phys.* **2003**, *204*, 1160-1168.

[123] For examples of cationic dithioester-based RAFT agents containing ammonium groups distal to their dithio moieties, see: (a) Baussard, J.-F.; Habib-Jiwan, J.-L.; Laschewsky, A.; Mertoglu, M.; Storsberg, J. *Polymer* **2004**, *45*, 3615-3626. (b) Mertoglu, M.; Laschewsky, A.; Skrabania, K.; Wieland, C. *Macromolecules* **2005**, *38*, 3601-3614. (c) Samakande, A.; Sanderson, R. D.; Hartmann, P. C. *Synth. Commun.* **2007**, *37*, 3861-3872. For an example of a RAFT polymerization mediated by a quarternary dithiocarbamate, see: Kanagasabapathy, S.; Sudalai, A.; Benicewicz, B. C. *Macromol. Rapid Commun*. **2001**, *22*, 1076-1080.

[124] (b) Herrmann, W. A.; Köcher, C. *Angew. Chem., Int. Ed. Engl*. **1997**, *36*, 2163-2165.

[125] (a) Peris, E.; Crabtree, R. H. Coord. *Chem. Rev.* **2004**, *248*, 2239-2258. (b) Hillier, A. C.; Gasa, G. A.; Viciu, M. S.; Lee, H. M.; Yang, C. L.; Nolan, S. P. *J. Organomet. Chem.* **2002**, *653*, 69-82.

[126] (b) Boydston, A. J.; Bielawski, C. W. *Dalton Trans.* **2006**, 4073-4077.

[127] For a report describing the utility of 2 in Suzuki–Miyaura reactions, see: Tudose, A.; Delaude, L.; André, B.; Demonceau, A. *Tetrahedron Lett.* **2006**, *47*, 8529-8533.

[128] Rotational barriers were calculated at the Hartree-Fock 6-31G* level of theory, as implemented in the Spartan **2004** software package (Wavefunction, Inc., Irvine, CA 92612).

[129] For examples of dithioester-based RAFT agents where the dithioester moiety is attached to the 1- or 5-position of an imidazole system, see: (a) Carter, S.; Rimmer, S.; Sturdy, A.; Webb, M. *Macromol. Biosci.* **2005**, *5,* 373-378. (b) Zhou, D.; Zhu, X.; Zhu, J.; Yin, H. *J. Polym. Sci., Part A: Polym. Chem.* **2005**, *43*, 4849-4856. (c) Mayadunne, R. T. A; Rizzardo, E.; Chiefari, J.; Chong, B. Y. K.; Moad, G.; Thang, S. H. *Macromolecules* **1999**, *32*, 6977-6980.

[130] As a control, polymerizations were performed in the absence of AIBN using styrene : CTA ratios of 200 : 1. After 2 d at 110 °C, no polymer was observed when either 3 or 4 was used at the CTA which suggested to us that AIBN was essential for forming active radicals, and hence polymer.

[131] Molecular weights and polydispersities were determined using gel permeation chromatography (eluent = DMF/LiBr or THF) and are reported relative to polystyrene standards.

[132] $M_{n,theory} = ([Mon]_0/[CTA]_0) \times FW_{mon} \times \%$ mon. conv. $+ FW_{CTA}$

[133] Solvent was removed under vacuum at 85 °C and ^1H NMR was taken in $CDCl_3$

[134] Vu, P. D.; Boydston, A. J.; Bielawski, C. W. *Green Chem.* **2007**, *9,* 1158-1159.

[135] The synthesis of 3 is similar to protocols used to prepare dithioester-based CTAs commonly used in RAFT polymerizations, see: Wood, M. R.; Duncalf, D. J.; Rannard, S. P.; Perrier, S. *Org. Lett.* **2006**, *8*, 553-556.

[136] Alberti, G.; Casciola, M. *Solid State Ionics* **2001**, *145*, 3–16.

[137] (a) Souzy, R.; Ameduri, B. *Prog. Polym. Sci.* **2005**, *30*, 644–687. (b) Mauritz, K. A.; Moore, R. B. *Chem. Rev.* **2004**, *104*, 4535–4586.

[138] (a) Fu, Y.; Manthiram, A.; Guiver, M. D. *Electrochem. Commun.* **2006**, *8*, 1386–1390. (b) Munch, W.; Kreuer, K. D.; Silvestri, W.; Maier, J.; Seifert, G. *Solid State Ionics* **2001**, *145*, 437–443. (b) Li, Q.; He, R.; Jensen, J. O.; Bjerrum, N. J. *Chem. Mater.* **2003**, *15*, 4896–4915.

[139] (a) Wainright, J. S.; Wang, J. T.; Weng, D.; Savinell, R. F.; Litt, M. *J. Electrochem. Soc.* **1995**, *142*, L121–L123. (b) Savinell, R. F.; Litt, M. H. US Patent **1996**,

5,525,436. (c) Bouchet, R.; Siebert, E. *Solid State Ionics* **1999**, *118* 287–299. (d) Ma, Y. L.; Wainright, J. S.; Litt, M. H.; Savinell, R. F. *J. Electrochem. Soc.* **2004**, *151*, A8–A16.

[140] (a) Smitha, B.; Sridhar, S,; Khan, A. A. *J. Membrane Sci.* **2003**, *225*, 63–76. (b) Kim, J.; Kim, B.; Jung, B. *J. Membrane Sci.* **2002**, *207*, 129–137. (c) Sangeetha, D. *Eur. Polym. J.* **2005**, *41*, 2644–2652. (d) Shin, J. P.; Chang, B. J.; Kim, J. H.; Lee, S. B.; Suh, D. H. *J. Membr. Sci.* **2005**, *251*, 247–254.

[141] (a) Lafitte, B.; Karlsson, L. E.; Jannasch, P. *Macromol. Rapid Commun.* **2002**, *23*, 896–900. (b) Karlsson, L. E.; Jannasch, P. *Electrochimica Acta* **2005**, *50*, 1939–1946. (c) Park, H. B.; Shin, H. S.; Lee, Y. M.; Rhim, J. W. *J. Membr. Sci.* **2005**, *247*, 103–110.

[142] (a) Kopitzke, R. W.; Linkous, C. A.; Anderson, H. R.; Nelson, G. L. *J. Electrochem. Soc.* **2000**, *147*, 1677–1681. (b) Kreuer, K. D. *J. Membr. Sci.* **2001**, *185*, 29–39. (c) Li, L.; Zhang, J.; Wang, Y. *J. Membr. Sci.* **2003**, *226*, 159–167.

[143] Yang, B.; Manthiram, A. *Electrochem. Solid-State Lett.* **2003**, *6*, A229–A231.

[144] (a) Kreuer, K.D.; Fuchs A.; Ise M.; Spaeth, M.; Maier J. *Electrochimica Acta* **1998**, *43,* 1281–1288. (b) Pu, H.; Qin, Y.; Tang, L.; Teng, X; Chang, Z. *Electrochimica Acta* **2009**, *54,* 2603–2609. (c) Schechter, A.; Savinell, R.F. *Solid State Ionics* **2002**, *147*, 181–187.

[145] Yang, C.; Costamagna, P.; Srinivasan, S.; Benziger, J.; Bocarsly, A. B. *J. Power Sources* **2001**, *103*, 19.

[146] Yamada, M.; Honma, I. *Polymer* **2005**, *46*, 2986–2992.

[147] Dillon, R.; Srinivasan, S.; Aricò, A.S.; Antonucci, V. *J. Power Sources* **2004,** *127*, 112.

[148] Neburchilov, V.; Martin, J.; Wang, H.; Zhang, J. *J. Power Sources* **2007**, *169,* 2, 221.

[149] Li, Q.; He, R.; Jensen, J.O.; Bjerrum, N.J. *Chem Mater* **2003,** *15,* 4896.

[150] V. Tricoli, N. Carretta, M. Bartolozzi, J. Electrochem. Soc. **2000**, 147, 1286.

[151] Kreuer, K. D. *J. Membr. Sci.* **2001**, *185*, 29–39.

[152] (a) Li, W.; Norris, B.C.; Snodgrass, P.; Prasad, K.; Stockett, A. S.; Pryamitsyn, V.; Ganesan, V.; Bielawski, C. W.; Manthiram, A. *J. Phys. Chem. B* **2009**, *113*, 10063.

[153] Yang, C.; Costamagna, P.; Srinivasan, S.; Benziger, J.; Bocarsly, A.B.; *J. Power Sources* **2001,** *103,* 1.

[154] Kreuer, K.D.; Paddison, S.J.; Spohr, E.; Schuster, M. *Chem. Rev.* **2004,** *104*, 4637.

[155] Herz, H.G.; Kreuer, K.D.; Maier, J.; Scharfenberger, G.; Schuster, M.F.H.; Meyer, W.H. *Electrochim. Acta* **2003,** *48*, 2165.

[156] Saxena, A.; Tripathi, B. P.; Shahi, V. K. *J. Phys. Chem. B.* **2007**, *111*, 12454.

[157] J Jeong, M-H.; Lee, K-S.; Lee, J-S. *Macromolecules* **2009** *42, 5*, 1652.

[158] Kerres, J. A. *Fuel Cells* **2005,** *5*, 2, 230.

[159] Kerres J. A. *J. Membrane Sci.* **2001,** *185*, 3.

[160] Xu, N.; Guo, X.; Fang, J.; Xu, H.; Yin, J. *Polym. Sci.,Part A: Polym. Chem.* **2009,** *47*, 6992.

[161] Zhang, G.; Guo, X.; Fang, J.; Chen, K.; Okamoto, K.-i. *J. Membr. Sci.* **2009***, 326*, 708.

[162] Meldal, M.; Tornøe, C. W. *Chem. Rev.*, **2008**, *108*, 8, 2952-3015.

[163] Kolb, H.C.; Finn, M. G.;Sharpless, K.B. *Angew. Chem. Int. Ed.* **2001**, *40*, 2004.

[164] Abboud, J-L. M.; Roces-Foces, C.; Notario, R.; Trifonov, R.E..; Volovodenko, A.P.; Ostrovskii, V.A.; Alkorta, I,; Elguero, J. *Eur. J. Org. Chem.* **2001**, 3013.

[165] Zhou, Z.; Li, S.; Zhang, Y.; Liu, M.; Li, W. *J. Am. Chem. Soc.* **2005**, *127* , 10824.

[166] Li, W.; Manthiram, A.; Guiver, M.D.; Liu, B. *Electrochemistry Communications* **2010**, *12*, 607.

[167] Karlsson, L E.; Jannash P. *Journal of Membrane Science*, **2004**, *230,* 61.

[168] Lee, H-S.; Badami, A. S.; Roy, A.; McGrath, J. E. *Journal of Polymer Science: Part A: Polymer Chemistry*, **2007**, *45*, 4879.

[169] Lafitte, B.; Jannasch, P. *Adv. Funct. Mater.* **2007,** *17*, 2823..

[170] Kerres, J.; Zhang, W.; Cui, W. *J. Polym. Sci.: Part A: Polym. Chem.* **1998,** *36,* 1441-1448.

[171] Dudek S. P.; Pouderoijen M.; Abbel R.; Schenning A. P. H. J.; Meijer E. W. *J. Am Chem Soc.* **2005**, *127,* 11768.

[172] Hahn F. E.; Wittenbecher, L.; Boese, R.; Bläser, D. *Chem. Eur J.* **1999**, *6*, 1931.

[173] Coady, D. J.; Khramov, D. M.; Norris, B. C.; Tennyson, A. G.; Bielawski, C. W. *Angew. Chem. Int. Ed.* **2009**, 5187.

[174] Werstiuk N. H.; Kadai T. *Can. J. Chem.* **1974**, *52*, 2169.

[175] D. L. Herring, *J. Org. Chem*. **1961**, *26*, 3998.

[176] M. Minato, P. M. Lahti, H. Willigen, *J. Am. Chem. Soc*. **1993**, *115*, 4532.

[177] S. P. Dudek, M. Pouderoijen, R. Abbel, A. P. H. Schenning, E. W. Meijer, *J. Am. Chem. Soc.* **2005**, *127*, 11763.

[178] S. S. Berg, D. T. Cowling, *J. Chem. Soc. C: Org.* **1971**, 1653.

[179] J. H. Brannon, D. Magde, *J. Phys. Chem.* **1978**, *82*, 705.

[180] D. M. Khramov, A. J. Boydston, C. W. Bielawski, *Org. Lett.* **2006**, *8*, 1831.

[181] Grasa, G. A.; Viciu, M. S.; Huang, J.; Nolan, S. P. *J. Org, Chem*. **2001**, *66*, 7729-7730.

[182] Akutagawa, T.; Saito, G. *Bull. Chem. Soc. Jap.* **1995**, *68*, 1753–1773.

[183] Jordan, D. O.; Taylor, H. F. W. *J. Chem. Soc.* **1946**, 994–997.

[184] K. Okamoto, Y. Yin, O. Yamada, M.N. Islam, T. Honda, T. Mishima, Y. Suto, K. Tanaka, H. Kita, *J. Membr. Sci.* **2005**, *258,* 115.

[185] Zhai, F.; Guo, X.; Fang. J.; Xu, H. *J. Membr. Sci.* **2007,** *296*,102.

[186] Guiver, M.D.; Robertson, G.P. *Macromolecules* **1995,** *28*, 1, 294.

Vita

Brent Carl Norris was born on June 17, 1981 in Houston, Texas to parents Jan and Susan Norris. He attended Robert E. Lee High School, and then the Texas A&M Univesity. After receiving his B.S. in chemistry during the winter of 2004 he moved to Austin to attend graduate school at The University of Texas at Austin. Once in Austin Brent joined the research group of Dr. Christopher W. Bielawski. While being advised by Dr. Bielawski, he mainly worked on small molecule synthesis, polymer synthesis and post polymerization modification for his various polymer research areas.

Permanent address: 18321 Lake Edge Court, Pflugerville, TX, 78660
This dissertation was typed by Brent Carl Norris.